

Universität Bielefeld

# Optic Flow in Behavior and Brain Function of the Zebra Finch

Doctoral Thesis

by Dennis Eckmeier

Bielefeld University, October 2010



# Danksagung

Selbstverständlich gilt mein Dank zunächst den Menschen, die mich in meinem Werdegang immer unterstützt und einen Großteil davon überhaupt erst möglich gemacht haben, meinen Eltern.

Im Weiteren möchte ich den Kommilitonen aus Köln danken, die mich in der Entscheidung bekräftigt haben, mich auf die Stelle zu bewerben, die ich hier in Bielefeld dann auch über nun fast vier Jahre ausfüllen durfte - natürlich nicht, weil sie mich hätten loswerden wollen, oder ich sie, sondern weil sie mein Bestes im Sinne hatten. Dies richtet sich vor allen Dingen an Bart Geurten, der ebenfalls in Bielefeld promoviert, und Moritz Pähler, und einige andere.

Sehr wichtige Bezugspersonen waren natürlich meine Betreuer Prof. Dr. Hans-Joachim Bischof, Prof. Dr. Martin Egelhaaf und Dr. Roland Kern, die mir mit ihrer Erfahrung und mit materieller Unterstützung eine persönlich gewinnbringende und auch wissenschaftlich erfolgreiche Arbeit sowie einen großen Erfahrungszuwachs in wissenschaftlichen Belangen ermöglichten, und mich auch darüber hinaus in meinen Bemühungen um eine Anstellung im Anschluss an die Promotion sehr unterstützten.

Schlussendlich danke ich natürlich auch allen Postdocs, Doktoranden und Studenten der Verhaltensforschung und der Neurobiologie, die das Umfeld erst entstehen lassen, in dem ein erfolgreiches Arbeiten möglich ist.

# Erklärung

Hiermit erkläre ich, dass ich die Arbeit selbstständig, also ohne Zuhilfenahme unzulässiger Mittel oder unzulässiger Hilfestellung Dritter, verfasst habe. Zitate habe ich in der üblichen Form kenntlich gemacht.



# Table of Content

<b>Summary</b>	<b>7</b>
<b>Disquisition</b>	<b>9</b>
<b>Introduction</b>	<b>11</b>
The Impact of Optic Flow on the Behavior of Insects	14
Behavioral Optimization of the Visual Input in Birds	16
Central Processing of Visual Motion Information in the Avian Brain	19
<b>The Authors Scientific Contribution to...</b>	<b>21</b>
... the Influence of Optic Flow on Gaze Shift in Freely Flying Birds	21
... the Control Mechanism for Optokinetic Reactions	22
... Motion Processing in the Tectofugal Visual System of the Zebra Finch	24
<b>References</b>	<b>26</b>
<b>The Optokinetic Response in Wild Type and White Zebra Finches</b>	<b>33</b>
<b>Abstract</b>	<b>33</b>
<b>Introduction</b>	<b>35</b>
<b>Material and Methods</b>	<b>37</b>
<b>Results</b>	<b>39</b>
Monocular and Binocular OKR	39
Illumination Level Dependency of OKR	41
Comparison of Low Illumination and Daylight Results	43
<b>Discussion</b>	<b>43</b>
Dependency of OKR on Illumination Levels	43
Comparison of White and Wild Type Zebra Finches	44
<b>References</b>	<b>45</b>

<b>Gaze Strategy in the Free Flying Zebra Finch (<i>Taeniopygia guttata</i>)</b>	<b>49</b>
Abstract	49
Introduction	51
Material and Methods	53
Results	57
Discussion	60
Acknowledgement	61
References	61
<b>New Insights into Object Detection in the Zebra Finch Brain Revealed by Complex Visual Motion Stimuli</b>	<b>63</b>
Abstract	63
Introduction	65
Material and Methods	66
Naturalistic Visual Stimulation and Data Analysis	71
Results	72
Responses to Conventional Self-Motion Stimuli	72
Receptive Field Estimation	76
Looming Stimuli	79
Naturalistic Replay	81
Discussion	87
I. Comparison of our findings to those from other studies on birds.	87
II. Adding realism to a stimulus gives rise to unexpected response properties.	89
III. Flies and birds show similar aspects of response to a naturalistic replay.	89
Acknowledgements	90
References	91

# - Chapter I -

## Summary

**Dennis Eckmeier**

My dissertation focused on the impact of optic flow on the behavior and brain function of the zebra finch in three approaches. First we demonstrated that the zebra finch controls its gaze in way that facilitates the perception of depth in the optic flow. Then we studied the control mechanism that underlies this strategy and added to the knowledge about the properties of this mechanism. Finally we studied the actual processing of object related information during presentation of naturalistic self motion and found neurons coding for specific behaviorally relevant characteristics of the optic flow that correlate with the approach towards objects.

Optic flow is the displacement of the retinal image during self motion. Due to basic optic phenomena, the flow field provides information about the distance to objects in the visual scene and about self motion. Distance information, however, can only be acquired from optic flow generated from straight (translational) self motion.

Birds highly depend on such cues and use them, for example, for the control of flight maneuvers. The need to use optic flow emerges from anatomical properties of the bird's skull. Laterally positioned eyes and a short interocular distance are common across avian species. These properties cause binocular vision to be insufficient for stereoptic depth perception. Pigeons, for example, can estimate depth from binocular cues in a range of only 5 to 19 cm distance – impractically short for fast locomotion in an unknown environment. Behavioral evidence for the actual usage of such cues was reported for birds that controlled flight maneuvers on the basis of optic flow.

Insects also depend on optic flow, due to their size and anatomy. The impact of optic flow on the behavior of insects is omnipresent especially in airborne species. One example would be the typical flight and gaze strategy in flies. Since depth information can only be derived from optic flow that is generated by straight (translational) self-motion, flies avoid flying in curves but change flight direction in fast saccadic body turns. Between such saccadic turns, they move translational. The visual input is further optimized by facilitating head movements.

To find whether zebra finches would show a similar behavior, we analyzed their head movements in free flight. We recorded high speed videos of zebra finches circling around an obstacle. The obstacle forced the birds into a curved flight during which rotational self motion components occurred. In analogy to the blowfly zebra finches changed the orientation of the gaze in geocentric coordinates only in saccades. These saccades, however, were not produced by body turns. They rather were generated by head turns instead. Between saccades gaze orientation did not change. This must have been achieved by head turns that compensated the rotational component of the flight path, as well as body turns occurring in maneuvers, such as braking. This gaze strategy optimizes the visual input for depth information. We concluded that the birds used optic flow to achieve information about the structure of the environment, e.g. the distance to the obstacle.

This gaze strategy is controlled by the optic flow produced during rotational self motion. The compensation of rotationally induced optic flow is done via optokinetic reactions that control the neck muscles according to the overall motion of the visual scene. The optokinetic reaction can be demonstrated in the rotating drum paradigm. The bird is tethered while the visual scene – consisting of the inner walls of a drum – is being rotated around the

birds. The optokinetic reaction stabilizes the retinal image by turning the head accordingly in the so called ‘slow phase’ of the response. The head is then turned back in a fast head movement during the ‘fast phase’. This is repeated as long as the visual scene is rotated.

It was assumed that the slow phase correlates with the intersaccadic intervals in free flight during which the orientation of the head in geocentric coordinates does not change. The fast phase of the optokinetic reaction in this case would correlate with the saccadic gaze shift we observed.

We used the rotating drum paradigm to test the optokinetic reaction in different conditions. The visual input to the mechanism controlling the optokinetic reaction is provided by the accessory optic system. At the first level of this visual upstream, retinal input is transferred to the nucleus lentiformis mesencephali and the nucleus of the basal optic root which code for self motion in different directions. The signal is then further processed in the inferior olive and the vestibulocerebellum.

An open question had been to what extent nucleus lentiformis mesencephali and nucleus of the basal optic root contribute to the optokinetic reaction. From our results we concluded that the contribution of nucleus of the basal optic root was insignificant or not existing. In another experiment we found that the performance of mechanism controlling the optokinetic reaction depends on illumination in a way that indicates the function of photoreceptors to be the only limiting factor for optokinetic reactions.

We then focused on the processing of optic flow in an object motion processing area, the nucleus rotundus of the tectofugal visual system. We presented anaesthetized zebra finches visual motion stimuli on a panoramic LED display during multi-unit recordings.

Due to previous results from other groups working on pigeons, areas of the tectofugal visual system were assumed to respond only to small objects but be inhibited by global motion. In our study, however, rotundal neurons responded to such stimuli with a significant increase in spike rate. We even found neurons preferring either motion patterns of virtual self-translation or such of virtual self-rotation. We concluded that the novel stimuli that provided optic flow including depth information and a panoramic stimulation allowed us to find previously unknown response properties.

In a further step towards more realistic motion stimuli we presented a virtual flight in the perspective of the bird. This was constructed from data acquired by our previous behavioral study.

We found neurons responding to objects in the visual scene of the naturalistic stimulus. One neuron signaled precisely when the obstacle appeared within its receptive field. Since the receptive field was located in the lateral part of the visual field, the neuron signaled that the object was being passed. Two other neurons produced peaks in spike rate when an object was located in heading direction. In other words, these neurons signaled the approach towards an object.

Our data indicates some parallels to the research conducted on the blowfly. Approach signaling neurons were found to prefer rotationally induced optic flow in the previously described test. In the blowfly, a neuron assumed to code for horizontal rotational self motion (yaw turns) was found to signal the spatial relation between the fly and the walls in a naturalistic replay experiment. In both animals the visual motion induced by saccadic gaze shifts did not elicit a response as it would have been expected if the neuron’s purpose was to signal rotational self motion.

Taken together, we were able to demonstrate new response properties in single neurons which could not be predicted by the response to more conventional stimuli like it was also shown for the blowfly. Realistic stimuli allowed us a new perspective on the function of motion selective neurons.

# - Chapter II -

## Disquisition

Dennis Eckmeier



## Introduction

To prevent injury, a moving animal needs to detect objects in its environment and determine whether there is a risk of collision. Birds move with high velocity when flying and are therefore especially depending on a fast and reliable mechanism to achieve obstacle avoidance.

The most commonly known mechanism for three-dimensional vision, stereopsis, does not function in birds very well. For stereopsis, two images that are simultaneously perceived by the two eyes are being compared. The quality of depth information in this case depends on the difference between the two pictures and the size of the area in the visual scene that is viewed by both eyes and can be compared. Most birds have relatively small heads. The eyes therefore usually are located very closely, so that the angles between the eyes and a perceived object do not differ very much. In consequence, the parts of the two perceived images that are to be compared do not differ much, too. Further, most birds have lateral eyes which leads to a very small area of overlap in the images of both eyes and makes it impossible to converge the lines of sight in one point (figure 1). These constraints limit the ran-

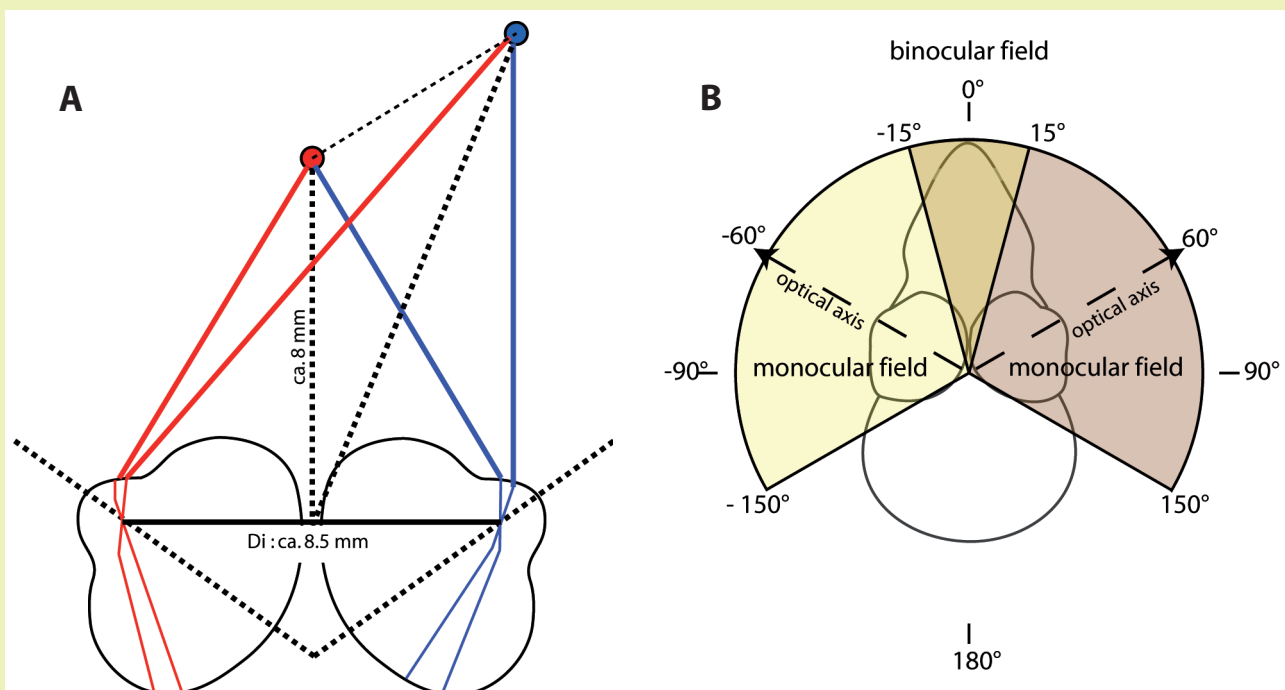


**figure 1 - In birds with lateral eyes, anatomical properties of the skull are malicious for stereoptical depth perception.**

A indicates the function of stereopsis (adapted for the zebra finch, original from McFadden, 1993). Both eyes need to view the same objects to determine the distance between them. The interocular distance is depicted for the zebra finch (8.5 mm, DE). The optical axes deviate from the center of the visual field by  $60^\circ$  (Bischof, 1988). B depicts the properties of the visual field. The optical axes (dashed lines with arrows) deviate from the center ( $0^\circ$ ) by  $60^\circ$ . The visual field extends from  $-15^\circ$  to  $150^\circ$  for the right eye or  $15^\circ$  to  $-150^\circ$  for the left eye, respectively. The binocular field therefore lies between  $-15^\circ$  and  $15^\circ$  and is  $30^\circ$  wide. In the rear there is a  $60^\circ$ -wide gap where the bird can not see (illustration adapted from Bischof, 1988).

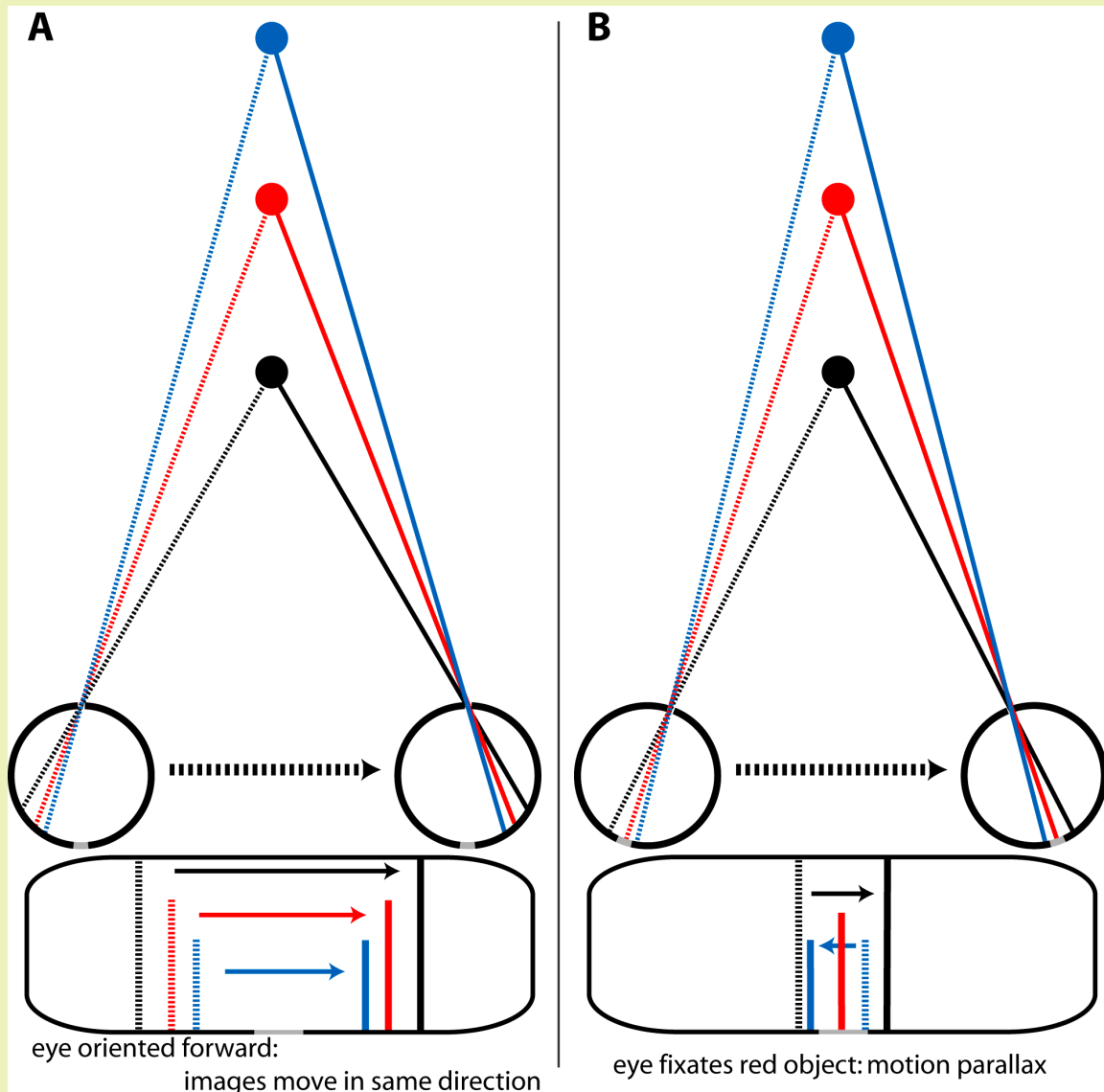


**figure 2 - Depth estimation from image velocities.**

In the upper part, three objects (blue, red and black filled circles) are observed by the same eye from two consecutive positions during translational self motion (from left to right, indicated by broad dashed arrow). The lens of the eye is indicated by a gap in the circle illustrating the eye ball. A grey area in the circle indicates a fovea. Lines indicate the projection of the objects to the retina. dashed lines correlate with first eye position, solid lines correlate with second eye position. In the lower part the motion of the images on the retina is indicated. Colors correlated to object colors, dashed lines indicate first position, solid lines indicate second position. Arrows indicate direction and approximate velocity of image displacement. A: When the eye does not change in orientation, all images move in the same direction but with different velocities depending on the distance between eye and object. B: The eye fixates the red object during translational self motion. The image of the fixated object does not move on the retina, since the eye rotates to keep it in the foveal area. Retinal images of objects in front and behind the fixated object move in opposite directions, velocities depend on the distance of the object to the eye (motion parallax). One may define the situation in A as motion parallax with the 'fixated' depth plane lying in infinite distance.

## Chapter II : Disquisition

ge of sight to which stereoscopic vision can be used for depth perception (Martin, 2007; McFadden, 1993). For pigeons, behavioral tests revealed that the efficient range in which they could be trained to use stereoscopic clues was limited to 5 to 19 cm (McFadden, 1993). This would already be too short for fast flying birds to avoid objects on collision course. From considerations of anatomical properties, our test animal, the zebra finch, is even more constricted in the use of stereopsis since the interocular distance is less than half of that measured in pigeons (ca 8.5 mm, DE; McFadden, 1993).

Birds therefore use another visual source of information to estimate the three-dimensional composition of the environment: the image motion on the retina during self motion (Gibson, 1950). This so called optic flow can be experienced in every day live. An object that is far away looks small because the size of its image on the retina is small. When the observer is close to the same object, its image on the retina is big. In consequence the image of an object expands during approach and contracts when departing. Also, the velocity of expansion or contraction is higher for closer objects than for objects further away. Since this happens for all images of all objects in sight, the image in heading direction expands during straight forward motion and contracts in the opposite direction. The origin of the expanding image in the visual field is called 'focus of expansion' and marks the direction of current heading. Its counterpart is called 'focus of contraction'. From the properties of the optic flow, the visual system can estimate distances to objects in the visual field, such as the heading direction. The velocity of ongoing self motion can be determined by the integration of motion vectors over the whole visual field (Gibson, 1950; Koenderink, 1986).

Another optic flow phenomenon is motion parallax. When looking sideways during translational self motion, e.g. out of the window of a train, one is looking on the transition between the expanding part of the visual flow field and the contracting part. Here, motion vectors are nearly horizontal. When the observer focuses on a defined position in a certain depth plane (humans do this spontaneously), the eyes are automatically moved to keep this position tracked for a moment and then reorient to fixate another point in the flow field very fast. One can observe these eye movements (optokinetic nystagmus) when watching another person who is looking out of a moving vehicle. The effect of this behavior is that the images of objects behind the focused depth plane not only move slower but also in opposite direction than images of objects in front of the depth plane (figure 2). In this case rotational eye movements, which contribute to the overall self motion induced flow in a compensatory fashion, facilitate depth estimation by adding direction of image motion as a further cue (Gibson, 1950).

However, in most cases, distance information can only be processed from the optic flow as long as the overall self motion (locomotion vectors + head motion vectors + eye motion vectors) is translational. During rotational motion, e.g. when rotating on the spot, the images of all objects in the visual scene move from one side to the other in the same velocity. The image motion is not correlated to the distance to the objects. Therefore, optic flow emerging from rotational self motion does not incorporate depth information.

Moving on a curved path combines translational and rotational self motion. In this case the motion vectors emerging from the rotational component of the movement are added to those generated by the translational component. This leads to a disruption of depth cues in the optic flow. Animals known to heavily rely on optic flow for depth estimation therefore evolved locomotion and gaze strategies to separate rotational from translational self motion (Schilstra and van Hateren, 1998, see below).

Usage of optic flow has many advantages since the information can be obtained very fast, but precise gaze control is necessary to acquire depth information from the optic flow.

accessory optic system    tectofugal visual system

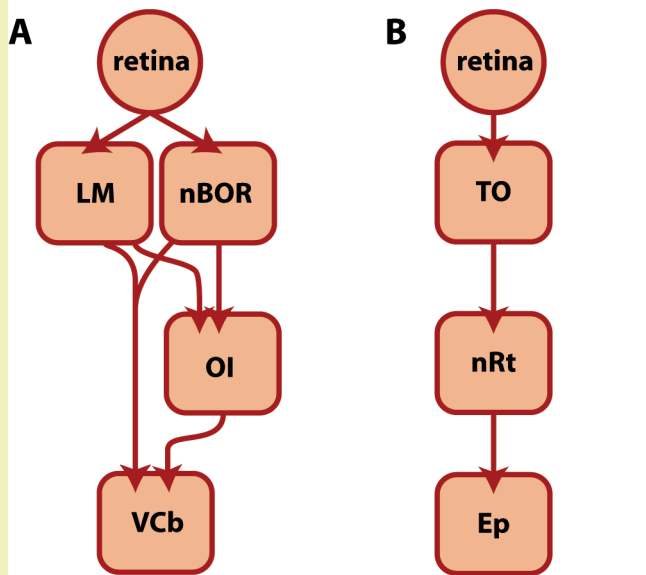


**figure 3 - motion processing pathways in the avian brain.**

A: The accessory optic system receives direct retinal input from displaced retinal ganglion cells which is projected to the nucleus of the basal optic root (nBOR) and nucleus lentiformis mesencephali (LM) of the contralateral hemisphere. It is further transmitted to the vestibulocerebellum (VCb) on the ipsilateral hemisphere either directly or via contralateral inferior olive.

B: The tectofugal visual system receives direct retinal input at the contralateral tectum opticum (TO). Signals are further projected to the thalamic nucleus rotundus (nRt). The Entoplallium (Ep) receives input from the nRt.

## The Impact of Optic Flow on the Behavior of Insects

Direct evidence of birds making use of optic flow parameters in flight is sparse. Insects, on the other hand, serve as good examples to illustrate to which extent optic flow can be used for the control of behavior (Srinivasan and Zhang, 2000). Due to the anatomy of their eyes, insects rely heavily on optic flow. Especially the very small interocular distance is malicious for stereoptic depth perception. The compound eyes are fixed to the head which reduces the degrees of freedom by which the visual input can be optimized by compensatory movements. To solve this problem, insects often need to adjust their whole body movement. In consequence, the impact of optic flow on the behavior of insects is omnipresent.

### Control of Locomotion

Insects control velocity, altitude and path of flight by the optic flow. The according control mechanisms process velocity information in different parts of the visual field (Srinivasan and Zhang, 2000).

To control flight velocity, bees estimate their flight speed by the visual motion velocity and keep it constant. When a honey bee flies in an experimental tunnel with walls textured with a pattern of high spatial frequency the number of contrast changes over time at a given flight speed is high as well. High rates of contrast changes were either interpreted as a high self motion velocity or as flying in a very narrow environment. In such cases, bees tend to fly slowly to reduce the frequency of contrast changes. When over the course of the tunnel the spatial frequency of the texture was reduced, bees accelerated accordingly (Srinivasan et al., 1996; Baird et al., 2005). For the fruit fly similar results had been reported earlier (David, 1982).

In order to fly along the centre line of an experimental tunnel, a honey bee keeps the frequency of contrast changes in the left and right visual field equal. Again the optic flow serves as information source for the distance

to a wall. Because the images of near objects move faster than those of farther objects, a high frequency of contrast changes is interpreted as being close to a wall and a low frequency correlates to being farther away from the wall. In a tunnel of equally textured walls, controlling the position between the walls by keeping the visual input on both sides equal, leads to a well centered flight path. When one of the walls was moved, bees flew closer to the one which produced the lower image velocities (Srinivasan et al., 1991).

For the fruit fly, it has been hypothesized that, in order to fly straight in an open environment, it fixates targets that are visible at the focus of expansion. It shows an alternation of sharp turns and longer straight forward flight when observed in free flight. This behavior is typical for flies and is explained below.

However, straight flight needs to be visually guided. But in a tethered flight paradigm *Drosophila melanogaster* steers away from the point of expansion most likely to avoid a collision. This would usually make straight flight impossible since the focus of expansion emerges from straight flight. Reiser and Dickinson (2010) showed that the expansion-avoidance reaction is inhibited when there is a vertical object in flight direction that can be targeted. Reviewing the literature, the authors further found that in other studies straight flight usually only occurred when there was an edge or object available that would suit as goal. Here, two visual cues for navigation - optic flow and goal directed navigation - form a mechanism for the control of straight locomotion.

For a smooth landing, honey bees approach the surface during forward flight (meaning in a forward and downward pointing vector) and keep the perceived ground velocity constant. By this, they automatically slow down while reducing the distance to the ground which results in zero velocity when touching the ground (Srinivasan et al. 2000).

### Optic Flow Based Navigation

When a foraging honey bee is flying to a location that provides food, it estimates the distance flown by integrating optic flow over travelling time. This is called a visually driven odometer (Esch and Burns, 1995, 1996; Srinivasan et al., 1996, 1997, 2000; Esch et al., 2001; Si et al., 2003).

Similar to the effects found in the locomotion control mechanisms, distance is measured in the count of changes in contrast over time rather than in absolute distance information. In consequence, altering the checkerboard texture of an experimental flight tunnel from low to high spatial frequency leads to an overestimation of flown distance within the tunnel. The honey bees begin the search for a known feeder at a position closer to the entrance. In natural situation a forced detour around an object that induces many contrast changes, has a similar effect (Esch et al., 2001; Tautz et al., 2004).

When a bee reaches the terrain close to a known feeding site, it finds the exact position of a feeder or flower using an 'optic flow snapshot'. The original theory of snapshot matching was that a bee memorizes the exact image of the visual scene at the feeding site – a snapshot of the environment at the correct position (e.g. Cartwright and Collett, 1983). According to Dittmar et al. (2010), this rigid concept would not explain the flight trajectories they found in bees searching for the correct site. Most probably bees do not or not only memorize a static image but an impression of the scene which is based on optic flow amplitudes. This theory is more robust than the image matching approach since it incorporates a three-dimensional representation of landmarks in the vicinity of the goal.

## **Optimizing Visual Input: Active Sensing and Optokinetic Gaze Stabilization**

Two main principles are to be considered when the information content of the visual input has to be enhanced. First, the animal needs to prohibit gaze shifts that interfere with the quality of perception, like blurring effects. Second, gaze has to be actively controlled when peering at an object or memorizing the location of a feeding source. Each solution can be found in animal kingdom to be implemented by sets of behaviors that often are tightly linked to each other. In insects where gaze shifts can not be facilitated by eye movements, the whole body movement may be involved. I want to give two examples of behavior in insects each of which involve both aspects.

A praying mantis uses side-to-side gaze shifts to estimate the distance to its prey. This peering behavior is accomplished by moving the whole body. The animal adjusts translational movements according to the distance to the object. The farther away the object is, the bigger are the side-to-side movements. Translational gaze shift induces an optic flow that gives depth cues. The mantis uses these cues to jump on prey very precisely (Poteser and Kral, 1995).

Bees stabilize the orientation of the head using whole field visual flow. Like mantis, they show whole-body side-to-side movements when peering for example a feeding location, but they do it during flight. To change direction in flight a bee needs to rotate its thorax so that the beating wings produce the according drift. However, the head does not rotate with the thorax but is kept perfectly upright (Boeddeker and Hemmi, 2010). By manipulating large portions of the visual flow, the authors of the according article were able to manipulate the orientation of the head. This demonstrates that the stabilization mechanism that keeps the head upright uses wide field optic flow, which usually is generated by self motion - such as a rolling body. The mechanism induces a counter movement of the head. This stabilizes the gaze and the occurrence of rotational optic flow is avoided. Gaze shifts or gaze stabilization behaviors that are driven by visual motion in this way are called 'optokinetic responses' and have been found in virtually all seeing animals.

Freely flying blowflies evolved a saccadic flight strategy to reduce rotational components in their self motion to short moments. When navigating, a curved flight path would introduce rotational self motion that interfered with the necessity of generating optic flow including depth information. Schilstra and van Hateren (1998) observed that instead of flying on curved paths, the blowfly moves in a straight way for a while and then rapidly changes body orientation before flying off straight in the new direction. The saccadic body turns are accompanied by facilitating head movements. This behavior separates translational and rotational components of self motion in time. Necessary rotations are concentrated to short moments while most of the time translational self motion induces optic flow including cues about the three-dimensional composition of the environment.

## **Behavioral Optimization of the Visual Input in Birds**

### **Behavioral evidence for the Use of Optic Flow Parameters in Free Flight**

As mentioned in the previous section, there is only little direct evidence of birds making use of optic flow parameters in flight. While there are many studies on optokinetic gaze stabilization during walking and electrophysiological evidence for motion processing in anaesthetized birds (see below), only few studies showed that the control of flight maneuvers may be influenced by the retinal flow field.

## Chapter II : Disquisition

The main reason for this lack of data is the size and speed of freely flying birds which limit the feasibility of experiments in the laboratory. On the one hand, birds need relatively large space to perform flight maneuvers compared to that needed by maneuvering insects. On the other hand, a high spatial and temporal resolution is necessary to measure the fast movements of avian flight maneuvers sufficiently accurate. Recording techniques only recently became efficient enough to study such behavior in greater detail. This allows the observation of a relatively large space with high resolution using high speed cameras. However, the few older studies focusing on behavior that can be observed more easily provide a good basis for the study of optic flow usage in birds.

Lee and Reddish (1981) reported that during plummeting, gannets use an optic flow parameter ( $\tau$ ) to stretch their wings back just in time and avoid injury from hitting the water surface. The parameter  $\tau$  stands for the concurrent time to contact during an approach with constant velocity. This parameter can be calculated by the expanding flow field generated during the dive by the reflections on the water surface.

During a dive towards the water surface a gannet, like any other object, constantly accelerates due to gravity. The higher the starting point is over the water surface, the higher is the velocity before contact. Since  $\tau$  stands for the time to collision for a constant velocity, for different diving durations a specific value of  $\tau$  is reached at different times before the water surface is actually reached. The authors calculated this function and called it the ' $\tau$  strategy'. They found the behavioral data to fit the  $\tau$  strategy but not other possible strategies like using the correct time to collision or a specific height to trigger the behavior.

For a landing hawk, Davies and Green (1990) demonstrated that foot extension was also triggered by  $\tau$ . In contrast, pigeons did not use  $\tau$  for foot extension at landing. In a following article, Lee et al. (1993) found that pigeons use  $\tau$  not to trigger foot extension but for the control of flight velocity. By keeping the rate of change in  $\tau$  constant, the pigeon continuously decelerates during approach of a perch. In a fixed absolute distance to the perch the pigeon then extends its feet and grabs the perch.

### Optokinetic Reactions: Compensation of Rotational Movements

A set of visually driven (optokinetic) reactions facilitates the avoidance of optic flow from rotational self motion. In humans the optokinetic nystagmus is a common phenomenon. Between fast gaze corrections, eye movements compensate for the image displacements when the visual scene translates from one side to the other in the visual field - for example when looking out of the window in a moving train. This produces the motion parallax effect. The same eye movements can be observed when the observer turns on the spot.

However, birds do not move their eyes as readily as mammals do. They rather move the head in an optokinetic head nystagmus. The reaction is also called 'optocollic reaction' because it is executed by the neck muscles. Gianni (1988a,b) showed that eye movements make up to only 10-20% of the overall gaze shift while performing such an optokinetic reaction. The advantage of controlling head rather than eye movements to compensate body movements would be to not only stabilize vision but also the vestibular input. Additionally, the neck of birds is very flexible and allows gaze stabilization versus body movements of much higher amplitude than possible by eye rotations (Warrick et al., 2002).

The kinematics of rotational movements can be described as the sum of movements about three perpendicular axes of rotation: yaw, pitch and roll. In a yaw rotation the head or body turns left or right about the vertical axis. A pitch rotation describes the up and down turns about the transverse axis. Roll rotations are turns about the longitudinal axis.

Warrick et al. (2002) stated that birds isolate their heads from body accelerations during flight. The very flexible neck of birds allows the compensation of body turns and up and down body movements occurring in flapping

flight and maneuvers. For example, pigeons keep the head upright during body rolls of over 270°. This was explained by an optokinetic roll reaction.

The most often studied optokinetic reaction was the head nystagmus that compensates yaw rotations (e.g. Bilo and Bilo, 1978; Fite et al., 1979; Gioanni, 1988a,b, Maurice and Gioanni, 2004a,b,2006; Eckmeier and Bischof, 2008; Masseck and Hoffmann, 2009) during the slow phase. This has been tested in the rotating drum paradigm which we used for the study depicted in chapter III (Eckmeier and Bischof, 2008). Here, instead of inducing yaw self motion, the visual scene which consists of the inner walls of a turning drum, is rotated around the tethered bird. The bird's head follows the rotation of the drum in the slow phase of the nystagmus, stabilizing the visual input, and is then rotated back in the fast phase. However, the optokinetic roll reaction has also been studied (Gioanni 1988a; named ,vertical optokinetic nystagmus') in the same way.

### **Head Bobbing: Compensation of Forward Translation?**

Head bobbing is an optokinetic behavior typical for many birds (Dagg, 1977ab; Davies and Green, 1988; Green and Davies, 1994; Necker, 2007). During head bobbing the head moves back and forth in regard to the body while walking or otherwise locomoting slowly. In regard to the visual scene, however, the head does not move backwards. It rather is held stable in space while the body catches up with the head. Thus a head bobbing cycle consists of a ,hold phase' which compensates translational movement and a fast forward movement during ,thrust phase' (first to describe: Dunlap and Mowrer, 1930). Since the kinematics of head bobbing are controlled by optic flow it is assumed that it is an active sensing behavior that optimizes visual input (Friedman, 1975; Frost, 1978; Troje and Frost, 1999; 2000; Cronin, 2005).

What tasks for the processing mechanism demand a visual input like it emerges from head bobbing? Does it make sense to compensate translational self motion? Especially analysis of head bobbing during different modes of locomotion revealed further cues that may lead to an answer.

When walking, the hold phase is discussed to facilitate object recognition by the reduction of motion blur or to enhance the ability to detect moving objects by avoiding additional motion vectors from self motion. This is supported by the results of Pratt (1982) who studied the occurrence of eye movements during head bobbing in chicken. He did not find saccadic eye movements during hold phases but during 80% of thrust phases. An everyday observation also facilitates this idea: when holding a chicken it tries to keep its head completely stabilized regardless of the way and direction its body is moved. In this case the head bobbing cycle would emerge from the necessity to reposition the head regularly during forward locomotion.

But the hold phase is highly dependent on locomotion velocity. The faster the bird moves – regardless of the mode of locomotion – the shorter are the hold phases. Additionally, if a certain threshold velocity is reached, the head is not completely stabilized anymore but keeps moving forward slowly. At even faster velocities, the duration of the hold phase is reduced until no head bobbing can be observed anymore (Davies and Green, 1988; Cronin et al., 2005).

On the other hand, the thrust phase may generate translational motion used to estimate the distance to objects in the lateral visual field. It was shown that head bobbing often occurs when the bird is foraging on the ground (Cronin et al., 2005). Pigeons show head bobbing when peering at a perch they are about to target (Green et al., 1994). It was also shown that pigeons are able to discriminate objects during the thrust phase (Jiménez Ortega et al., 2009) which in parts contradicts the idea of a hold phase being necessary for object detection. The question about the actual function of head bobbing is therefore still open.

### Central Processing of Visual Motion Information in the Avian Brain

#### Self Motion Processing in the Accessory Optic System

To control optokinetic reactions, the ongoing self motion needs to be carefully monitored. Self motion is associated with whole-field motion. The processing of whole-field motion in the avian brain is accomplished by the accessory optic system.

The accessory optic system provides a bottom-up processing pathway in the avian visual system (figure 3A). Displaced retinal ganglion cells project to the nucleus of the basal optic root and the nucleus lentiformis mesencephali; Karten et al. 1977; Fite et al., 1981; Wöhrn et al., 1998; Mey and Thanos, 2000). From here, information is further transferred to the ocular motor complex and vestibulocerebellum via the inferior olive (Brauth, 1977; Brecha and Karten, 1979; Giovanni et al. 1983a, b; Simpson, 1984).

Already in the retina selectivity for motion direction is found (e.g. Borg-Graham, 2001). So called starburst amacrine cells integrate the input of the photoreceptors in their vicinity. These neurons respond selectively for one direction and project to direction selective retinal ganglion cells (e.g. He and Masland, 1997). Whether these include the displaced retinal ganglion cells that project into the accessory optic system is unknown. It is also unknown whether the displaced retinal ganglion cells show direction selectivity.

However, studies on the distribution of displaced retinal ganglion cells revealed a mosaic of exceptional high regularity. While analysis of the distribution of single displaced retinal ganglion cells did not reveal a conclusive regularity, Deplano and Pedemonte (2001) found that these cells clustered in groups of 3-4. Taking into account the clusters gave rise to an exceptional degree of order in the distribution of displaced ganglion cells throughout the entire retina. This would facilitate precise estimation of self motion direction.

Nucleus lentiformis mesencephali and nucleus of the basal optic root both code for self motion. Most neurons in the two nuclei at the first stage of the accessory optic system have large receptive fields and are selective for large flow fields. They respond selectively to visual motion as it emerges from different directions of self-motion (Wylie and Frost, 1999; Wylie, 2000). Being spontaneously active these neurons show an increase in spike rate when stimulated with a grating moving in a preferred direction and a decrease in activity when stimulated in anti-preferred direction. These neurons could further be categorized by their preference for either high ('fast' neurons) or low temporal frequencies ('slow' neurons).

The two nuclei mainly differ in self motion direction preference of the fast neurons. While in nucleus lentiformis mesencephali neurons preferring a high spatial frequency almost exclusively responded to gratings moving from temporal to nasal, fast neurons in nucleus of the basal optic root responded to upwards and downwards moving gratings as well as to nasal to temporal moving ones.

Iwaniuk and Wylie (2007) found that the nucleus lentiformis mesencephali is hypertrophied in birds capable of hovering and backward flight. Since nucleus lentiformis mesencephali incorporates cells with a preference for temporal-to-nasal optic flow, this might reflect the increased necessity to use optic flow from backwards self-motion for position- and maneuver-control in those birds.

However, nucleus of the basal optic root and nucleus lentiformis mesencephali do not function independently. A massive projection from nucleus of the basal optic root to nucleus lentiformis mesencephali was found. In a study in which nucleus of the basal optic root was blocked Crowder et al. (2003) found an effect on the direction preference and related response properties of neurons in nucleus lentiformis mesencephali. Also, blockade of

nucleus lentiformis mesencephali lead to an altered direction selectivity tuning in more than 80% of neurons recorded in nucleus of the basal optic root (Wang et al., 2001).

In the medial column of the inferior olive, the next step in the accessory optic system, Winship and Wylie (2001) found neurons selective for rotational and translational self-motion along or around certain axes. The receptive fields of these neurons are panoramic, spanning the binocular visual field. Winship and Wylie (2001) assume that both, the selectivity and the size of receptive fields are based on the properties of nucleus lentiformis mesencephali and nucleus of the basal optic root.

The accessory optic system information re-crosses to the other hemisphere when the signal is transduced to the vestibulocerebellum. This input originates from nucleus lentiformis mesencephali, nucleus of the basal optic root and the medial column of the inferior olive (Wylie et al., 1999, Pakan et al., 2005, 2006; Pakan and Wylie, 2006; Wylie et al., 2007). Neurons responsive for translational and rotational self motion prefer the same directions as those in contralateral inferior olive (Winship and Wylie, 2001).

### **Object Motion Processing in the Tectofugal Visual System**

To detect objects in the visual scene the brain needs to find local discontinuities in the optic flow. Local motion occurs when the image of an object moves within the scene. Immobile objects herein produce motion vectors that are part of the whole field visual flow generated by self motion. Moving objects produce local flow fields where object motion generated vectors are added to self motion generated vectors. Therefore a visual system associates the occurrence of local motion with objects (Frost et al., 1990a).

This is processed in the tectofugal visual pathway. Retinal information is projected to the optic tectum and further to the nucleus rotundus and then the entopallium (figure 3B).

Apart from cells responsive to other object related information, subgroups of the neurons at all stations of this system show selectivity to ‚looming‘ stimuli that is expanding objects. Expansion is usually correlated with approach. These neurons are also assumed to process the time to collision with an obstacle (Frost et al., 1990a; Wang and Frost, 1992; Sun and Frost, 1998; Wu et al., 2005; Xiao et al., 2006).

The tectum opticum is an anatomically pronounced area in avian brains which has a layered architecture and a retinotopic presentation of the visual scene (Hamdi and Whitteridge, 1954; Frost et al., 1990b; Keary et al., 2010). Motion sensitive neurons are selective for small stimuli moving at moderate velocities in a preferred direction. The tuning for directions is rather broad (Jassik-Gerschenfeld and Guichard, 1972; Frost and DiFranco, 1976). When a background moves in the same direction, the response is inhibited and it is excited when object and background move in opposite directions (Frost and Nakayama, 1983).

When the information has been transferred to nucleus rotundus, the retinotopic representation is no longer detectable. Different properties of objects, such as color, luminance and of course motion, are represented in different subdivisions (Nixdorf and Bischof, 1982; Wang et al., 1993). Motion specific neurons were either excited or inhibited by small objects in a wide receptive field (approximately 100° diameter). Excited neurons had a low spontaneous activity while in inhibited neurons spontaneous activity was high (Wang et al., 1993).

The entopallium is the first station receiving information from the thalamic nucleus rotundus. Here, direction selective neurons and looming selective neurons have also been shown (Frost et al., 1990; Bischof and Watanabe, 1997; Sun and Frost, 1998; Gu et al., 2002). The different categories of motion sensitive neurons are being found in different subdivisions of the entopallium, indicating that the parallel processing seen in n. rotundus is preserved also at the telencephalon (Nixdorf and Bischof, 1982).

### Integration of Self-Motion Information into Object Motion Processing

All studies on the tectofugal system that deal with motion processing and tested background or whole-field motion so far reported that these types of stimuli did not lead to excitatory responses (Frost et al., 1990; Wang et al., 1993). On the other hand, it has been reported that background motion modulates the response to object motion (Frost et al., 1990; Wang et al., 2000; Xiao and Frost, 2009). A background moving in the same direction as the object inhibits the response to it. A background moving in the opposite direction excites it. Similar findings were made for looming selective neurons.

It has also been shown that the nucleus of the basal optic root projects to the nucleus rotundus (Wang et al., 2000; Diekamp et al., 2001). In context of looming sensitive neurons, these response properties were discussed by Frost and Sun (2004) to function as discriminator between an approaching and a targeted object.

## The Authors Scientific Contribution to...

### ... the Influence of Optic Flow on Gaze Shift in Freely Flying Birds

We found evidence for the use of optic flow in the zebra finch (chapter IV). Zebra finches in free flight control their gaze in a way to optimize the resulting optic flow for a higher information density on depth clues.

We assumed that birds would follow a gaze strategy that separates the translational motion components of the gaze shift from rotational ones, as it was found in the blowfly. Instead of flying in curves, it alternates between straight forward flight and saccadic changes of flight direction. The effect on visual processing is an enhancement of the time where the fly experiences a visual flow field with high information content for depth information, within the intersaccadic intervals. The stream of information is interrupted only for a few milliseconds, while the fly performs a body saccade to change flight direction.

To find such a gaze strategy, we observed curved flights of zebra finches in an obstacle avoidance task. We built a test arena which consisted of a center cage and two outer divisions; one on each side of the center cage. From one outer division the test bird entered the center cage by a window and exited into the other outer division through another window at the opposite wall. We forced the birds into a curved flight by introducing an incomplete wall between entrance and exit which the bird had to circle around in order to get to the exit.

We measured gaze direction by means of head orientation in geocentric coordinates. For the reconstruction of the flight trajectories and head orientations, the obstacle avoidance flights were synchronously video recorded with two high speed cameras (500 frames/s) from perpendicular angles (in front of the cage and above). The beak tip was marked manually in every single frame of all footage. The head yaw orientation was measured by additionally marking the base of the beak in the videos shot from above. From the pixel coordinates in the video frames we calculated the trajectory in "real world" units.

We found that over the main course of all recorded flights the birds held a stable head orientation (not position!) in geocentric coordinates and shifted gaze in 1-3 saccadic head turns. The birds were able to stabilize head orientation, although the body moved along a curved trajectory and performed rotations of high amplitude for steering the head orientation (not position!) was kept constant.

According to our results, zebra finches do make use of the depth information in an expanding optic flow field as it is generated from translational self motion. Due to inertia, birds can not perform body saccades like the blowfly. Instead, the head is moved to compensate for the rotations of the body keeping its orientation in geocentric space unchanged.

An important question in this context addresses the contribution of eye movements to gaze direction. As mentioned above, in this study gaze direction was estimated from the orientation of the head. However, in contrast to blowflies, birds have moveable eyes that may contribute to the overall gaze shift to up to 20% (Gioanni, 1988a, b). Analogues to the combined body and head movement in blowflies, combined head and eye movements may be necessary for an optimally controlled gaze displacement during flight in birds.

This is supported by the finding of Maurice and Gioanni (2004) that in pigeons head and eye movements are synchronized in the rotating drum paradigm in a facilitating rather than a compensating manner. Unpublished data from my work suggests that this also is the case in the zebra finch. The kinematics of the optokinetic nystagmus performed with the eyes by head-fixed zebra finches were similar to those of the optokinetic head nystagmus in head-free birds.

What about eye movements occurring during intersaccadic intervals? Our model animal possesses lateral eyes. This leads to an approximately straight image displacement across large parts of the visual field of each eye. Such a flow field could elicit optokinetic nystagmus in each eye separately. This would be in accordance with the assumption of motion parallax as a fundamental origin of depth information in birds. However, the eyes would be moving front-to-back and forth again synchronously leading to a constantly changing visual field. Voss and Bischof (2009) showed that at least during fixating saccades birds tend to keep their visual field consistent. This dilemma might be solved by having both eyes perform an optokinetic nystagmus according to the visual input of only one eye and alternating the 'leading eye'. However, it would be easier to completely suppress eye movements during intersaccadic intervals and process depth from translational optic flow instead of motion parallax. Since the eye movements during translation could not be observed in our video data this is still an open question that should be addressed in further experiments.

### **... the Control Mechanism for Optokinetic Reactions**

It is suggested that the same mechanism that induces the gaze strategy in free flight also generates the optokinetic reaction in tethered birds. For the visual input to the mechanism that controls the optokinetic head nystagmus we reported evidence regarding the roles of nucleus lentiformis mesencephali and the nucleus of the basal optic root. We also determined the dependency of the control mechanism on the illumination level.

#### **Monocular and Binocular optokinetic head nystagmus**

Motor areas that control optokinetic reactions get self motion information from the accessory optic system. Lesion studies designed to investigate the role of the nucleus of the basal optic root and the nucleus lentiformis mesencephali (first level areas of the accessory optic system) for the control of the optokinetic head nystagmus gained contradictory results. Fite et al. (1979) reported that lesions of the nucleus of the basal optic root had little to no effect on the optokinetic head nystagmus, while Gioanni et al. (1983) found a complementary effect of the nucleus of the basal optic root lesions on optokinetic head nystagmus.

The optokinetic head nystagmus is usually tested in a rotating drum paradigm. Here the bird is tethered head-free in the center of a drum. The walls of the drum are textured with vertical stripes. The drum is then rotated which for the bird results in a horizontal whole field motion like during self rotation. In order to stabilize this

## Chapter II : Disquisition

visual motion the bird turns its head in accordance to the moving wall of the drum in the slow phase of the optokinetic reaction and then turns it back in a fast phase.

When the velocity of the turning drum exceeds a certain threshold the bird stops performing the reaction. This threshold velocity changes under different test conditions and is used to determine the efficacy of an optokinetic reaction.

From studies on the optokinetic head nystagmus under monocular conditions (one eye blindfolded), the monocular asymmetry of the reaction was already known in pigeons. Gioanni (1988; Gioanni et al. 1981) demonstrated that in monocular conditions the optokinetic head nystagmus can be evoked at high rotational velocities when the visual motion induced by the drum ran from temporal to nasal. When the drum turned in opposite direction (nasal to temporal), the performance was weaker.

With regard to horizontal visual motion, nucleus lentiformis mesencephali codes for temporal to nasal visual movement and the nucleus of the basal optic root codes for motion in the opposite direction. Since in monocular condition temporal to nasal motion evokes higher performance, this is in favor of the findings from Fite (1979) who state that the nucleus lentiformis mesencephali provides sufficient input for the optokinetic head nystagmus.

We assumed that a complementary effect of nucleus of the basal optic root as found by Gioanni (1983) would be due to activity of nucleus of the basal optic root in the hemisphere contralateral to according nucleus lentiformis mesencephali. For example, when the drum rotated clockwise, the visual scene would move from temporal to nasal in front of the left eye activating nucleus lentiformis mesencephali in the right hemisphere. In front of the right eye the visual scene would move from temporal to nasal activating nucleus of the basal optic root of the right hemisphere.

We hypothesized that if the eye that activates nucleus of the basal optic root gets occluded, nucleus lentiformis mesencephali would still drive the optokinetic head nystagmus. But if nucleus of the basal optic root had a complementary effect, the performance for optokinetic head nystagmus would be decreased in comparison to binocular condition.

This was tested in zebra finches in the rotating drum paradigm for monocular and binocular condition and clockwise and counter-clockwise rotation of the drum.

The results of this test showed that the monocular asymmetry of the optokinetic head nystagmus can be found in zebra finches. Like in the pigeon, the performance during monocular temporal to nasal stimulation was higher than during monocular nasal to temporal stimulation.

The performance during temporal to nasal stimulation did not differ from binocular performance so that our behavioral data do not confirm an influence of nucleus of the basal optic root on optokinetic head nystagmus, at least not for the contralateral nucleus of the basal optic root. The finding of Gioanni et al. (1983b) that nucleus of the basal optic root had an influence on optokinetic nystagmus may be due to the effect of the strong reciprocal connections between nucleus of the basal optic root and nucleus lentiformis mesencephali that influence tuning and receptive fields of motion selective neurons in both areas.

## Dependence of the optokinetic head nystagmus on Illumination

When one changes the illumination levels in the rotating drum paradigm, the contrast between the black and white vertical stripes of the texture of the walls is also changed.

To test how these changes influence the performance of optokinetic head nystagmus we tested zebra finches in the rotating drum. The illumination was preset to a certain illumination level (between 1 and 200 lx). Then the drum was accelerated in darkness. Finally the light was turned on and the occurrence of an optokinetic head nystagmus was observed. This was repeated for different illumination levels.

We found that the performance of optokinetic head nystagmus increased in a logarithmical fashion with increasing illumination. This indicates that it follows Fechner's law which describes the function of photoreceptors.

Since we did not reach the plateau which Fechner's law predicts under lab illumination levels, we measured the average optokinetic head nystagmus performance in daylight which was about 5000 to 11000 lx. The highest performance we found under artificial light conditions was already close to the performance during daylight. From regression analysis of the results from the artificial light condition we approximated the illumination at which the performance would have reached daylight performance between 240 and 290 lx. The maximum drum speed that evoked optokinetic head nystagmus was at  $349^\circ/\text{s} \pm 67^\circ/\text{s}$  in daylight condition.

## ... Motion Processing in the Tectofugal Visual System of the Zebra Finch

The main motivation for my most recent study (Eckmeier et al., submitted; chapter V) was to find motion sensitive neurons responsive to discontinuities in realistic optic flow that are related to objects. Since object motion is processed in the tectofugal visual system we chose to conduct multi-unit recordings in the nucleus rotundus of anaesthetized zebra finches. Nucleus rotundus provides a topographic representation of object features rather than a retinotopic representation which makes it a more promising target than the optic tectum.

We hypothesized that neurons confronted with realistic optic flow revealed response properties that were more conclusive about the actual function of these neurons than those found with more simplified stimuli. Especially naturalistic stimuli would provide an optic flow optimized for depth perception by natural gaze control.

We developed a set of experimenter-controlled stimuli to characterize the response properties in a conventional way before comparing the results to those from naturalistic experiments. These stimuli included global motion stimuli resembling the optic flow experienced during self motion, as well as a quick scan for the size and position of the receptive field and other stimuli.

For the naturalistic replay experiment we used a reconstructed real flight in the bird's perspective. The original flight was recorded in our previous behavioral study on the gaze strategy during free flight (Eckmeier et al., 2008; chapter IV).

We found two groups of rotundal motion sensitive neurons regarding response latency. Similar results were found in an earlier study on the zebra finch (Schmidt and Bischof, 2001) as well as studies on the pigeon (Folta et al., 2004, 2007).

## Chapter II : Disquisition

In these earlier studies the cause for the differences in response latency was assumed to be correlated with the origin of the visual input. Early responding neurons received input from the contralateral eye while late responding neurons received input from the ipsilateral eye. Folta et al. (2004, 2007) stated that input from the ipsilateral eye was mediated via a top-down pathway while contralateral input would reach nucleus rotundus in a bottom-up pathway. The difference in response latency would thus be caused by the longer transmission path for ipsilateral input.

The idea of a longer transmission path for ipsilateral input to cause one group of neurons to respond later does not seem to hold true in our experiment. We found neurons with receptive fields in the area covered by the contralateral eye as well as neurons with a binocular receptive field. However, early and late responding neurons possessed binocular receptive fields. Thus, binocular input seems to reach some neurons of nucleus rotundus via a shorter pathway than assumed by Folta et al. (2004), possibly via the direct inter-hemispherical rotundo-rotundal connection.

The influence of global motion on the response of rotundal motion selective neurons was confirmed in a surprising way. Previous work from other laboratories indicated, that background motion had an effect on the processing of the motion of objects (Wang et al., 2000; Diekamp et al., 2001; Xiao and Frost, 2009). Pure background motion, however, was shown to inhibit neuronal activity (Frost et al., 1990). It was therefore assumed that motion selective neurons in nucleus rotundus as well as other areas of the tectofugal visual system would not respond to global flow fields like they are perceived during self motion.

Here we could demonstrate that neurons in nucleus rotundus respond to pure self motion resembling flow fields. The reason for this would be that we used a panoramic presentation of motion and included depth cues. Conventional tests showed an object in front of a plane background (e.g. Frost et al., 1990; Diekamp et al., 2001; Xiao and Frost, 2009). The background in our stimulus consisted of many objects distributed over a depth continuum, surrounding the bird. Thus, our stimulus was built to be more complex and show more realistic motion patterns. We conclude that this causes the different response properties found in our data.

The next step was the naturalistic replay of a flight during which an obstacle was avoided. Neurons did not respond as was expected from our own conventional motion stimuli. Two neurons we found to respond selectively to rotational self motion signaled the approach towards an object in the naturalistic condition. Also, the response to objects being approached did not show similarities to the response to looming objects in the receptive field. A neuron with lateral receptive field did not show any specific response properties in the conventional experiments. However, it precisely signaled the moment at which the obstacle moved through the receptive field.

These results demonstrate that response properties of single neurons in the tectofugal visual system differ largely between stimuli of different degrees of complexity. The additional perspective enhances the way in which the actual function of these neurons can be studied.

The response properties of neurons responding to discontinuities in the optic flow caused by single objects are reminiscent of findings in the blowfly. A decrease of response activity during stimulation with changing global motion stimuli was shown in our study. Results from the blowfly, which were acquired using a naturalistic replay hint towards a similar direction (Liang et al., 2008). There, motion sensitive neurons adapted to global motion. In the adapted state the base line of the membrane potential due to background motion was lower than in the non-adapted state. A novel object that evoked the same activation levels in both states was thus responded to with a clearer signal in the adapted state. In our study, the response to the naturalistic stimuli shows a high spike rate at the beginning that decreases over the course of the stimulus. Both objects, obstacle and window, evoked similar spike rates. However, due to the lower base line at the end of the stimulus and the bigger difference between baseline

and peak activity, the response to the later appearing window is a clearer signal than that to the early appearing obstacle (chapter V).

Neurons that signal the three-dimensional structure of the environment from optic flow discontinuities in the blowfly and in the zebra finch, share common properties. The two neurons signaling approach found in the zebra finch responded with a preference for horizontal rotational self-motion (yaw rotation). The responses to objects were obscured by slow head turns while fast head turns did not have an effect on the response. This is similar to the situation in the blowfly. Kern et al. (2005) showed that the motion dynamics generated by the saccadic gaze strategy of the blowfly lead to a representation of the spatial relation of a fly to its surroundings during intersaccadic intervals. They also found that these responses showed a clearer signal when residual body yaw rotations were compensated during intersaccadic intervals by stabilizing head movements (Kern et al., 2006). From studies that used conventional stimuli, the neuron they recorded (HSE; a neuron responsive to horizontal motion) were previously thought to signal self-rotation. The neurons also did not reliably signal saccadic gaze shifts as would have been expected for a self-rotation coding neuron. It seems that the velocity tuning of these neurons does not fit a representation of self-motion. Instead they signal behavioral relevant discontinuities within the optic flow during translational self motion (Kern et al., 2006).

## References

- Baird, E., Srinivasan, M. V., Zhang, S. and Cowling, A. (2005). Visual control of flight speed in honeybees. *J Exp Biol* 208, 3895-3905.
- Bilo, D. and Bilo, A. (1978). Wind Stimuli Control Vestibular And Optokinetic Reflexes In Pigeon. *Naturwissenschaften* 65, 161-162.
- Bischof, H. J. and Watanabe, S. (1997). On the structure and function of the tectofugal visual pathway in laterally eyed birds. *Eur J Morph* 35, 246-254.
- Boeddeker, N. and Hemmi, J. M. (2010). Visual gaze control during peering flight manoeuvres in honeybees. *Proc Biol Sci* 277, 1209-1217.
- Borg-Graham, L. J. (2001). The computation of directional selectivity in the retina occurs presynaptic to the ganglion cell. *Nat Neurosci* 4, 176-183.
- Brauth, S. E. (1977). Direct accessory optic projections to the vestibulo-cerebellum: a possible channel for oculomotor control systems. *Exp Brain Res* 28, 73-84.
- Brecha, N. and Karten, H. J. (1979). Accessory optic projections upon oculomotor nuclei and vestibulo-cerebellum. *Science* 203, 913-916.
- Burns, S. and Wallman, J. (1981). Relation of single unit properties to the oculomotor function of the nucleus of the basal optic root (accessory optic system) in chickens. *Exp Brain Res* 42, 171-180.
- Cartwright, B. A. and Collett, T. S. (1983). Landmark Learning In Bees - Experiments And Models. *J Comp Physiol* 151, 521-543.
- Cronin, T. W., Kinloch, M. R. and Olsen, G. H. (2005). Head-bobbing behavior in foraging whooping cranes favors visual fixation. *Curr Biol* 15, R243-244.
- Crowder, N. A., Lehmann, H., Parent, M. B. and Wylie, D. R. (2003). The accessory optic system contributes to the spatio-temporal tuning of motion-sensitive pretectal neurons. *J Neurophysiol* 90, 1140-1151.

## Chapter II : Disquisition

- Dagg, A. I. (1977). **Running, walking and jumping: the science of locomotion** / Anne Innis Dagg. London: Wykeham Publications.
- Dagg, A. I. (1977). **Walk Of Silver Gull (*Larus-Novaehollandiae*) And Of Other Birds**. J Zoology 182, 529-540.
- David, C. T. (1982). **Compensation for height in the control of groundspeed by *Drosophila* in a new, barber's pole' wind tunnel**. J Comp Physiol A 147, 485-493.
- Davies, M. N. and Green, P. R. (1988). **Head-Bobbing during Walking, Running and Flying: Relative Motion Perception in the Pigeon**. J Exp Biol 138, 71-91.
- Davies, M. N. and Green, P. R. (1990). **Optic flow-field variables trigger landing in hawk but not in pigeons**. Naturwissenschaften 77, 142-144.
- Deplano, S. and Pedemonte, N. (2002). **Spatial organization of displaced ganglion cells in the chick retina**. Vis Neurosci 19, 727-734.
- Diekamp, B., Hellmann, B., Troje, N. F., Wang, S. R. and Gunturkun, O. (2001). **Electrophysiological and anatomical evidence for a direct projection from the nucleus of the basal optic root to the nucleus rotundus in pigeons**. Neurosci Lett 305, 103-106.
- Dittmar, L., Sturzl, W., Baird, E., Boeddeker, N. and Egelhaaf, M. (2010). **Goal seeking in honeybees: matching of optic flow snapshots?** J Exp Biol 213, 2913-2923.
- Dunlap, K. and Mowrer, O. H. (1930). **Head movements and eye functions of birds**. J Comp Psych 11, 99-113.
- Eckmeier, D. and Bischof, H. J. (2008). **The optokinetic response in wild type and white zebra finches**. J Comp Physiol A 194, 871-878.
- Eckmeier, D., Geurten, B. R., Kress, D., Mertes, M., Kern, R., Egelhaaf, M. and Bischof, H. J. (2008). **Gaze strategy in the free flying zebra finch (*Taeniopygia guttata*)**. PLoS ONE 3, e3956.
- Esch, H. and Burns, J. (1996). **Distance estimation by foraging honeybees**. J Exp Biol 199, 155-162.
- Esch, H. E. and Burns, J. E. (1995). **Honeybees Use Optic Flow To Measure The Distance Of A Food Source**. Naturwissenschaften 82, 38-40.
- Esch, H. E., Zhang, S., Srinivasan, M. V. and Tautz, J. (2001). **Honeybee dances communicate distances measured by optic flow**. Nature 411, 581-583.
- Fite, K. V., Brecha, N., Karten, H. J. and Hunt, S. P. (1981). **Displaced ganglion cells and the accessory optic system of pigeon**. J Comp Neurol 195, 279-288.
- Fite, K. V., Reiner, A. and Hunt, S. P. (1979). **Optokinetic nystagmus and the accessory optic system of pigeon and turtle**. Brain Behav Evol 16, 192-202.
- Friedmann, M. B. (1975). **Visual control of head movements during avian locomotion**. nature 255, 67-69.
- Frost, B. J. (1978). **Optokinetic Basis Of Head-Bobbing In Pigeon**. J Exp Biol 74, 187-195.
- Frost, B. J. and DiFranco, D. E. (1976). **Motion characteristics of single units in the pigeon optic tectum**. Vis Res, 16, 1229-1234
- Frost, B. J. and Nakayama, K. (1983). **Single visual neurons code opposing motion independent of direction**. Science, 220, 744-745.

- Frost, B. J. and Sun, H. J. (2004). **The biological basis of time to collision computation.** In: Hecht, H., Savelsbergh, G.J.P. (Eds.), *Theories of Time to Contact: Adv. Psychol.*, Amsterdam, Chapter 2. Elsevier, North Holland, 13-27.
- Frost, B. J., Wise, L. Z., Morgan, B. and Bird, D. (1990). **Retinotopic representation of the bifoveate eye of the kestrel (*Falco sparverius*) on the optic tectum.** *Visual Neuroscience* 5, 231-239
- Frost, B. J., Wylie, D. R. and Wang, Y. C. (1990). **The processing of object and self-motion in the tectofugal and accessory optic pathways of birds.** *Vision Res* 30, 1677-1688.
- Fu, Y. X., Xiao, Q. A., Gao, H. F. and Wang, S. R. (1998). **Stimulus features eliciting visual responses from neurons in the nucleus lentiformis mesencephali in pigeons.** *Vis Neurosci* 15, 1079-1087.
- Gibson, J. J. (1950). **The perception of visual surfaces.** *Am J Psychol* 63, 367-384.
- Gioanni, H. (1988). **Stabilizing Gaze Reflexes In The Pigeon (*Columba-Livia*).1. Horizontal And Vertical Optokinetic Eye (Okn) And Head (Ocr) Reflexes.** *Exp Brain Res* 69, 567-582.
- Gioanni, H. (1988). **Stabilizing Gaze Reflexes In The Pigeon (*Columba-Livia*).2. Vestibulo-Ocular (Vor) And Vestibulo-Collic (Closed-Loop Vcr) Reflexes.** *Exp Brain Res* 69, 583-593.
- Green, P. R., Davies, M. N. O. and Thorpe, P. H. (1994). **Head-Bobbing And Head Orientation During Landing Flights Of Pigeons.** *J Comp Physiol A* 174, 249-256.
- Gu, Y., Wang, Y. and Wang, S. R. (2002). **Visual responses of neurons in the nucleus of the basal optic root to stationary stimuli in pigeons.** *J Neurosci Res* 67, 698-704.
- Hamdi, F. A. and Whitteridge, D. (1954). **The Representation of the Retina on the Optic Tectum of the Pigeon.** *Exp Physiol* 39, 111-119.
- He, S. and Masland, R. H. (1997). **Retinal direction selectivity after targeted laser ablation of starburst amacrine cells.** *Nature* 389, 378-82.
- Iwaniuk, A. N. and Wylie, D. R. (2007). **Neural specialization for hovering in hummingbirds: hypertrophy of the pretectal nucleus Lentiformis mesencephali.** *J Comp Neurol* 500, 211-221.
- Jassik-Gerschenfeld, D. and Guichard, J. (1972). **Visual receptive fields of single cells in the pigeon's optic tectum.** 40, 303-317.
- Jimenez Ortega, L., Stoppa, K., Gunturkun, O. and Troje, N. F. (2009). **Vision during head bobbing: are pigeons capable of shape discrimination during the thrust phase?** *Exp Brain Res* 199, 313-321.
- Karmeier, K., van Hateren, J. H., Kern, R. and Egelhaaf, M. (2006). **Encoding of naturalistic optic flow by a population of blowfly motion-sensitive neurons.** *J Neurophysiol* 96, 1602-1614.
- Karten, J. H., Fite, K. V. and Brecha, N. (1977). **Specific projection of displaced retinal ganglion cells upon the accessory optic system in the pigeon (*Columbia livia*).** *Proc Natl Acad Sci U S A* 74, 1753-1756.
- Keary, N., Voss, J., Lehmann, K., Bischof, H. J. and Lowel, S. (2010). **Optical imaging of retinotopic maps in a small songbird, the zebra finch.** *PLoS One* 5.
- Kern, R., van Hateren, J. H. and Egelhaaf, M. (2006). **Representation of behaviourally relevant information by blowfly motion-sensitive visual interneurons requires precise compensatory head movements.** *J Exp Biol* 209, 1251-1260.

## Chapter II : Disquisition

- Kern, R., van Hateren, J. H., Michaelis, C., Lindemann, J. P. and Egelhaaf, M. (2005). Function of a fly motion-sensitive neuron matches eye movements during free flight. *PLoS Biol* 3, e171.
- Koenderink, J. J. (1986). Optic flow. *Vis Res* 26, 161-179.
- Laverghetta, A. V. and Shimizu, T. (2003). Organization of the ectostriatum based on afferent connections in the zebra finch (*Taeniopygia guttata*). *Brain Res*, 963, 101-112.
- Lee, D. N., Davies, M. N. O., Green, P. R. and Vanderweel, F. R. R. (1993). Visual Control of Velocity of Approach by Pigeons When Landing. *J Exp Biol* 180, 85-104.
- Lee, D. N. and Reddish, P. E. (1981). Plummeting Gannets - A Paradigm Of Ecological Optics. *Nature* 293, 293-294.
- Liang, P., Kern, R. and Egelhaaf, M. (2008). Motion adaptation enhances object-induced neural activity in three-dimensional virtual environment. *J Neurosci* 28, 11328-11332.
- Lindemann, J. P., Kern, R., Michaelis, C., Meyer, P., van Hateren, J. H. and Egelhaaf, M. (2003). FliMax, a novel stimulus device for panoramic and highspeed presentation of behaviourally generated optic flow. *Vision Res* 43, 779-791.
- Martin, G. R. (2007). Visual fields and their functions in birds. *J Ornithol* 148 (Suppl 2), S547-S562.
- Masseck, O. A. and Hoffmann, K. P. (2009). Comparative neurobiology of the optokinetic reflex. *Ann N Y Acad Sci* 1164, 430-439.
- Maurice, M. and Gioanni, H. (2004). Eye-neck coupling during optokinetic responses in head-fixed pigeons (*Columba livia*): Influence of the flying behaviour. *Neuroscience* 125, 521-531.
- Maurice, M. and Gioanni, H. (2004). Role of the cervico-ocular reflex in the „flying“ pigeon: interactions with the optokinetic reflex. *Vis Neurosci* 21, 167-180.
- Maurice, M., Gioanni, H. and Abourachid, A. (2006). Influence of the behavioural context on the optocollic reflex (OCR) in pigeons (*Columba livia*). *J Exp Biol* 209, 292-301.
- McFadden, S. (1993). Constructing the Three-Dimensional Image. In: Zeigler, H.P. und Bischof, H.-J.(eds.): *Vision, Brain and Behavior in Birds*. MIT Press, Cambridge, Mass., London (1993).
- Mey, J. and Thanos, S. (2000). Development of the visual system of the chick. I. Cell differentiation and histogenesis. *Brain Res Rev* 32, 343-379.
- Necker, R. (2007). Head-bobbing of walking birds. *J Comp Physiol A* 193, 1177-1183.
- Nixdorf, B. E. and Bischof, H. J. (1982). Afferent Connections Of The Ectostriatum And Visual Wulst In The Zebra Finch (*Taeniopygia-Guttata-Castanotis-Gould*) - An Hrp Study. *Brain Res* 248, 9-17.
- Pakan, J. M., Krueger, K., Kelcher, E., Cooper, S., Todd, K. G. and Wylie, D. R. (2006). Projections of the nucleus lentiformis mesencephali in pigeons (*Columba livia*): a comparison of the morphology and distribution of neurons with different efferent projections. *J Comp Neurol* 495, 84-99.
- Pakan, J. M., Todd, K. G., Nguyen, A. P., Winship, I. R., Hurd, P. L., Jantzie, L. L. and Wylie, D. R. (2005). Inferior olivary neurons innervate multiple zones of the flocculus in pigeons (*Columba livia*). *J Comp Neurol* 486, 159-168.
- Pakan, J. M. and Wylie, D. R. (2006). Two optic flow pathways from the pretectal nucleus lentiformis mesencephali to the cerebellum in pigeons (*Columba livia*). *J Comp Neurol* 499, 732-744.

- Poteser, M. and Kral, K. (1995). The significance of head movements in distance discrimination in praying mantis larvae. *J Exp Biol* 198, 2127-2137.
- Pratt, D. W. (1982). Saccadic eye movements are coordinated with head movements in walking chickens. *J Exp Biol* 97, 217-223.
- Reiser, M. B. and Dickinson, M. H. (2010). *Drosophila* fly straight by fixating objects in the face of expanding optic flow. *J Exp Biol* 213, 1771-1781.
- Schilstra, C. and van Hateren, J. H. (1998). Stabilizing gaze in flying blowflies. *Nature* 395, 654.
- Si, A., Srinivasan, M. V. and Zhang, S. (2003). Honeybee navigation: properties of the visually driven „odometer“. *J Exp Biol* 206, 1265-1273.
- Simpson, J. I. (1984). The accessory optic system. *Annu Rev Neurosci* 7, 13-41.
- Srinivasan, M., Zhang, S. and Bidwell, N. (1997). Visually mediated odometry in honeybees. *J Exp Biol* 200, 2513-2522.
- Srinivasan, M., Zhang, S., Lehrer, M. and Collett, T. (1996). Honeybee navigation en route to the goal: visual flight control and odometry. *J Exp Biol* 199, 237-244.
- Srinivasan, M. V., Lehrer, M., Kirchner, W. H. and Zhang, S. W. (1991). Range perception through apparent image speed in freely flying honeybees. *Vis Neurosci* 6, 519-535.
- Srinivasan, M. V., Zhang, S., Altwein, M. and Tautz, J. (2000). Honeybee navigation: nature and calibration of the „odometer“. *Science* 287, 851-853.
- Srinivasan, M. V. and Zhang, S. W. (2000). Visual navigation in flying insects. *Int Rev Neurobiol* 44, 67-92.
- Srinivasan, M. V., Zhang, S. W., Chahl, J. S., Barth, E. and Venkatesh, S. (2000). How honeybees make grazing landings on flat surfaces. *Biol Cybern* 83, 171-183.
- Sun, H. and Frost, B. J. (1998). Computation of different optical variables of looming objects in pigeon nucleus rotundus neurons. *Nat Neurosci* 1, 296-303.
- Tautz, J., Zhang, S. W., Spaethe, J., Brockmann, A., Si, A. and Srinivasan, M. (2004). Honeybee odometry: Performance in varying natural terrain. *Plos Biology* 2, 915-923.
- Troje, N. F. and Frost, B. J. (1999). Evidence for active vision during the thrust-phase of the pigeon's head-bobbing. Paper presented at the Ninth Annual Meeting of the Canadian Society for Brain, Behaviour and Cognitive Science, Edmonton, Alberta.
- Troje, N. F. and Frost, B. J. (2000). Head-bobbing in pigeons: how stable is the hold phase? *J Exp Biol* 203, 935-940.
- van Hateren, J. H., Kern, R., Schwerdtfeger, G. and Egelhaaf, M. (2005). Function and coding in the blowfly H1 neuron during naturalistic optic flow. *J Neurosci* 25, 4343-4352.
- Voss, J. and Bischof, H. J. (2009). Eye movements of laterally eyed birds are not independent. *J Exp Biol* 212, 1568-1575.
- Wang, Y. and Frost, B. J. (1992). Time to collision is signalled by neurons in the nucleus rotundus of pigeons. *Nature* 356, 236-238.

## Chapter II : Disquisition

- Wang, Y., Gu, Y. and Wang, S. R. (2000). Modulatory effects of the nucleus of the basal optic root on rotundal neurons in pigeons. *Brain Behav Evol* 56, 287-292.
- Wang, Y., Gu, Y. and Wang, S. R. (2001). Directional responses of basal optic neurons are modulated by the nucleus lentiformis mesencephali in pigeons. *Neurosci Lett* 311, 33-36.
- Wang, Y. C., Jiang, S. and Frost, B. J. (1993). Visual processing in pigeon nucleus rotundus: luminance, color, motion, and looming subdivisions. *Vis Neurosci* 10, 21-30.
- Warrick, D. R., Bundle, M. W. and Dial, K. P. (2002). Bird maneuvering flight: Blurred bodies, clear heads. *Integrative And Comparative Biology* 42, 141-148.
- Winship, I. R. and Wylie, D. R. (2001). Responses of neurons in the medial column of the inferior olive in pigeons to translational and rotational optic flowfields. *Exp Brain Res* 141, 63-78.
- Winterson, B. J. and Brauth, S. E. (1985). Direction-Selective Single Units In The Nucleus Lentiformis Mesencephali Of The Pigeon (*Columba-Livia*). *Experimental Brain Research* 60, 215-226.
- Wohrn, J. C., Puellas, L., Nakagawa, S., Takeichi, M. and Redies, C. (1998). Cadherin expression in the retina and retinofugal pathways of the chicken embryo. *J Comp Neurol* 396, 20-38.
- Wu, L. Q., Niu, Y. Q., Yang, J. and Wang, S. R. (2005). Tectal neurons signal impending collision of looming objects in the pigeon. *Eur J Neurosci* 22, 2325-2331.
- Wylie, D. R. (2000). Binocular neurons in the nucleus lentiformis mesencephali in pigeons: responses to translational and rotational optic flowfields. *Neurosci Lett* 291, 9-12.
- Wylie, D. R. and Crowder, N. A. (2000). Spatiotemporal properties of fast and slow neurons in the pretectal nucleus lentiformis mesencephali in pigeons. *J Neurophysiol* 84, 2529-2540.
- Wylie, D. R. and Frost, B. J. (1999). Responses of neurons in the nucleus of the basal optic root to translational and rotational flowfields. *J Neurophysiol* 81, 267-276.
- Wylie, D. R., Lau, K. L., Lu, X., Glover, R. G. and Valsangkar-Smyth, M. (1999). Projections of purkinje cells in the translation and rotation zones of the vestibulocerebellum in pigeon (*Columba livia*). *J Comp Neurol* 413, 480-493.
- Wylie, D. R., Pakan, J. M., Elliott, C. A., Graham, D. J. and Iwaniuk, A. N. (2007). Projections of the nucleus of the basal optic root in pigeons (*Columba livia*): A comparison of the morphology and distribution of neurons with different efferent projections. *Vis Neurosci*, 1-17.
- Xiao, Q. and Frost, B. J. (2009). Looming responses of telencephalic neurons in the pigeon are modulated by optic flow. *Brain Res* 1305, 40-46.
- Xiao, Q., Li, D. P. and Wang, S. R. (2006). Looming-sensitive responses and receptive field organization of telencephalic neurons in the pigeon. *Brain Res Bull* 68, 322-328.



# - Chapter III -

## The Optokinetic Response in Wild Type and White Zebra Finches

Dennis Eckmeier and Hans-Joachim Bischof

### Abstract

Optic flow is a main source of information about self movement and the three-dimensional composition of the environment during locomotion. In mammals and birds the accessory optic system (AOS) processes optic flow. It feeds to several areas that generate different optokinetic driven behaviours such as obstacle avoidance, self motion experience or oculomotor response.

The optokinetic response (OKR) is triggered by rotational optic flow, e.g. in a rotating drum lined with vertical stripes. We investigated here the effect of the rotational component on the optokinetic response (OKR) in white and wild type zebra finches. White birds were investigated because previous studies revealed strong deviations of the wiring of the visual system. However, concerning the OKR there was no difference between colour morphs. Monocular exposure exhibited an asymmetric OKR with a much stronger temporal to nasal component, while the binocularly induced OKR was symmetrical. OKR merging frequency was dependent on the illumination level in agreement with Fechner's law, saturation was reached at about 560 lx. In bright daylight, white birds did not show optokinetic responses. We conclude that the accessory optic system, which is processing optic flow in birds, does not show wiring deviations like other visual areas in white zebra finches. The unwillingness of responding with OKR at bright daylight by white birds may be due to a strong lack of inhibition within the visual system which we have demonstrated in earlier studies and which may enhance the sensibility to glare.

**This chapter has been published:**

**Eckmeier, D. and Bischof, H. J. (2008).** The optokinetic response in wild type and white zebra finches. *J Comp Physiol A Neuroethol Sens Neural Behav Physiol* 194, 871-8.

**additional illustration: Two types (morphs) of zebra finches.**



**above: the wild type zebra finch.**

The typical colors are found. Gender is easily identified by the sexual dimorphism of the feather colors. Males have the typical zebra pattern on their neck and breast as well as brown patches with white dots at their sides and an orange patch on the cheek.

**right: the white morph.**

All feathers are white. The sexual dimorphism in feather color is therefore not visual. Beak and eyes, however, show normal coloration.



**(the content of this box was not included in the original publication)**

## Introduction

Moving around in an unpredictable environment appears to be an easy task, judged from the observation of animals walking or flying in their natural habitat. However, its complexity becomes obvious if one analyses the sensory and motor demands for perfect orientation and manoeuvring skills which can be observed for example in birds. On the motor side, a lot of adaptations like weight reduction, metabolism enhancement and the special construction of the wings are examples for the optimization of the avian body for flight. On the sensory side, it is mainly the visual system which has been optimized for fast processing of sensory information as it is necessary during flight. This paper describes experiments aiming to investigate processing of optic flow by the visual system of birds. Self-motion of the animal induces motion of the visual scene on the retina. This optic flow can be translational or rotational, dependent on whether the motion is straight (forward, backward, up, down) or involves a rotation or turn of the head. Translational optic flow has been shown to be a major sensory cue which the animal can use for navigation. It contains information about the three-dimensional composition of the environment, for example the distance between objects. Most support for this role of optic flow has been obtained with flying insects (rev. Lappe 2000, Kern et al. 2001), but there is also evidence that birds use it for manoeuvring (e. g. Davis and Green, 1990, 1991; Lee and Davis, 1993). Rotational optic flow does not contain such information, and it has been shown that insects avoid contaminating the translational optic flow by concentrating the necessary turns inducing rotational flow to short saccades (Kern et al. 2005).

A similar reaction to rotation, the optokinetic response (OKR), has been observed in all animals examined so far. When a subject is situated inside a rotating drum with vertical stripes, the eye (or head) responds to the optic stimulation by following the movement of the stripes. Traditionally, it has been interpreted as a mechanism which stabilizes an image on the retina for better object identification, but it may also play a role for stabilization of translational optic flow. Among vertebrates, it is a specific characteristic of birds to follow the rotation of a pattern with the head instead of moving only the eyes. It has been demonstrated that the head response in birds is coupled so strongly to the eye response that measurements of both give almost identical results (Gioanni et al, 1988).

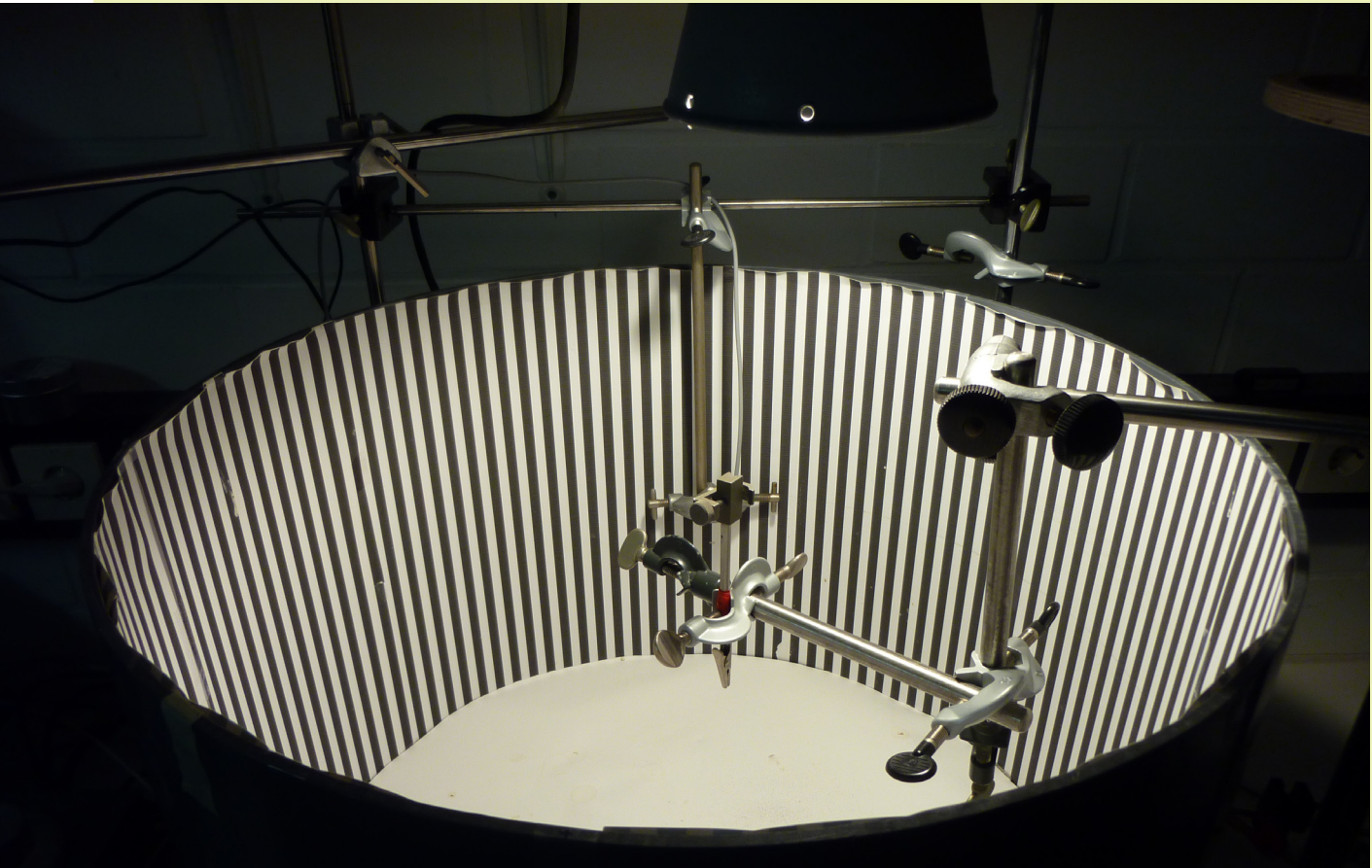
The OKR has been examined to obtain information of the processing capacities of the visual system, for example to measure the visual merging frequency, that is the maximal number of perceivable contrast changes, or the fastest speed detectable by the visual system (Bischof 1988). It has also been used as a diagnostic tool to detect deficits due to genetic or other disorders of the visual system.

In vertebrates, one of the three main visual pathways, the so called accessory optic system (AOS) is specialized for the processing of optic flow. Together with a closely connected pretectal nucleus (n. lentiformis mesencephali) it receives direct retinal input from the displaced ganglion cells, a subpopulation of retinal ganglion cells located outside of the ganglion cell layer. The information from these nuclei is then fed to optokinetic reaction control nuclei (oculomotor nuclear complex and vestibulocerebellum; Gioanni et al. 1983, Brauth and Karten 1977, Brecha and Karten 1978). It also transfers information to brain areas calculating the time to collision of objects approaching on a collision course (e. g. *N. rotundus*, Wang and Frost 1992, Wylie et al. 1997, Diekamp et al., 2001) and controlling self motion (vestibulocerebellum, Brauth and Karten 1977, Wylie et al. 1997, 1998).

All information available for birds as yet stems from research on the pigeon. From the biggest avian group, the passerines, no information is available. We therefore decided to investigate the optokinetic response in the zebra finch, a small songbird from Australia, the visual system of which we have explored over the last 30 years.

Another reason to investigate the OKR was its suitability as a diagnostic tool for the function of the accessory optic system. A number of studies has demonstrated that in albino animals the optokinetic reactions are reduced

## additional illustration: The rotating drum.



### above: the drum.

The drum is illuminated by a light adjustable in illumination. The walls of the drum are lined with vertical stripes. Turning direction can be changed from clockwise to counter clockwise.

### right: zebra finch in the drum.

The test bird is wrapped in cloth. The bird is then attached to a holder in the center of the drum via the cloth. The drum covers most of the visual field. When it is turning the bird therefore begins stabilizing the visual flow by performing the optokinetic nystagmus (see introduction).



(the content of this box was not included in the original publication)

(albino rabbit, Collewijn et al. 1985) or absent (albino ferrets, Hoffmann et al. 2004). Collewijn et al. speculated that the induction of the OKR in rabbits might be due to normally nondecussating fibers from the temporal retina which cause an inversion of the OKR response in the anterior sector of the visual field. Hoffmann et al. were able to show that the deficit was due to changes within the NOT (nucleus of the optic tract) which is the mammalian homologue of the LM (n. lentiformis mesencephali) in birds, and not in motor areas. The mammalian albino visual system differs from that of the normal animal by strongly reduced ipsilaterally projecting retinal ganglion cell fibers. This lack of binocular information within the NOT may be responsible for the OKR deficit (Hoffmann et al. 2004).

The white morph of the zebra finch is a partial albino. In contrast to full albinos, its eye is pigmented and normally structured (Bredenkötter and Bischof 1996). However, it develops strong deviations in the central visual system (Leminski and Bischof 1996). The optic nerve, which is totally crossing in birds, is unaffected, while the recrossing fibers, conveying information of the eye from contralateral visual areas back to the ipsilateral hemisphere, are strongly enhanced. This leads to an enhancement of neuronal responses within the visual brain areas ipsilateral to the stimulated eye (Engelage and Bischof 1988, Bredenkötter and Bischof 1996).

Given these strong physiological changes we proposed that behavioural reactions in white zebra finches may also be altered. The optokinetic nystagmus seemed to be a good first choice to investigate behaviour, because albinism has been shown to induce strong alterations in other albinotic animals (Collewijn et al. 1985, Hoffman et al. 2004). Due to the wiring of the visual system of birds without direct visual input of the ipsilateral eye to the nuclei of the AOS, we expected asymmetries of the OKR for clockwise and counter-clockwise rotation if only one eye could be used. Because the recrossing visual projections are stronger in white zebra finches, we speculated that this asymmetry could be smaller in white animals.

## Material and Methods

Twelve white and twelve wild type zebra finches from the institute's stock were used for the experiments testing the OKR with binocular and monocular viewing. Another six males of each morph were tested in experiments under variable illumination conditions.

The bird was wrapped into a poncho-like piece of cloth with its head free and then attached to a holder by a clamp. It was positioned in the middle of a rotating drum (59 cm inner diameter; 38.5 cm height) facing its walls which were lined with vertical black and white stripes of equal width ( $3.24^\circ$ ). The drum was illuminated from above by a light bulb (200W) which could be regulated at the power supply. The bird's head was monitored by a video camera from above to avoid distractions by direct observation.

The drum was rotated by a small electric motor. Velocities were adjusted by regulating the current supply and measured by a photo sensor monitoring the frequency of black-white transitions passing the point of measurement. For experiments with low illumination, a calibration curve was established in addition to determine the frequency as a function of the applied voltage.

The illumination level was measured in lux [lx] by a hand-held illumination meter positioned within the drum facing the same area of the drum's wall as the bird's head.

To cover an eye for the monocular condition, we used eye caps made from soft plastic foil usually used as table cover. To manufacture these caps, the foil was firmly attached to one side of a plexiglass box which had numerous holes of 6 mm diameter on that side. The box was attached to a vacuum pump by high pressure tubing. By eva-

**figure 1: box-whisker plot: comparison of clockwise and counter-clockwise stimulation.**

Means for each morph (wild type and white) and each eye opened (left and right), there is one mean value for clockwise (CW) and counter-clockwise (CCW) stimulation as indicated by the arrows. Boxes indicate SEM, whiskers SDM.

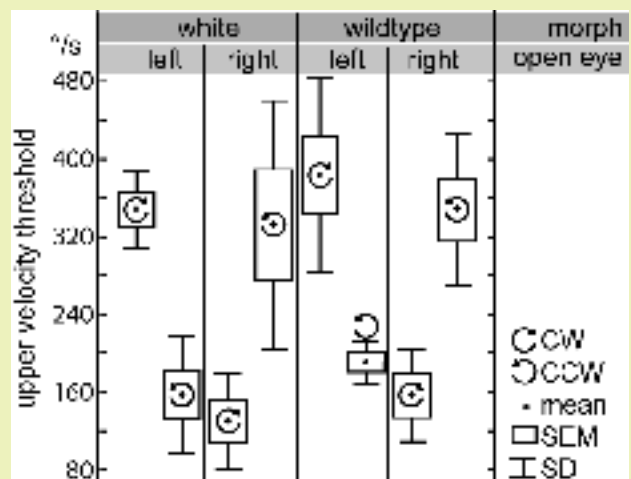
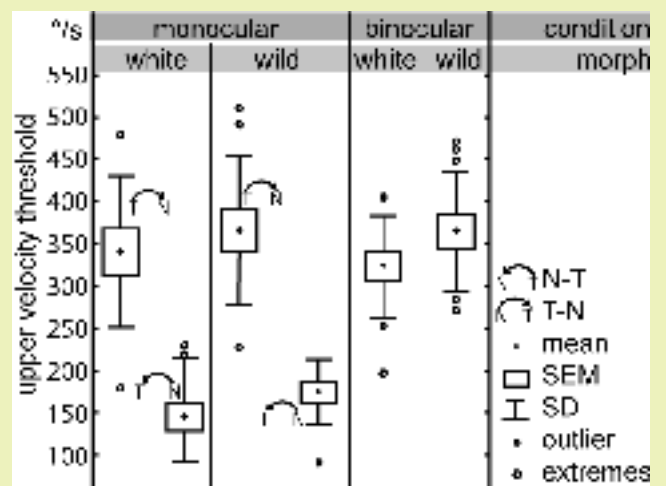


**figure 2: box-whisker plot of results with constant illumination.**

Means for monocular and binocular conditions. Monocular: for each morph (white and wild type) there is the mean visual merging frequency for N-T and that for T-N stimulation. Binocular: the mean visual merging frequency for each morph. Boxes indicate SEM, whiskers SDM.



coating the box with the pump, the plastic foil was pressed onto the holes. The foil was then slightly warmed with a hot fan until it was soft enough to be sucked gently into the holes. With quite a lot of experience, hemispherical plastic caps could be produced, which were glued on the feathers around the eye with a silicone medical adhesive normally used for artificial stomata. The caps could be removed easily after the experiment.

For determination of the effects of monocular and binocular viewing, the illumination was set to the highest level possible. The drum accelerated while the bird was watching. At a certain velocity the bird stopped head movements and the corresponding frequency was recorded.

For experiments with variable light conditions, the lamp was first set to a certain illumination level and then turned off. In darkness the rotation speed of the drum was set. Then the light was turned on again with preset brightness. By this method, the resulting merging frequency could not be contaminated by movements of the bird's head induced by lower speed of the drum before the merging frequency was reached. We measured in steps of 6.4 Hz (0.5 V), starting with 28.6 Hz (5 V). The frequency was registered at which the birds did not respond optokinetically when the light was turned on again.

To examine the merging frequency under daylight the method used in the previous experiment was not applicable. Therefore we accelerated the drum while the birds were able to watch the moving stripes. For a comparison with lower illumination levels, we also measured a threshold curve under increasing light level as we did in the experiment before.

## Results

### Monocular and Binocular OKR

This experiment was run to examine the asymmetry of the OKR if only one eye is open. Because the symmetry of the optokinetic response may depend on the amount of ipsilateral input to the AOS, we presumed that the asymmetry would be smaller in white birds which have enhanced ipsilateral projections. The variable condition for this test was monocular (left or right) and binocular viewing. Individuals were tested ten times during counter-clockwise (ccw) and another ten times during clockwise (cw) rotation of the drum for each condition. The results were statistically analyzed with ANOVA and posthoc Newman-Keuls tests.

#### Wild Type

For wild type animals, measurement of OKR with both eyes open revealed a mean visual merging frequency of 111.5 ( $\pm 8.55$  Hz SEM) for clockwise and 113.6 ( $\pm 9.90$  Hz SEM) for counter-clockwise rotations of the drum (figure 1). There was no significant difference between the two rotation directions (ANOVA;  $F = 0.099$ ,  $P = 0.755$ ). The mean of the both conditions was 112.55 Hz ( $\pm 9.44$  Hz SEM).

Monocular tests revealed a mean visual merging frequency of 118.26 ( $\pm 12.59$  Hz SEM) for an open left eye, when the drum rotated clockwise. In counter-clockwise condition with open left eye the mean visual merging frequency was 58.86 ( $\pm 2.99$  Hz SEM). When the right eye was open, we recorded mean frequencies of 48.2 ( $\pm 7.30$  Hz SEM) for clockwise and 107.42 ( $\pm 9.97$  Hz SEM) for counter-clockwise rotation. There was thus a strong asymmetry of the OKR in tests with monocular viewing (ANOVA,  $F = 37.421$ ,  $p < 0.001$ ). In any case, the temporal to nasal rotations of the drum caused higher merging frequencies compared to the nasotemporal rotation.

Statistical analysis showed no significant difference between an open left eye paired with ccw stimulation and an open right eye paired with cw stimulation (post hoc Newman-Keuls:  $p = 0,713$ ) and vice versa, but significant differences for all complementary pairings ( $p < 0.003$ ). We therefore pooled the results to two classes: temporal to

**figure 3: dependency of the visual merging frequency on illumination levels.**

Acceleration of the drum in the dark (see text) CCW: counter clockwise stimulation; CW: clockwise stimulation; grey squares: wild type zebra finches; black triangles: white zebra finches; grey line: line of best fit for wild type birds during low illumination [CCW:  $R^2 = 0,9842$ ;  $f(x) = 7,8596 \ln(x) + 38,402$  - CW:  $R^2 = 0,991$ ;  $f(x) = 7,7795 \ln(x) + 38,745$ ]; grey line: line of best fit for white birds during low illumination [CCW:  $R^2 = 0,9724$ ;  $f(x) = 7,7825 \ln(x) + 35,151$  - CW:  $R^2 = 0,9931$ ;  $f(x) = 8,5113 \ln(x) + 35,428$ ]. Bars indicate SDM.

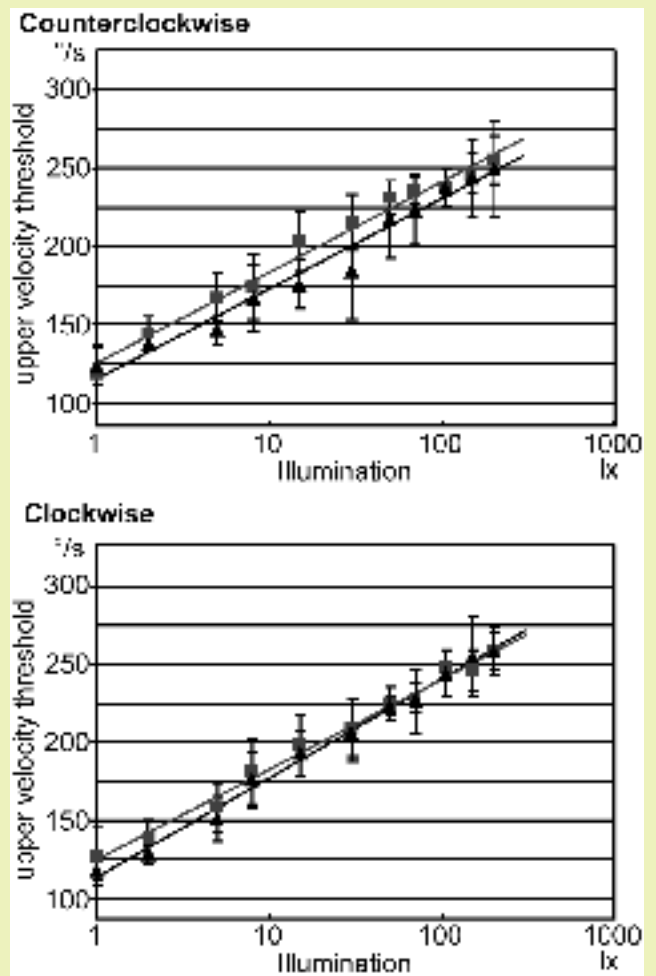
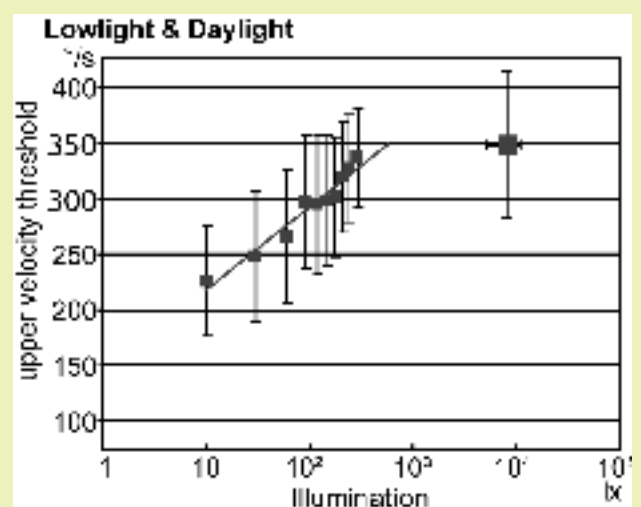


**figure 4: dependency of the visual merging frequency on illumination levels.**

Acceleration of the drum with light on (see text). Small squares: mean visual merging frequency for a given illumination; big square: mean daylight data point; line: line of best fit for low illumination [ $R^2 = 0.9475$ ;  $f(x) = 10.04 \ln(x) + 43,827$ ]. Bars indicate SDM.



nasal (T-N; left eye open with cw rotation and right eye open with ccw rotation) stimulation and nasal to temporal (N-T; left eye open with ccw rotation and right eye open with cw rotation) stimulation. N-T stimulations resulted in significantly lower visual merging frequencies compared to T-N (Anova;  $F = 50.38$ ,  $P < 0.0001$ ).

Comparison of monocular and binocular conditions (figure 2) revealed differences (Anova;  $F = 23.53$ ,  $p < 0.001$ ). While T-N and binocular performances were not different (Newman-Keuls;  $p = 0.975$ ), the OKR induced by N-T stimulation was lower than the binocularly induced ones ( $p < 0.001$ ).

### White Morph

In contrast to our expectations, the results for white birds were very similar to those obtained in the wild type animals (figure 1). The visual merging frequency for OKR with binocular viewing was 97.31 Hz ( $\pm 5.63$  Hz SEM) for clockwise rotation of the drum and 102.22 Hz ( $\pm 9.57$  Hz SEM) for counter-clockwise rotation. The difference was not significant (Anova;  $F = 3,234$ ,  $p = 0.078$ ). The mean of both conditions amounted to 99.76 Hz ( $\pm 9.44$  Hz SEM).

When the left eye was open, the mean visual merging frequency was 48.30 ( $\pm 7.61$  Hz SEM) for counter-clockwise rotation and 107.16 Hz ( $\pm 5.38$  Hz SEM) for the clockwise condition. With the right eye open, we recorded mean visual merging frequencies of 40.31 Hz ( $\pm 6.76$  Hz SEM) for clockwise and 102.78 Hz ( $\pm 17.71$  Hz SEM) for counter-clockwise stimulation.

There were significant differences between the different monocular conditions (Anova;  $F = 11.87$ ,  $p < 0.001$ ). Comparing the results of an open left eye paired with ccw stimulation and an open right eye paired with cw stimulation (Newman-Keuls;  $p = 0.593$ ) and vice versa showed no significant difference ( $p = 0.769$ ). Tests of the reverse conditions showed significant differences ( $p < 0.003$ ). As in the wild type animals, this showed that there was a strong asymmetry in tests with monocular viewing, with higher merging frequencies for the temporal to nasal rotations compared to the nasal to temporal ones. Lumping together the two temporal to nasal and nasal to temporal conditions (figure 2), respectively, revealed that this difference was significant (Anova,  $F = 50.388$ ,  $p < 0.0001$ ). Again, the binocular results were not different from the nasal to temporal condition ( $p = 0.975$ ), but from the T-N results ( $p < 0.001$ ). Comparison of the Morphs

The performances of both morphs for binocularly induced OKR do not differ significantly (Newman-Keuls:  $p = 0.36$ ). The same was found for T-N ( $p = 0.672$ ) and N-T ( $p = 0.310$ ) stimulations in the monocular condition (figure 1 and 2).

### Illumination Level Dependency of OKR

We tested each individual at twelve illumination levels from 1 to 200 lx once per stimulation direction. Figure 3 shows that visual merging frequencies strongly correlated with illumination. There was no difference between white and wild type zebra finches (Anova;  $F = 0.39$ ,  $p = 0.5$ ). In agreement with the results of the experiments to test the influence of the eyes, we found no significant difference between stimulus directions (Anova;  $F = 0.5$ ,  $p = 0.89$ ).

### Daylight

In daylight all wild type, but only one white zebra finch showed optokinetic responses sufficient for data analysis. Each bird was tested three times for each stimulus, the corresponding illumination was measured directly thereafter.

As illumination undergoes fast changes during daylight, we were not able to achieve more than one measurement for a given illumination level. Therefore we calculated the means of the illuminations and of the corresponding visual merging frequencies to obtain one single value (figure 4). Mean daylight illumination was  $8133.5 \pm 2909$  lx, the corresponding merging frequency  $107.38$  Hz  $\pm 20.47$  Hz).

## In short: The avian accessory optic system (AOS).

So-called displaced retinal ganglion cells project to two areas of the accessory optic system: nucleus of the basal optic root (nBOR) and nucleus lentiformis mesencephali (LM). The optic nerve hereby crosses completely to the contralateral hemisphere of the brain. LM and nBOR are characterized by their selectivity for (self motion generated) whole field motion and differ in preferred direction of movement. In context of the rotating drum paradigm, nBOR and LM of the same hemisphere primarily code for opposing directions.

Information about whole field motion direction is further projected to the vestibulocerebellum (VCb) directly and indirectly via the inferior olive. From there it is further transduced to brain areas controlling optokinetic reactions.

From our data we conclude that the main input for the optokinetic response originates from the LM (see discussion).

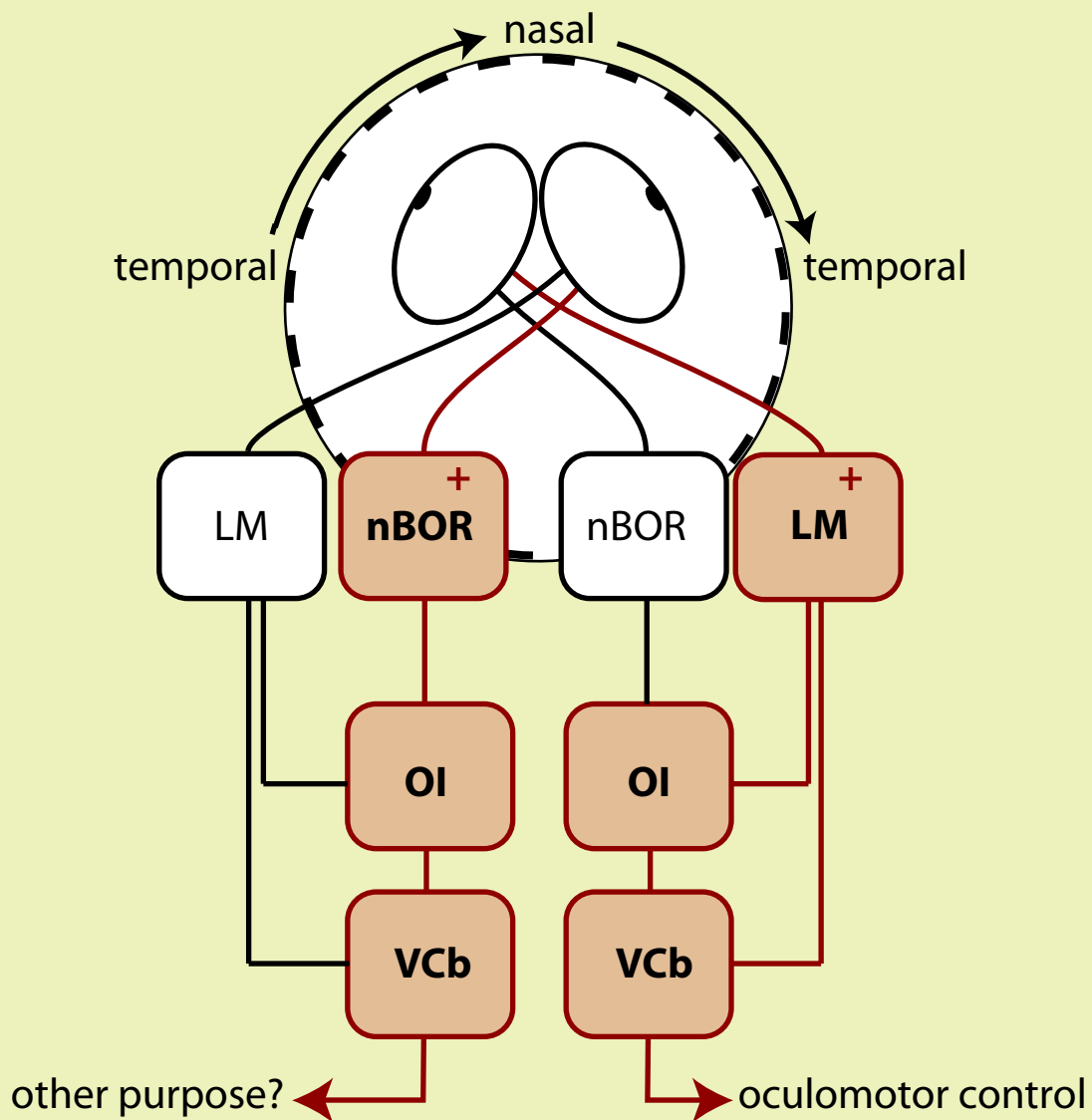


figure: The avian AOS in the rotating drum paradigm.

Dotted circle indicates a drum turning clock wise. Stripes move from temporal to nasal for the left eye and from nasal to temporal for the right eye. In the left hemisphere nBOR is stimulated with preferred direction and consecutive areas are activated. In the right hemisphere LM is elicited by motion in preferred direction, which via following areas finally contributes to optomotor control.

(the content of this box was not included in the original publication)

### Comparison of Low Illumination and Daylight Results

The daylight datapoints fit well to the calculated lines of best fit from the previous mentioned results in low light (figure 3). But considering that the reaction to moving stripes should reach a plateau somewhere at higher illuminations, and because daylight should actually be at the saturation level, this result was not acceptable. So we did another experiment with other birds under low light conditions. In contrast to the previous experiments, the light was not switched off before acceleration of the drum.

The results are shown in figure 4. This experimental variation lead to higher results for the visual merging frequency, which got close to daylight results already at relatively low illumination levels (between 240 and 290 lx). The standard error of the mean became higher, too (SEM between 5.54 and 7.88 Hz when watching the acceleration and between  $\pm 0.54$  and 3.92 Hz when the light was turned off during acceleration).

The calculated line of best fit had a coefficient of determination ( $R^2$ ) of 0.95. According to its equation ( $f(x) = 10.04 \ln(x) + 43.827$ ), we estimated the saturation point to be reached at about 530 to 590 lx, with a corresponding visual merging frequency of about 107 Hz.

## Discussion

Our results concerning the optokinetic response in the zebra finch, a songbird, are comparable to findings in the pigeon (Gioanni, 1981; 1988). Temporal to nasal (T-N) and nasal to temporal (N-T) movements of the stimulus exhibit different results if only one eye is open. A stimulus moving in T-N-direction leads to higher merging frequencies compared to stimulation in N-T direction. Performance during T-N directed stimulation was equal to that achieved with both eyes open.

The information about the rotational optic flow is transferred from the retina to the pretectal nucleus LM (lenticiformis mesencephali) and to nBOR (nucleus of the basal optic root) of the accessory optic system. LM receives additional input from the contralateral nBOR. Both nuclei project to the inferior olive where the input is combined and further transferred to the cerebellum. At least within the cerebellum, information from both hemispheres is combined forming one output controlling the OKR. Neurons of the LM specifically represent the T-N direction of whole field movement with only a few units reacting to other stimulus directions (Wylie and Crowder 2000, Fu et al. 1998, Winterson et al. 1985), indicating that this nucleus is the main processing unit for the OKR. nBOR exhibits responses for all other directions of environmental movements, with the exception of T-N directed ones. nBOR may thus probably modulate the OKR. (Burns and Wallman, 1981; Wylie and Frost, 1999). Gioanni et al. (1983) and Fite et al (1979) described contradictory results concerning such modulation. According to Fite, the nBOR has little to no effect on horizontal OKR, while Gioanni et al. described complementary effect of nBOR compared with LM.

With both eyes open, the stimulus moves in T-N direction for one eye and in N-T direction for the other. In this case, the N-T coding cells in the nBOR might enhance the effect of T-N cells of the contralateral LM on OKR. With one eye covered, this activation of N-T neurons does not occur. If the contralateral nBOR enhances the ipsilateral LM performance, we would therefore expect the performance in monocular experiments with T-N stimulation to be weaker than in binocular experiments. This is not the case, indicating that LM provides the dominant input for OKR control in zebra finches and is not additionally supported by contralateral nBOR input.

### Dependency of OKR on Illumination Levels

Because we did not find significant differences between white and wild type zebra finches in the previous experiments, we also investigated whether there were differences concerning the dependency of the OKR on the

illumination level. There were, however, again no significant differences between the colour morphs. When the light was turned off between the tests so that the birds were not able to see the drum accelerate, the results were very clear with small standard errors. When plotted on a logarithmic scale, the progression became linear indicating that the curves are following Fechner's law. The lines of best fit (least squares analysis) matched the data at the 97-99% level. The maximum visual merging frequency reached in this experiment was about 80 Hz at 210 lx illumination.

The experiment described above provided a very clear OKR-illumination relation with small standard deviations. It had, however, the disadvantage that the birds were adapted to the dark when they were asked to react to the moving stimulus. This may have effects on the merging frequency which we measured. We therefore also investigated which visual merging frequencies we achieved if the drums were accelerated with lights on. Indeed, the merging frequencies were in this case some 20 Hz higher. If one considers that with this experiment the frequencies measured might be slightly too high because of a "hysteresis" effect which may keep the birds moving their heads a bit longer than they perceived the moving stripes, the "real" merging frequency might be between our two measurements.

The linearity of the curves in a logarithmic scale indicates that the illumination level – OKR curve is dependent on the function of the photoreceptors. In this case and also if the curve might be more determined by the motor response, there should be a saturation level with higher illumination. Because we did not reach this with the artificial light experiment, we transferred our experimental setup to daylight. According to these daylight measurements, saturation may be reached at around 560 lx, so that the highest illumination levels at the experimental condition were already near to the saturation point.

## **Comparison of White and Wild Type Zebra Finches**

Although there were a couple of reasons to speculate about a difference between white and wild type zebra finches, we did find only one deviation in white birds, namely their unwillingness to perform OKR in bright daylight. Neither the performance under monocular conditions nor the dependency of the merging frequency on the illumination level were different. We can thus state that, in contrast to albino rabbits (Collewijn et al. 1985) and to albino ferrets (Hoffmann et al. 2004) the white zebra finches do not seem to have any defect of the OKR system. The reasons are as yet unclear. It might be that the accessory optic system, in contrast to the other visual projections (Bredenkötter and Bischof 1996) is not affected by the albino mutation. It may also be that binocular interaction, although demonstrated for the AOS (e. g. Wylie, 2000) is not as important in birds as to affect the OKR, because there were no differences between binocular performance and monocular performance with stimulation in the preferred direction. However, more experiments are certainly necessary.

The refusal of the white zebra finches to perform OKR under daylight conditions came not fully unexpected. Our initial reason to investigate the visual system of the white birds was the observation that they had big orientation difficulties at occasions where an animal caretaker entered the aviary. As yet, we presumed that it was the stressful situation causing the behavioural deficits. Our present results indicate that it could be the level of illumination (there is daylight in all our aviaries) which probably glares the birds and causes enhanced stress. The pupil reflexes, however, were normal in the white birds. Probably, such glare could be induced by a photoreceptor deviation. It could, however, also be caused by the lack of inhibition which we showed for almost all areas of the visual system of white birds (Bredenkötter and Bischof 1996). Again, further experiments are necessary to decide between these alternatives.

## References

- Bischof HJ (1988) The visual-field and visually guided behavior in the zebra finch (*Taeniopygia guttata*). J Comp Physiol A 163:329-337
- Bischof HJ, Watanabe S (1997) On the structure and function of the tectofugal visual pathway in laterally eyed birds. Europ J Morph 35:246-254
- Brauth SE (1977) Direct accessory optic projections to the vestibulo-cerebellum: a possible channel for oculomotor control systems. Exp Brain Res 28:73-84
- Brecha N, Karten H (1978) Projection of the accessory optic nuclei and vestibular nuclei upon the oculomotor nuclear complex in pigeon. Ann Rec 190:605-606
- Bredenkötter M, Bischof HJ (2003) Unusual postnatal development of visually evoked potentials in four brain areas of white zebra finches. Brain Res 978:155-161
- Bredenkötter M, Engelage J, Bischof H-J (1996) Visual system alterations in white zebra finches. Brain Behav Evol 47:23-32
- Collewijn H, Winterson BJ, Dubois MF (1978) Optokinetic eye movements in albino rabbits: inversion in anterior visual field. Science 199:1351-1353
- Collewijn H, Apkarian P, Spekreijse H (1985) The oculomotor behaviour of human albinos. Brain 108:1-28
- Davies MN, Green PR (1990) Optic flow-field variables trigger landing in hawk but not in pigeons. Naturwiss 77:142-144
- Davies MNO, Green PR (1991) The adaptability of visuomotor control in the pigeon during landing flight. Zool Jb-Abt allg Zool Physiol 95:331-338
- Diekamp B, Hellmann B, Troje NF, Wang SR, Güntürkün O (2001) Electrophysiological and anatomical evidence for a direct projection from the nucleus of the basal optic root to the nucleus rotundus in pigeons. Neurosci Lett 305:103-106
- Dunn-Meynell AA, Prasada Rao PD, Sharma SC (1983) The ipsilateral retinotectal projection in normal and albino channel catfish. Neurosci Lett 36:25-31
- Engelage J, Bischof HJ (1988) Enucleation enhances ipsilateral flash evoked responses in the ectostriatum of the zebra finch (*Taeniopygia guttata castanotis* Gould). Exp Brain Res 70:79-89
- Engelage J, Bischof H-J (1993) The organization of the tectofugal pathway in birds: A comparative review. In: Zeigler HP, Bischof H-J (eds) Vision, Brain and Behavior in Birds. MIT Press, Cambridge, Mass, London, pp 137-158
- Fite KV, Montgomery N, Whitney T, Boissy R, Smyth JR, Jr. (1982) Inherited retinal degeneration and ocular amelanosis in the domestic chicken (*Gallus domesticus*). Curr Eye Res 2:109-115
- Frost BJ, Wylie DR, Wang YC (1990) The processing of object and self-motion in the tectofugal and accessory optic pathways of birds. Vision Res 30:1677-1688
- Garipis N, Hoffmann KP (2003) Visual field defects in albino ferrets (*Mustela putorius furo*). Vision Res

- Gioanni H (1988) Stabilizing gaze reflexes in the pigeon (*Columba-Livia*).1. Horizontal and vertical optokinetic eye (OKN) and head (OCR) reflexes. Exp Brain Res 69:567-582**
- Gioanni H, Villalobos J, Rey J, Dalbera A (1983) Optokinetic nystagmus in the pigeon (*Columba-Livia*). 3. Role of the nucleus ectomamillaris (nEM) - Interactions in the accessory optic-system (AOS). Exp Brain Res 50:248-258**
- Gioanni H, Rey J, Villalobos J, Bouyer JJ, Gioanni Y (1981) Optokinetic nystagmus in the pigeon (*Columba-Livia*). 1. Study in monocular and binocular vision. Exp Brain Res 44:362-370**
- Gioanni H, Rey J, Villalobos J, Richard D, Dalbera A (1983) Optokinetic nystagmus in the pigeon (*Columba-Livia*). 2. Role of the pretectal nucleus of the accessory optic-system (AOS). Exp Brain Res 50:237-247**
- Guillery RW (1986) Neural abnormalities of albinos. TINS 9:364-367**
- Güntürkün O (1997) Avian visual lateralization: a review. Neurorep 8:iii-xi**
- Hoffmann KP, Garipis N, Distler C (2004) Optokinetic deficits in albino ferrets (*Mustela putorius furo*): a behavioral and electrophysiological study. J Neurosci 24:4061-4069**
- Hoperskaya OA (1975) The development of animals homozygous for a mutation causing periodic albinism (ap) in *Xenopus laevis*. J Embryol Exp Morphol 34:253-264**
- Kern R, Petereit C, Egelhaaf M (2001) Neural processing of naturalistic optic flow. J Neurosci 21:RC139**
- Kern R, Lutterklas M, Petereit C, Lindemann JP, Egelhaaf M (2001) Neuronal processing of behaviourally generated optic flow: experiments and model simulations. Network 12:351-369**
- Lappe M (2000) Neuronal processing of optic flow. Int Rev Neurobiol 44. Academic Press, San Diego, CA**
- Lauber JK (1964) Sex-linked albinism in the Japanese quail. Science 146:948-950**
- Lauber JK, Vriend J (1989) Melatonin reduction by lithium and albinism in quail and hamsters. Gen Comp Endocrinol 76:414-420**
- LaVail JH, Nixon RA, Sidman RL (1978) Genetic control of retinal ganglion cell projections. J Comp Neurol 182:399-421**
- Lee DN, Davies MNO, Green PR, Vanderweel FRR (1993) Visual control of velocity of approach by pigeons when landing. J Exp Biol 180:85-104**
- Leminski S, Bischof HJ (1996) Morphological alterations of the visual system in white zebra finches. Neurorep 7:557-561**
- Loshin DS, Browning RA (1983) Contrast sensitivity in albinotic patients. Am J Optom Physiol Opt 60:158-166**
- Lund RD (1965) Uncrossed visual pathways of hooded and albino rats. Science 149:1506-1507**
- Maurice M, Gioanni H (2004) Eye-neck coupling during optokinetic responses in head-fixed pigeons (*Columba livia*): Influence of the flying behaviour. Neurosci 125:521-531**

### Chapter III : Eckmeier and Bischof, 2008

- McKenna OC, Wallman J (1985) Accessory optic-system and pretectum of birds - comparisons with those of other Vertebrates. *Brain Behav Evol* 26:91-116
- Takatsuji K, Ito H, Watanabe M, Ikushima M, Nakamura A (1984) Histopathological changes of the retina and optic nerve in the albino mutant quail (*Coturnix coturnix japonica*). *J Comp Pathol* 94:387-404
- Wang YC, Frost BJ (1992) Time to collision is signaled by neurons in the nucleus rotundus of pigeons. *Nature* 356:236-238
- Watanabe M, Takatsuji K, Ito H, Masai H, Kawahara T (1984) Degeneration of retinal ganglion-cells in the cataract affected albino quail (*Coturnix-Coturnix-Japonica*). *Z Tierzucht Zuchtungsbiologie - J Anim Breed Gen* 101:153-158
- Weidner C, Reperant J, Miceli D, Rio JP, Desroches AM, Kirpichnikova E (1988) Visual system degeneration in the glaucomatous albino quail. *J Hirnforsch* 29:299-314
- Wylie DR, Frost BJ (1999) Responses of neurons in the nucleus of the basal optic root to translational and rotational flowfields. *J Neurophysiol* 81:267-276
- Wylie DR, Linkenhoker B, Lau KL (1997) Projections of the nucleus of the basal optic root in pigeons (*Columba livia*) revealed with biotinylated dextran amine. *J Comp Neurol* 384:517-536
- Wylie DR, Bischof WF, Frost BJ (1998) Common reference frame for neural coding of translational and rotational optic flow. *Nature* 392:278-282
- Zhang HY, Hoffmann KP (1993) Retinal projections to the pretectum, accessory optic system and superior colliculus in pigmented and albino ferrets. *Eur J Neurosci* 5:486-500



# - Chapter IV -

## Gaze Strategy in the Free Flying Zebra Finch (*Taeniopygia guttata*)

Dennis Eckmeier, Bart RH Geurten, Daniel Kress, Marcel Mertes, Roland Kern, Martin Egelhaaf and Hans-Joachim Bischof

### Abstract

Fast moving animals depend on cues derived from the optic flow on their retina. Optic flow from translational locomotion includes information about the three-dimensional composition of the environment, while optic flow experienced during a rotational self motion does not. Thus, a saccadic gaze strategy that segregates rotations from translational movements during locomotion will facilitate extraction of spatial information from the visual input.

We analysed whether birds use such a strategy by highspeed video recording zebra finches from two directions during an obstacle avoidance task. Each frame of the recording was examined to derive position and orientation of the beak in three-dimensional space was derived. The data show that in all flights the head orientation was shifted in a saccadic fashion and was kept straight between saccades.

Therefore, birds use a gaze strategy that actively stabilizes their gaze during translation to simplify optic flow based navigation. This is the first evidence of birds actively optimizing optic flow during flight.

**This chapter has been published:**

**Eckmeier, D., Geurten, B. R., Kress, D., Mertes, M., Kern, R., Egelhaaf, M. and Bischof, H. J. (2008).**  
Gaze strategy in the free flying zebra finch (*Taeniopygia guttata*). PLoS ONE 3, e3956.



## Introduction

Navigating through a complex environment requires a specific set of information. It is essential to quickly get an impression of the three dimensional composition of the environment. This impression would consist of the distances between the observer and the objects in the environment, as well as among those objects. Such information may be used to anticipate the future path of movement, and to decide when to execute manoeuvres necessary to follow that path without the risk of collisions.

Several mechanisms are known to allow the estimation of distance, but doing so during fast locomotion presents special challenges. Sharp retinal images of objects or edge detection are very difficult to obtain due to motion blur. Also, using accommodation mechanisms for distance estimation would be too slow for fast navigation in difficult and unknown terrain [1]. Stereopsis is a major cue for sensing depth, but it requires binocular viewing which is well developed only in predators [2]. Further, stereopsis works also only within a limited spatial range depending on the distance between the eyes and the spatial resolution [3]. All these mechanisms are therefore not ideal for distance estimation during fast navigation, especially in rapidly flying animals such as many birds.

Optic flow fulfils the requirements for fast detection of information relevant for visually guided navigation of fast moving animals. It refers to the velocities with which environmental objects are displaced in the retinal image of the moving animal. Optic flow follows basic geometric rules that allow a moving human or animal observer to estimate its relative distance to environmental objects by analyzing these movements [4-6]. Detailed edge or object recognition is not necessary. It is sufficient to detect areas of different speed and direction of motion by means of optic flow.

Optic flow is produced by self motion: During straight (translational) motion, the retinal images of objects in the visual field move with different velocities according to their distances from the observer. The images of objects that are far away move slowly while those of near objects move fast. In addition, the images of approaching objects expand while images of receding objects contract. Hence an animal can estimate distances to and among objects from the optic flow experienced during translational self-motion. However, many movements have an additional rotational component due to turns of the head or the body. The optic flow generated by such rotational movement does not provide any distance information because the velocities of retinal images of differently distant objects do not differ [4]. This may complicate the processing of distance information provided by the translational optic flow component. The extraction of distance information from optic flow could thus be facilitated if its rotational component is reduced by an active gaze strategy. Schilstra and van Hateren [7-9] showed that blowflies separate rotational from translational motion by following a flight path with straight passages interrupted by very fast saccadic turns of the body and head instead of flying in smooth curves.

Here we investigate whether birds exhibit similar active gaze behaviour that would facilitate the use of optic flow during free flight. Many avian species move very fast in three dimensions and, therefore, may have evolved a well developed a navigational system based on optic flow. As yet, behavioural evidence that birds actually make use of optic flow during flight is rare, probably because their size and speed would require too much space. The few experiments that have been done focussed on a single task such as plummeting or landing [10-12].

We filmed zebra finches flying around an obstacle with two high-speed cameras, and analyzed the recorded head movements to obtain information on their gaze strategies during flight. Eye movements were neglected for methodological reasons. This protocol is justified by the findings of Gioanni et al [13, 14], who demonstrated that in the combined optokinetic and optocollic reflex, the head movements account for 80-90% of the overall gaze shift. So the birds mainly move their heads when changing gaze direction. If we could show that head turns

**Figure 1. The flight arena.**

During experiments the bird entered the middle division through one of the entrances, avoided the obstacle, and left through the opposite window. Roof and front were open for video recording. The walls were lined with random texture to make navigation by landmarks difficult. The floor was covered with single coloured paper to increase contrast in video recordings from above.

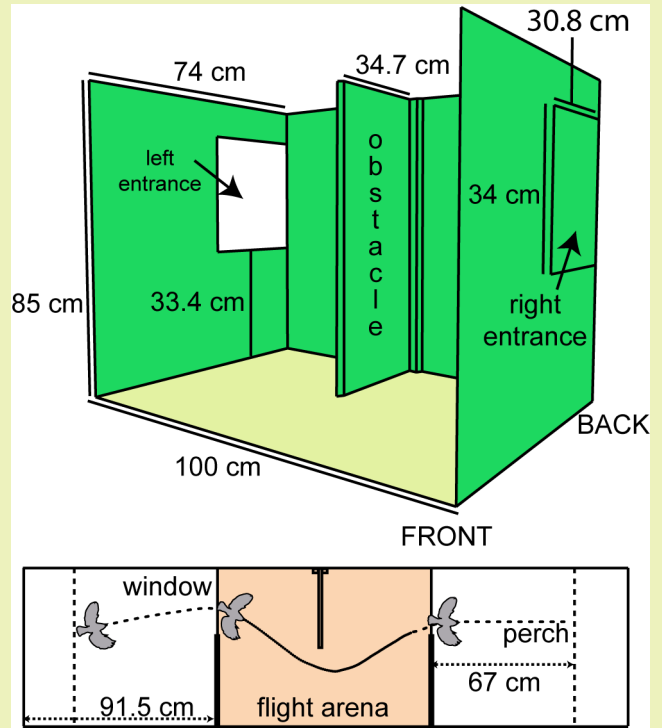
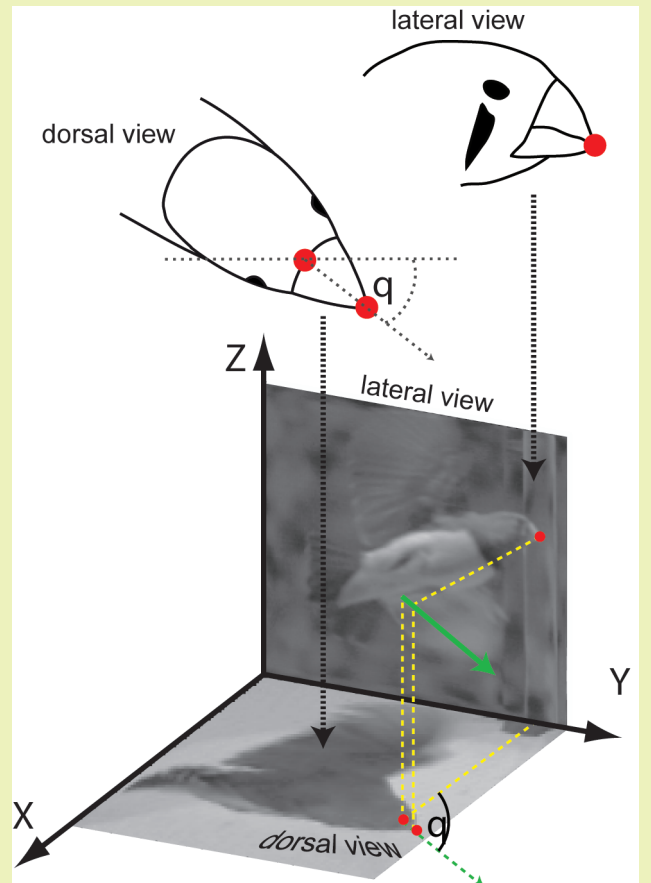


**Figure 2. Determination of the gaze direction.**

In a pair of image frames taken from different directions, the base and the tip of the beak were marked as is indicated by red dots. Theta ( $\Theta$ ) is the angle between the X axis and the beak axis from a dorsal view or the horizontal orientation angle of the beak. The three-dimensional position of the beak tip is determined from both pictures. Dotted green arrow indicates gaze direction in dorsal view; solid green arrow is projected in three dimensions.



were restricted to short periods of the flight, this would be a strong hint that the distance information needed for navigation might be obtained from optic flow cues.

For insights into natural optic flow processing in the brain, the flight behaviour of white zebra finches might be of special interest. This albinotic mutation is known to have strong anatomical and physiological changes of the central visual system leading to enhanced neuronal responses in areas ipsilateral to the stimulated eye [15-17]. Some of the areas with enhanced responses in the white birds feed information to nuclei of the accessory optic system that processes optic flow. Other areas involved in distance estimation like nucleus rotundus in turn receive input from the accessory optic system [18] This may lead to a less efficient flight performance. To relate possible deficits of flight behaviour to neuronal deviations may then help to identify the neuronal structures essential for the processing of optic flow.

The primary goal of the present experiments is to examine whether zebra finches use a behavioural strategy to separate the translational and the rotational component of optic flow. As stated above, only the translational component, that is optic flow induced by straight flight, contains the distance information needed for manoeuvring. Turning movements of the head, which add a rotational component of optic flow, should therefore be avoided. If turning movements are necessary as for example when flying around an obstacle, a bird should develop a strategy where turning movements and straight flight alternate instead of being intermingled. Demonstration of such a strategy would prove that optic flow is an important tool for flight path control and may be universally used throughout the animal kingdom.

## Material and Methods

The experiments were performed with the zebra finch (*Taeniopygia guttata*), a small Australian songbird, raised and kept at the department's animal care facilities. Ten individuals were accustomed to the flight arena, 5 of them being white, the others wild type birds of the normal grey colour.

The flight behaviour of the bird was examined in a cage especially built for this experiment. It was 283 cm long, 85 cm high and 74 cm deep and separated by wooden walls into three compartments. The central compartment was 100 cm long, the outer ones about 90 cm (fig. 1). The birds could enter and leave the central compartment by windows in the partitions, each 31 by 34 cm, located at the rear of the cage at a height of 38 cm above the floor. The central compartment was divided by a 1.5 cm thick wall (obstacle) reaching from bottom to roof and extending from the back end into the cage by 34.7 cm. In the front wall was a window (90 x 36 cm). The outer compartments of the flight arena had one perch each (67 cm away from the window and 40 cm from the floor) and walls of mesh wire (1.2 cm mesh width).

The walls and the obstacle were wallpapered with green to black randomly textured paper to make edge detection more difficult as we did not want the birds to navigate by landmarks. The roof and the floor were not wallpapered. The floor was covered with plain sand-coloured paper because wild type birds were hard to recognise on the video recordings from above when textured wallpaper was used. During experiments the roof was left open for illumination and for video recording from above. On top of the open roof, a box was installed with openings for spotlights and a camera. Lights and camera were mounted on top of the box. The second camera faced through the front window of the middle part of the flight arena (shown in fig.1), which was also left open to avoid reflections by an otherwise necessary glass window. During training the roof was covered with wire mesh and the front window was closed with a pane of glass. So the birds learned not to fly through these openings and none

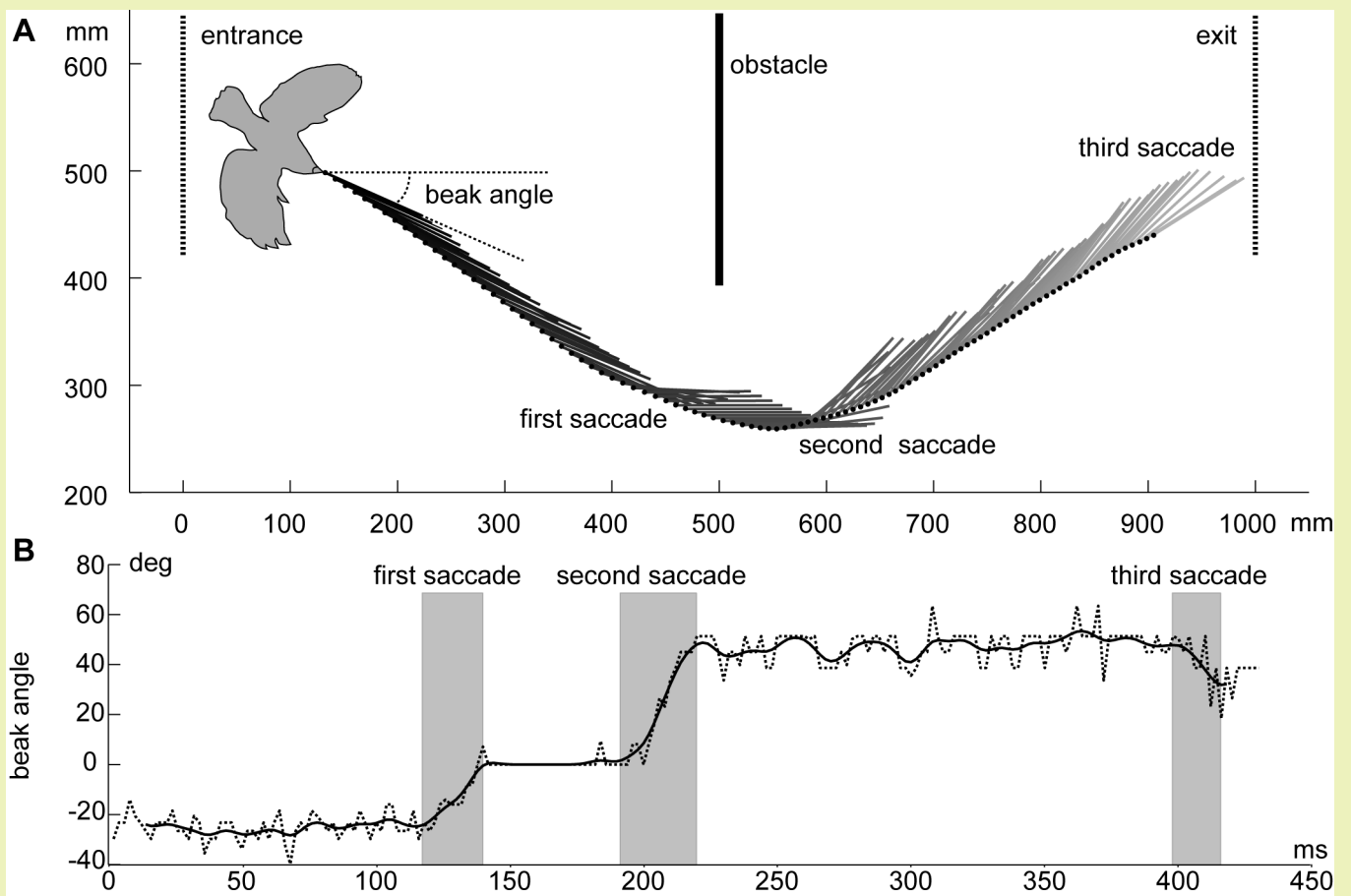


**Figure 3. Example of a flight trajectory.**

A: Position and head orientation of a bird shown every 4 ms within the middle division of the flight arena. Dots indicate beak tip position; lines indicate horizontal beak orientation and, thus, gaze direction in the middle section of the flight arena. The bird contour is taken from the first frame analysed and approximately sized relative to the indicated cage dimensions. Origin of XY plane is the front left corner of the middle division. Positions of entrance, exit and obstacle are marked. B: Time-dependent beak angle relative to long axis of flight arena over time. The dotted line indicates raw data and the solid line indicates filtered data.

of them did in the experiment. Additionally, the area in front of the cage was darkened by black cloth during the experiments. This prevented the birds from leaving the cage and eliminated unwanted hints by landmarks outside the cage. The second camera was installed within this darkened area for video recordings from the front.

For training as well as during the experiments, a bird was put into one of the outer compartments and perched there. It was then forced to fly by approaching the cage or by a piece of cloth applied to a string and moved from the outside of the cage. In response to these actions, the bird then entered the central compartment through one of the windows, flew around the obstacle, left the central compartment through the other window, and perched at the other outer compartment. It was then forced to fly into the opposite direction. Flights in both directions were recorded during experiments. Training continued for four days until every bird passed the middle compartment without landing inside or touching the (transparent) glass window at the front side of the cage. Then the glass pane at the front and the mesh wire at the top of the central compartment were removed to allow video recordings. As stated above, the birds did not attempt to fly through these opening during experiments.

High speed cameras (Red Lake Motion Pro; 500 frames/s) were used for video recording. The top camera was situated 125 cm above the upper rim of the cage with a 12.5 mm objective. The front camera stood 153 cm away from the front rim of the cage. For later analysis the recordings of both cameras had to be synchronized. This was accomplished by using the Red Lake 'Midas' software.

To reconstruct the position and orientation of the bird's head we manually marked discrete points of the bird's beak in every frame of both recordings with the help of 'Fly Trace' [19], a custom made software that returns pixel coordinates of marked positions in a bitmap picture. In single frames of videos taken from above, the tip and the base of the beak were marked. In videos taken from the front, providing a side view of the flight, only the beak tip was marked in each frame (fig. 2). Noise introduced by this manual tracing was accounted for by smoothing the data using a Gaussian filter. The frequencies that had to be filtered out were determined by analysing the frequency spectrum of the noise generated by ten different people, who digitized the same video sequence. The resulting pixel coordinates obtained from both views were stereo-triangulated to derive three-dimensional position and orientation of the beak as projected into the horizontal plane (fig 2).

We calculated the beak orientation within the horizontal plane from the position data of the base and the tip of the beak to estimate gaze direction (see Discussion for the problem of "gaze direction" in birds). Eye movements could not be measured, but given that head movements account for up to 90% of a gaze shift [13, 14], the beak direction was interpreted to coincide with the gaze direction (fig 2, 3). The angular velocities of gaze changes were calculated by determining the changes in beak orientation between two frames and relating them to the video frame rate (500 frames/s).

As we wanted to reconstruct the position and orientation of the head in three dimensions, we had to obtain calibration data that allowed us to calculate the real spatial position from the pixel coordinates. This was done with the J.Y. Bouguett camera calibration toolbox for Matlab (MathWorks USA) [20]. We used 31 interpolation points that were physically defined as the tops of upright bars on a so called 'Manhattan' model. The bars were of different but defined heights and positions within the flight arena (removed before training and experiments). Pixel coordinates of these interpolation points were taken from single frames. We employed an optimisation routine to choose four points, which then were used to build a translational matrix. Based on this translational matrix, we also derived a rotational transformation matrix. With these matrices we were finally able to calculate the real position of the objects in the arena from the pixel coordinates derived from the recordings. The calculations were done using Matlab (Mathworks Inc.). Most scripts used here were based on scripts previously developed in our group, but adjusted or rewritten for the purposes of the current study.

To search the data for sequences of high rotational head velocities, that is saccadic gaze shifts, we defined two search parameters. First, the angular velocity had to be larger than  $400^\circ/\text{s}$  for at least four consecutive frames (i.e. for at least 8ms). Second, the angular velocity had to reach a peak of at least  $700^\circ/\text{s}$  during such a turn.

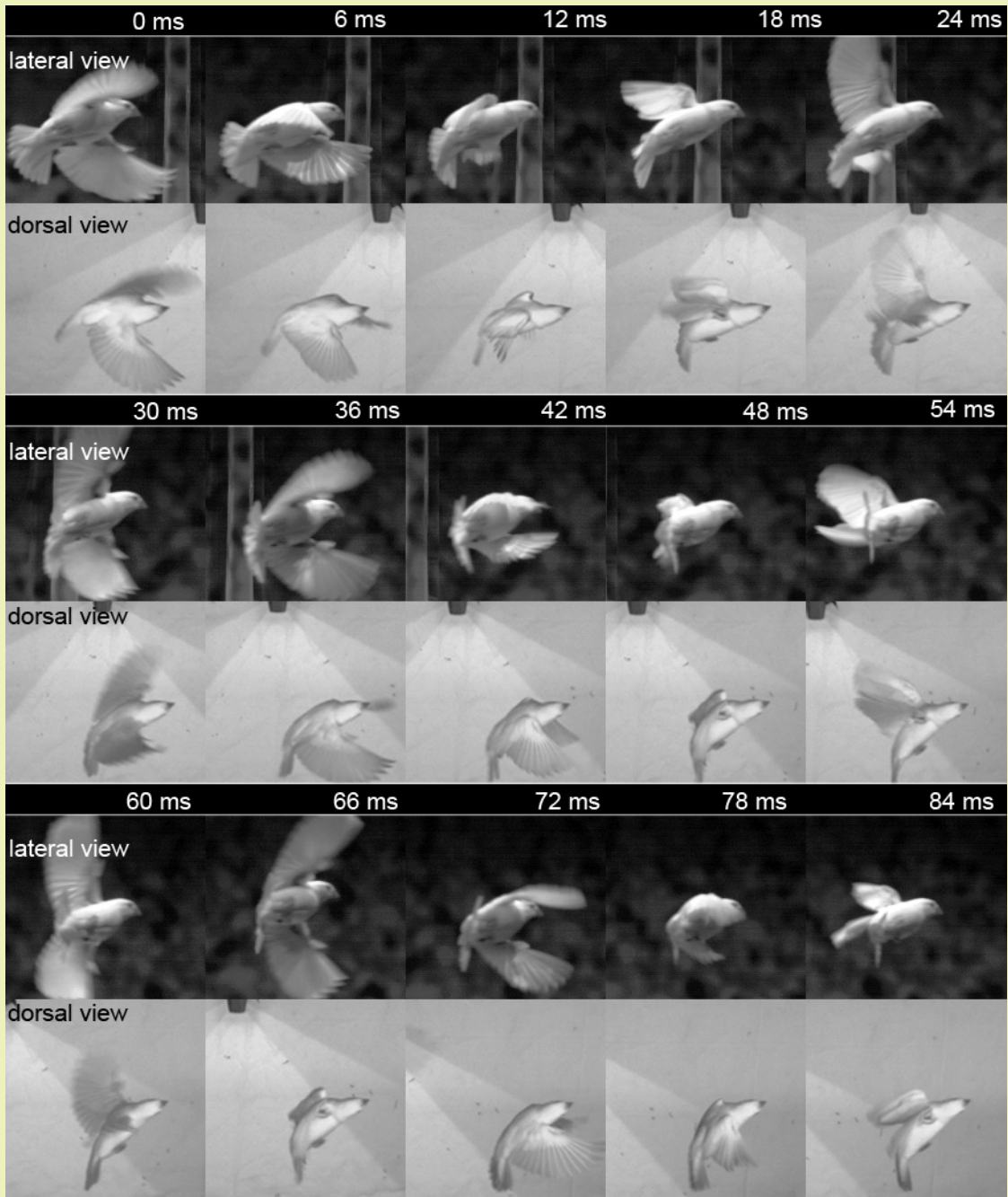


**Figure 4. Sequence of a manoeuvring bird.**

As shown in this series of picture pairs, during a braking manoeuvre the head stays steady while the body turns and the tail feathers are spread.

Finally we examined the orientation of the head in the vertical plane. We randomly selected three birds of each morph and analysed the recordings of the lateral view of their flights. Only the short flight path intercepts where the birds flew parallel to the frontal border of the cage (almost perpendicular to the camera axis) allowed us to obtain the pitch angle of the head exactly enough. The raw head orientation values within each flight were normalised by subtracting the mean orientation to get a single dataset for each bird.

The original research reported herein was performed under guidelines established by the German Welfare Law.

## Results

We recorded 97 flights in a flight arena with an obstacle. Fifty of these were performed by white zebra finches, 47 by wild type birds. Due to the experimental procedure, about half of the flights (46) were from left to right comprising a left turn around the obstacle in the central compartment, the other half (51 flights) was from the right to the left with a left turn around the obstacle. Neither the colour morph nor the flight direction affected the experimental results. We therefore pooled the entire data set.

The recordings were made after the birds had been acclimatized to the cage and reliably traversed the central compartment without colliding with the obstacle or arena walls. The birds flew with a relatively high speed of  $2.49 \pm 0.033$  m/s, so that the central compartment was usually crossed in less than half a second. Accordingly, few wing beats were performed. The wings were opened only when a bird changed its flight direction. In between, they were flattened along the body.

The birds had to fly into the middle compartment of the cage through an entrance facing the obstacle. Therefore, a bird entering at the left entrance first had to turn right, then perform a leftwards turn to fly around the obstacle and eventually turn right to reach the exit window. Accordingly the turns were in opposite direction when the bird entered the central cage from the right entrance. Although the birds executed two or three turns in the setup, only the turn around the obstacle was reliably recorded. The other turns occurred at the beginning or end of the flight and were often recorded incompletely or not at all. We, therefore, limited our analysis to the turn around the obstacle.

When the bird flew around the obstacle, it decelerated and turned into the new direction of its flight path. During this manoeuvre, the wings were opened and the body turned and pushed forward relative to the head while the tail feathers were spread (fig. 4). Then the body turned into the new flight direction facilitated by wing beats. Although the body showed substantial twisting during these turns (fig 4), the head kept its orientation in space, suggesting that the bird kept its gaze constant between turns. During breaking in turns the height of the birds decreased for a short period; nonetheless, up and down movements were small. The differences between the highest and lowest point ranged between 2 and 30 cm and on average across flights, amounted to  $10.49 \pm 5.65$  cm.

Fig. 3A shows an example of a flight from the left to the right with a left turn around the obstacle. The dots along the flight path depict the position of the beak tip (used as a marker for the position of the head) every second frame. The direction of the short lines represents the gaze direction. Although the movement of the head is a smooth curve, the gaze direction remains relatively constant over quite long periods of time. Such phases of relatively constant gaze are interrupted by short and fast changes of head direction, i.e., by head saccades. Hence, the head is not turned continuously, but changes its orientation in short distinct phases. This is demonstrated in figure 3B.

**Figure 5. Percentage of saccade counts per flight.**

The figure is subdivided into 1 to 3 saccades for each morph and summed for all birds (n = 174).

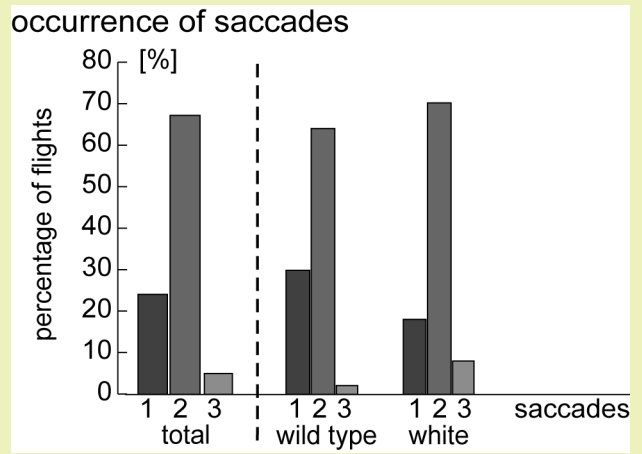


**Figure 6. Mean flight speed.**

Mean flight speed for flights with 1 to 3 saccades (n = 95). The small squares indicate means, boxes indicate the standard error of the mean, and whiskers indicate standard deviations.

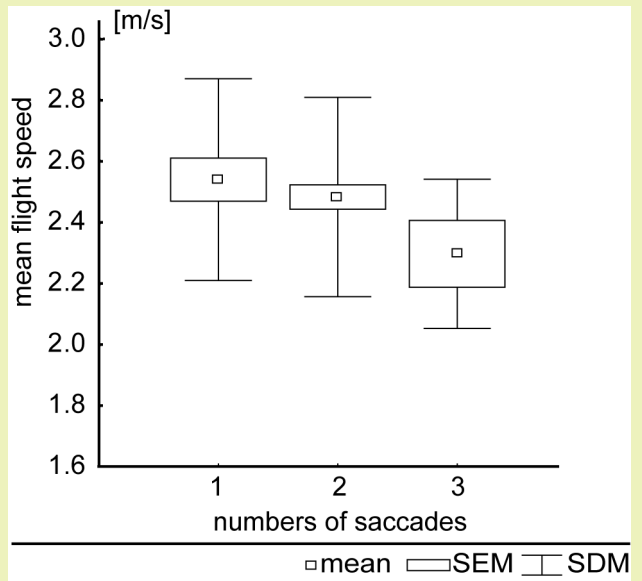
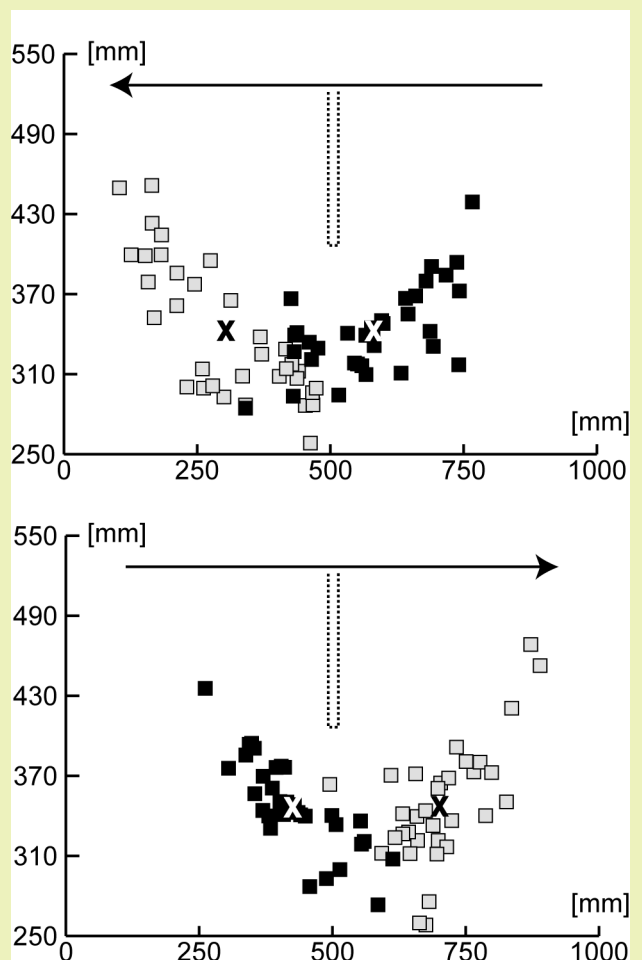


**Figure 7. Saccade positions of flights with two saccades.**

The axes correspond to long and transverse axes of the middle division of the flight arena. The dotted line indicates the position of the obstacle. The arrow indicates the flight direction while squares indicate beak position at the beginning of the saccade (black squares: first saccade; white squares: second saccade). X indicates the position of the mean value (white X: first saccade; black X: second saccade).



To define criteria for a computer-based identification of saccades we examined results such as presented in fig 3B. Earlier results that showed that the zebra finch does not respond optokinetically to rotational flowfields faster than  $349 (\pm 67) ^\circ/\text{s}$  further supports our decision [21]. For this reason we defined saccades as being the periods in which the absolute value of the angular velocity of the beak was above  $400^\circ/\text{s}$  for at least 8 ms, and with the peak maximum being at least  $700^\circ/\text{s}$ . By applying these criteria, we found at least one saccade in every flight (fig.5) except one. Two saccades were observed for 66 (68%) of the flights. Only one saccade was found in 22 (23%) flights. Few flights showed three saccades (7; 7%), and one (1%) flight even comprised four saccades. There was one flight that did not reveal any saccade matching the search parameters, but the video showed smaller saccadic turns also for this flight. Despite this limitation, the parameters used for saccade detection probably are a good compromise between missing relevant saccades and the detection of spurious events that do not represent saccades. The saccade number distribution in white and wild type zebra finches was very similar (fig.5).

The number of saccades made during a flight depends on the speed of the bird along the flight trajectory. It slightly decreased with increasing speed (fig.6), although this trend is not statistically significant for our data base (Kruskal-Wallis-Anova:  $H = 1.236$ ,  $N = 97$ ,  $p = 0.8721$ ).

The spatial distribution of the first and second saccades (black squares and white squares, respectively) is rather broad, occurring almost at any location along the analysed section of the flight trajectories (fig.7). However, the distribution of the first and the second saccades is not symmetrical with respect to the obstacle (see the position of the crosses which depict the mean of the first and the second saccades, respectively). In both flight directions, the first saccade is closer to the obstacle than is the second one.

Up to now we have shown that birds are using a saccadic gaze strategy in our flight arena: they are alternating during flights on a curved path between times where they keep the head orientation relatively constant followed by saccadic head movements.

Figure 3 may cast doubts on the intersaccadic constancy of the head direction. The orientation of the beak fluctuates slightly even after filtering as long as it is not  $0^\circ$ . When we recognized this, we re-examined our videos and found intersaccadic intervals in 18 flights during which the beak was oriented around  $0^\circ$  (one of them depicted in fig. 3). In any case the fluctuations of beak orientation within these flight sections were almost negligible. A beak orientation of  $0^\circ$  indicates that the beak was oriented parallel to the X axis in the above view. We therefore think it likely that single pixels can be marked more exactly for a  $0^\circ$  beak orientation than is true for other angles and that fluctuations of the beak orientation during other intersaccadic intervals may be an artifact. Hence, we may conclude that the gaze direction is well stabilised during the intersaccadic intervals.

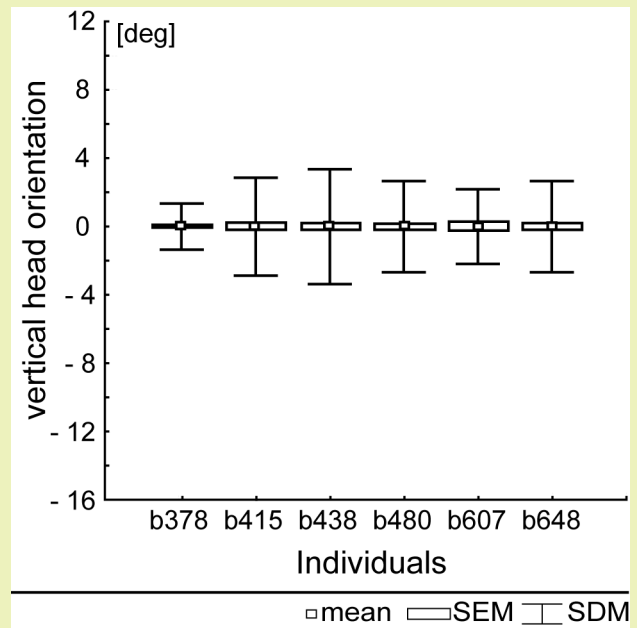
The mean angular velocity of saccades ( $n = 178$ ) was about  $1082.89 \pm 22.43 ^\circ/\text{s}$ , the fastest saccade reaching  $2154 ^\circ/\text{s}$ . Average angular speed of intersaccadic intervals ( $n=82$ ) was about  $114.75 \pm 7.86 ^\circ/\text{s}$ . So between saccades head rotational movements in the horizontal plane were relatively slow (see also the previous paragraph).

The mean duration of saccades (defined by velocities above  $400^\circ/\text{s}$ ) was  $15.6 \pm 0.4$  ms, while intersaccadic intervals endured  $91.9 \pm 3.93$  ms. This means that when seen from above, the head was held in a constant direction for 83% of the flight around an obstacle. However, constant translational flow can only be obtained if there is also no rotational motion component around other axes of the head either.

Usually, when examining rotations, changes and velocities are presented with algebraic signs to indicate direction. Here we pooled saccades of different direction and, therefore, used absolute values of the data. This could be done because all flights from one direction (left or right turn) only produced saccades of the same direction (see figure 3).

**Figure 8. Normalised vertical head orientation angles during intersaccadic intervals in 6 birds.**

Vertical orientation deviations taken from 42 selected flight sequences of six individuals. The mean vertical beak orientation is zero due to normalisation. The small squares indicate mean values and boxes indicate standard error of the mean while whiskers indicate standard deviations.



the environment while rotational components do not [4]. It is a known strategy of insects to behaviourally separate translational from rotational components which is likely to separate translational from rotational components. This facilitates extraction of spatial information from behaviourally generated optic flow. They perform fast body saccades which are supplemented by even faster head saccades, and look in a constant direction between saccades [7-9, 22]. We want to compare this behaviour to avian flight.

First of all, we did not observe saccadic fast body turns as was shown for the blowfly. The force that has to be overcome when changing direction is proportional to mass and velocity. Zebra finches have approximately ten times the length of a blowfly (12 cm) and 100-140 times the mass (10-14 g). The velocities of the zebra finches in our experiment reached up to 3.5 m/s while Schilstra and van Hateren [8] measured flight velocities of only up to 1.2 m/s for the blowfly. So while in flies a significant proportion of the gaze shift is done by body saccades, such behaviour is probably impossible for zebra finches due to inertia.

However, while the body moves smoothly the head either turns rapidly or is held constant in orientation even when manoeuvring (fig. 4). We use head orientation as a first approximation for estimating gaze direction. But in contrast to flies, birds have movable eyes which we assume to contribute to gaze shifts. A recent study (Voss and Bischof, submitted) demonstrated substantial eye movements in the zebra finch. Giovanni [13-14] showed that during horizontal optokinetic reflexes induced by a rotating drum, eye movements are synchronised with head movements. The eye movements accounted for up to 20% of the gaze shift in that study. Thus we presume that in the zebra finch eye movements add to saccadic head shifts to optimize the saccadic gaze shift. This would be analogue to the blowfly that executes head movements to add speed and accuracy to the gaze shift generated by the body saccade [9, 22]. Between saccades, eye movement compensates for slow head movement to keep the gaze direction fixed. However, eye movement could not be resolved in our study.

The gaze shifts of birds and flies are similar not only to the fact that there are phases of fast and slow head turns, but also to some parameter values of these phases. For example, the maximum angular velocity of saccades measured by Schilstra and van Hateren [8] was about 2000°/s and for the zebra finch the fastest saccade we found was at 2150 °/s. Also, rotational velocities of the gaze during intersaccadic intervals in the blowfly were found to be below 100-200 °/s [9]. In birds we found a mean velocity of 115 °/s during intersaccadic intervals, which presumably may further be reduced by compensatory eye movements. Schilstra and van Hateren state that these residual rotational velocities are slow enough to make motion blur from rotational optic flow negligible. They also

state that during the shortest saccades, the visual system experienced significant rotational motion blur for only 15-20 ms. Due to our search parameters we did not measure saccades shorter than 8 ms, and we only called a turn a saccade when the head moved faster than 400 °/s. So saccade durations given in this study always coincide with the experience of rotational motion blur. These saccade durations were 15.6 ms in mean.

We wanted to compare two morphs of zebra finches, because investigating optic flow processing in a deviating visual system such as that of the white morph might reveal some additional insight. Surprisingly, wild type and white zebra finches did not show significant differences. The strong deviations of the visual system in the white morph which were assumed to have some major influence on the AOS and thus on optic flow processing did not seem to have any effect on the overall flight performance. This is congruent to Eckmeier and Bischof [21] who did not find differences in the optokinetic nystagmus of the two morphs elicited by rotational optic flow.

Taken together, our experiments demonstrate that birds use a gaze strategy separating rotational and translational optic flow. This is achieved by an alternation of fast rotational head shifts and intersaccadic periods where head rotations are minimal. Eye movements probably enhance gaze shift during saccades and minimize it during intersaccadic intervals. To this end, head and eye saccades of birds appear to be analogous to body and head saccades in flies. Both, flies and birds, exhibit similar kinetic characteristics of gaze control. By exhibiting an active gaze strategy similar to that of the blowfly, zebra finches are able to use optic flow for distance estimation.

## Acknowledgement

This study was supported by the DFG – Deutsche Forschungsgemeinschaft, Germany (Ke 645/2-1).

## References

- 1 Martinoya C, Bloch S (1980) Depth perception in the pigeon: Looking for the participation of binocular cues. 28th International Congress of Physiological Sciences: 477-482
- 2 Martin GR (2007) Visual fields and their functions in birds. *J Ornithol* 148 (Suppl 2): S547-S562.
- 3 McFadden SA (1993) Constructing the three-dimensional Image. In: Zeigler HP, Bischof HJ, editors. *Vision, Brain and Behaviour in Birds*. MIT Press, pp. 47-61
- 4 Koenderink JJ (1986) Optic Flow. *Vision Res* 26(1): 161-179.
- 5 Gibson JJ (1950) The perception of visual surfaces. *Am J Psychol* 63(3): 367-384.
- 6 Vaina L, Beardsley S, Rushton S (2004) *Optic Flow and beyond*. Norwell: Kluwer Academic Publishers. 485 p.
- 7 Schilstra C, van Hateren JH (1998) Stabilizing gaze in flying blowflies. *Nature* 395(6703): 654.
- 8 Schilstra C, van Hateren JH (1999) Blowfly flight and optic flow. I. Thorax kinematics and flight dynamics. *J Exp Biol* 202 (Pt 11): 1481-1490.
- 9 van Hateren JH, Schilstra C (1999) Blowfly flight and optic flow. II. Head movements during flight. *J Exp Biol* 202 (Pt 11): 1491-1500.

- 10 Davies MN, Green PR (1990) Optic flow-field variables trigger landing in hawk but not in pigeons. *Naturwissenschaften* 77(3): 142-144.
- 11 Davies MNO, Green PR (1991) The adaptability of visuomotor control in the Pigeon during landing flight. *Zoologische Jahrbucher-Abteilung fur allgemeine Zoologie und Physiologie der Tiere* 95(3-4): 331-338.
- 12 Lee DN, Davies MNO, Green PR, Vanderweel FRR (1993) Visual control of velocity of approach by pigeons when landing. *Journal of Experimental Biology* 180: 85-104.
- 13 Gioanni H (1988) Stabilizing gaze reflexes in the pigeon (*Columba livia*).1. Horizontal and vertical optokinetic eye (OKN) and head (OCR) reflexes. *Experimental Brain Research* 69(3): 567-582.
- 14 Gioanni H (1988) Stabilizing gaze reflexes in the pigeon (*Columba livia*).2. Vestibulo-Ocular (VOR) and vestibulo-colic (Closed-Loop VCR) reflexes. *Experimental Brain Research* 69(3): 583-593.
- 15 Bredenkotter M, Engelage J, Bischof HJ (1996) Visual system alterations in white zebra finches. *Brain Behav Evol* 47(1): 23-32.
- 16 Voss J, Bischof HJ (2003) Regulation of ipsilateral visual information within the tectofugal visual system in zebra finches. *J Comp Physiol A Neuroethol Sens Neural Behav Physiol* 189(7): 545-553.
- 17 Engelage J, Bischof HJ (1988) Enuclation enhances ipsilateral flash evoked responses in the ectostriatum of the zebra finch (*Taeniopygia guttata castanotis*, Gould). *Exp Brain Res* 70(1): 79-89.
- 18 Wylie DR, Linkenhoker B, Lau KL (1997) Projections of the nucleus of the basal optic root in pigeons (*Columba livia*) revealed with biotinylated dextran amine. *J Comp Neurol* 384(4): 517-536.
- 19 Lindemann JP (2005) Visual navigation of a virtual blowfly. Dissertation, Bielefeld: Faculty of Technology
- 20 Bouguet JY, Perona P. (1998) 3D photography on your desk. Sixth International Conference on Computer Vision (ICCV'98) pp.43
- 21 Eckmeier D, Bischof HJ (2008) The optokinetic response in wild type and white zebra finches. *J Comp Physiol A* 194(10): 871-878.
- 22 Kern R, van Hateren JH, Egelhaaf M (2006) Representation of behaviourally relevant information by blowfly motion-sensitive visual interneurons requires precise compensatory head movements. *J Exp Biol* 209(Pt 7): 1251-1260.

# - Chapter V -

## New Insights into Object Detection in the Zebra Finch Brain Revealed by Complex Visual Motion Stimuli

Dennis Eckmeier, Roland Kern, Martin Egelhaaf and Hans-Joachim Bischof

### Abstract

Fast flying animals need reliable information about the position of objects within visual space, for example to avoid collisions. The main source for depth information is optic flow. At least blowflies and zebra finches have developed strategies to optimize the perception of optic flow. We here investigated how the brain processes optic flow information. Because conventionally used simplified stimuli often do not give reliable information about the function of optic flow processing neurons, we also used stimuli emulating the visual scene seen by a bird during natural flight.

Multi-units were recorded at nucleus rotundus of anaesthetized zebra finches. Motion stimuli were presented on a panoramic LED array display.

One type of stimuli was spheres moving in three-dimensional space emulating image displacements induced by self-motion. These stimuli lead to excitatory responses depending on the exact type of self motion in contrast to earlier studies suggesting inhibition of neuronal activity of n. rotundus by such stimuli.

With naturalistic stimuli resembling a flight around an obstacle in a bird's view, neurons signaled the approach towards an object or the passing of an obstacle. As in the blowfly, this reaction could not be predicted from responses to conventional stimuli.

We show that an area said to be involved in object recognition is also reacting to whole field motion. This indicates that there is not a strong separation of identification and localization processing within the visual system of birds. We also demonstrate that the use of more naturalistic stimuli in visual perception research is necessary because simplified stimuli are not sufficient to reveal the full spectrum of neuronal responses. The reaction patterns shown here indicate that in birds, like in the blowfly, the position of an object can be extracted from discontinuities in the optic flow caused by these objects.

**This chapter has been submitted:**

**Eckmeier, D., Kern, R., Egelhaaf, M. and Bischof, H. J. (submitted). New Insights into Object Detection in the Zebra Finch Brain Revealed by Complex Visual Motion Stimuli. PLoS ONE**



## Introduction

The crucial task for fast navigation in three dimensions is a fast and reliable estimation of distances to objects. The most often discussed mechanism for obtaining such distance information is stereopsis. However, stereopsis requires special anatomical features. To obtain a sufficiently large binocular overlap, the eyes have to be frontally placed. A large distance between the eyes is also necessary to provide image differences big enough to get reliable depth information. In most birds, the interocular distance is very small ( $\sim 8.5$  mm in zebra finches, unpublished) and the binocular field is very small due to the lateral position of the eyes ( $\sim 40^\circ$  in the zebra finch; [1]. The range within which depth perception by stereopsis functions efficiently is therefore limited. [2,3]. Pigeons, for example, exhibit an effective range for stereopsis guided tasks of about 5 to 19 cm [3]. Small fast moving animals like song birds or flying foxes may therefore predominantly depend on cues from optic flow to estimate distance and to control maneuvers like avoiding collisions with obstacles.

Optic flow is the retinal image change during locomotion or eye and head movements. When the observer moves, the entire retinal images are displaced. Local segments of these image displacements are related to the objects which constitute the environment. By processing global and local changes, the observer therefore obtains information about his/her self-motion as well as the three dimensional structure of the surroundings.

Integrated processing of optic flow over large parts of the visual field provides information about the speed and direction of self-motion, including eye and head movements. During translational self-motion (straight movement into any direction), images of immobile objects far away seem small but expand during approach. These image changes also accelerate during approach of objects. Finally, images of objects move from a central position towards a lateral position in the visual field when the observer passes by. For the visual pathway that processes the visual feedback of self-motion, translation is thus defined by a globally expanding image with a focus of expansion in the direction of movement. Local changes in the flow field that correlate to single objects in the environment provide information about the distance to and motion of these objects. From the expansion velocity of the image of an object on the retina, the visual system can compute the distance of this object. Whether the object or the observer is moving can be derived from differences between object-induced and self-motion-induced image changes.

If the optic flow results from rotational self-motion, it only contains information about the self-rotation but no depth information. This is because the images of objects do not change in size or motion dynamics. Instead, the entire image moves in one direction depending on speed and direction of self-rotation [4-6]. No relative image changes can be observed that emerge from positions or sizes of objects in the scene.

In an earlier behavioral study [7] we demonstrated that zebra finches during flight reduce head turns and thus rotational optic flow to fast short saccades, while in the time period between the saccades the head orientation is kept relatively constant in space. Translational and rotational movements are therefore separated from each other. This strategy minimizes the time during which optic flow from translational self-motion is superimposed by distracting motion vectors from rotational self-motion components and thus facilitates to extract reliable depth information.

Other behavioral evidence for the actual use of optic flow parameters for navigation in birds focuses on landing and plummeting behavior. Davies and Green ([8-10]) found in hawks a distinct time window before landing at during which the feet were extended while pigeons use the same optic flow parameter to control flight velocity during landing. Gannets lay back their wings just in time to avoid injuries which may be caused by collision with the water surface when plummeting into the sea to catch fish [11]. The authors suppose these behaviors to be based on a time to collision estimation from cues derived from optic flow.

In the avian brain, self-motion is processed by nuclei of the accessory optic system (AOS). A specific subgroup of retinal ganglion cells (displaced ganglion cells) project to the nucleus of the basal optic root and the nucleus lentiformis mesencephali [12,13]. Both nuclei are characterized by neurons selective for large flow fields as emerging from either self-translation or self-rotation [14,15]. From the accessory optic system, information is further transferred to the ocular motor complex and vestibulocerebellum [16-19] and, together with vestibular input, functions as control signal for gaze stabilizing head movements. Lesions of the accessory optic system, for example, affect the performance of optokinetic head reactions [19, 20]. It may also be involved in the compensation of visual field rotation to stabilize the head orientation during flight [21,7].

Object related information is being processed by the tectofugal visual system, which transfers information from the retina via optic tectum and nucleus rotundus to the entopallium. Next to units responding selectively to one or several other object related visual characteristics like color and luminance [22], there are neurons at all stations of this system responding selectively to approaching objects, also called 'looming' stimuli [22-25] Xiao et al., 2006). Subpopulations of these neurons have been shown to signal the time to collision with the approaching object, also in all stages of the tectofugal system [23, 24, 26, 27]. The response of motion sensitive units in tectofugal areas is, however, affected by self-motion related input from nBOR (tectum opticum: reviewed in [28]; nucleus rotundus: [29]; [30]). Also, background motion affects the response to looming stimuli [31,32]. Thus, object motion and self-motion are integrated at several stages of the tectofugal system. Diekamp et al. [30] who described a modulation of nucleus rotundus neurons by input from the accessory optic system presumed that this modulation facilitates to distinguish between self-and object motion.

For our study we characterized motion selective neurons of the nucleus rotundus in the tectofugal visual system of the zebra finch with different conventional and naturalistic visual motion stimuli. These were presented on a panoramic monitor ('FliMax'; [33]) during multi unit recordings. The naturalistic stimuli are based on data from our recent behavioral study [7] and reflect an obstacle avoidance task. We found neurons that responded to objects in the naturalistic replay in a way which was not predicted by the response to more conventional stimuli. Taken together, our study suggests that using more realistic motion stimuli may result in a better insight into a neuron's function in visual processing mechanisms.

## Material and Methods

All experimental procedures were performed according to the German Law on the Protection of Animals and had been approved by the local government, Landesamt für Natur, Umwelt und Verbraucherschutz Nordrhein-Westfalen, approval number AZ 9.93.2.10.36.07.105.

### Electrophysiology

Seventeen zebra finches (*Taeniopygia guttata*) of both sexes were examined. The animals were taken from the departments stock. Each bird was anesthetized by an injection of urethane (SIGMA Diagnostics, 0.01 ml, 20% PBS) into the flight muscle. After injection, the bird's foot was pinched occasionally until reflexes were not observed any longer. The bird's head was then attached to a head holder [34], i.e. fixated at the ear holes and the beak tip. Lidocain gel (Xylocain Gel 2%, Astra Zeneca GmbH, Wedel, Germany) was applied to the skin of the ear holes for additional local anesthesia.

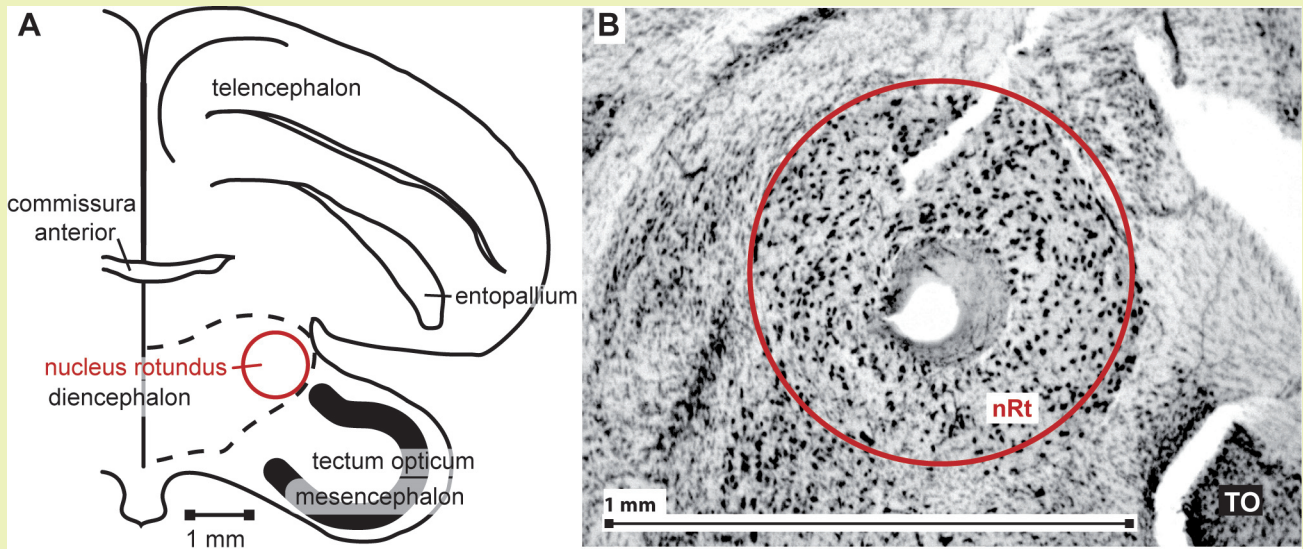


**Figure 1. Location of nucleus rotundus and histological verification of recording sites.**

A shows a schematic of a transverse section of the zebra finch brain according to Nixdorf-Bergweiler and Bischof (2007), 2.4 cm anterior to the Y-point (origin of coordinate system). B shows a photograph of a Giemsa-stained section. In the centre of n. rotundus (nRt) the lesion is visible. In the lower right corner of the photograph a small part of the optic tectum (TO) can be seen.

Feathers were removed and the skin was incised and retracted to expose the skull at the desired positions for electrode placement. The skull was then opened by removing the two bone layers. The dura was kept intact until it was penetrated with the electrode. To make visual stimulation possible, both eyelids were fixed by surgical adhesive in an open position shortly before the experiment started. The nictitating membrane remained intact and served to protect the eye from desiccation.

The head holder mentioned above was attached to a bar on which the bird's body was placed. The bar with the head holder was then mounted to a stand which carried the micro-manipulator, the pre-amplifier and electrodes in the correct angle to the bird's brain for a stereotaxic approach (figures 1 and 2).

The ground electrode was clamped to the skin of the head and moistened with saline (0.9 %). The recording electrode (tungsten in glass micro-electrode TM31A10, World Precision Instruments, Inc., Sarasota, USA, 0.9-1.0 M $\Omega$ , tip diameter 1-2  $\mu\text{m}$ , 1  $\mu\text{m}$  insulation thickness) was positioned according to coordinates (centre of n. rotundus: 2000  $\mu\text{m}$  lateral and 2430  $\mu\text{m}$  anterior of origin, depth 4000-5000  $\mu\text{m}$ ) taken from the stereotaxic atlas of the zebra finch [35]. After penetration of the dura, the electrode tip was forwarded to a depth of 500  $\mu\text{m}$ . Then a hood of fine wire mesh was attached to the stand to shield bird and electrode from electronic interference that otherwise were caused by the stimulus apparatus. The hood did not essentially obscure the bird's view. When these preparations were complete, the stand was placed within FliMax such that the position of the head center coincided with that of the center of the incomplete icosahedron formed by FliMax (see below; figure 2).

To reach the recording site the electrode was advanced into the tissue slowly in steps of 2  $\mu\text{m}$  with a motorized microdrive, avoiding damage of the tissue. About 500  $\mu\text{m}$  before the target area was reached (depth  $\sim$ 3500  $\mu\text{m}$ ), random visual stimuli were presented to the bird using a flashlight while further advancing the electrode. Response of visual neurons was detected and monitored via loudspeakers and an oscilloscope. Where neurons responded to the moving flashlight, the tests as described below were conducted. The search was stopped at a depth of 5500  $\mu\text{m}$

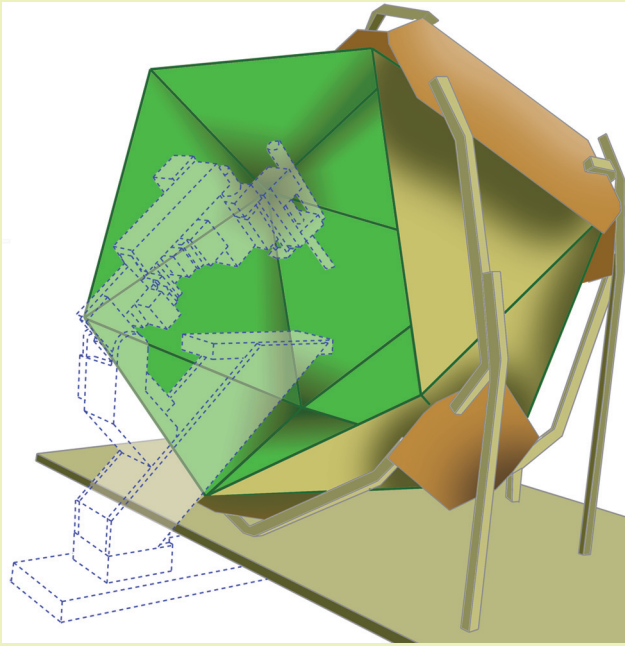


**Figure 2. Schematic of the stimulation device ‘FliMax’: a panoramic LED display.**

FliMax consists of 14 triangular circuit boards each equipped with 512 green LED. Brown plates indicate circuit boards that carry control electronics. It covers  $240^\circ$  ( $-120^\circ$  to  $+120^\circ$ ) azimuth at  $0^\circ$  elevation and from  $60^\circ$  to  $-90^\circ$  elevation of the visual field. The electrophysiology stand including micromanipulator and electrode holder is depicted transparently. The bird was placed on the plate in the centre of FliMax.

( $\sim 500 \mu\text{m}$  below the nucleus rotundus according to Nixdorf and Bischof, 2007). Then the electrode was retracted completely and re-inserted at slightly different coordinates for a new approach. The distance between recording sites was at least  $50 \mu\text{m}$  to avoid recording the same neuron twice.

The received signal was amplified ( $\times 1000$ ) and band pass filtered (300 Hz lower, 20 kHz upper cutoff frequency; A-M Systems Model 1800) before it was digitized (CED 1401 mkII, Cambridge Electronic Design) and stored (Spike 2 recording software, Cambridge Electronic Design).

The activity of different single neurons within a recording was separated offline using the spike sorting function provided by Spike 2 (a template matching procedure). The data was then related to the corresponding stimulus. To this end we recorded a trigger signal from the computer that controls the stimulus apparatus (FliMax). The trigger is given within 3 ms before the first movie frame. The resulting peristimulus-time histograms were further analyzed with self-written Matlab® (Mathworks) scripts.

At the end of each experiment, an electrical lesion was made to mark the position of the last electrode track. The brain was removed and stored for at least two days in fixative (4% paraformaldehyde in phosphate buffered saline (PBS) followed by 30% saccharose in PBS). Coronal  $40 \mu\text{m}$  sections were cut, mounted on glass slides and stained with Giemsa dye (SIGMA Diagnostics, St. Louis, USA).

## Conventional Visual Stimulation and Data Analysis

The stimulation device FliMax [33] used in the experiments has initially been constructed for experiments with flies. It is a segment of an icosahedron (44.8 cm in diameter; figure 2). More than 7000 green light emitting diodes (diameter 5mm, wavelength 567 nm; WU-2-53GD, Vossloh Wustlich Opto, Germany) are positioned equally spaced on 14 triangular circuit boards. The illumination of these diodes can be controlled by a computer program, so contrast can be changed if necessary. In principle, the device can be seen as a spherical computer screen with low spatial (LED separation  $2.3^\circ$  in the centre of a triangle,  $1.5^\circ$  at rims) but high temporal resolution (370Hz). The maximum luminance averaged over the array of LEDs is  $420 \text{ cd/m}^2$ . On this LED screen optic flow stimuli could be presented which were previously computed.

FliMax covers most but not all of the visual field of a zebra finch. It can illuminate an area of  $240^\circ$  ( $-120$  to  $+120^\circ$ ) azimuth at  $0^\circ$  elevation and from  $60$  to  $-90^\circ$  elevation. The visual field of the zebra finch covers an area of  $\sim 300^\circ$  ( $-150$  to  $+150^\circ$ ) azimuth [1]. According to Martin [2] there may be no blind area above the head. Martin observed that the blind area above the head depends on eye size. He hypothesized that animals with big eyes have greater problems with glare effects and thus develop a blind area to exclude the sun from the visual field. However, due to the data presented in his study, this area may even be covered binocularly in the zebra finch (eye size  $\sim 4.2$  mm diameter, unpublished). The visual field of a zebra finch therefore covers  $-90$  to  $90^\circ$  in elevation. The outmost areas of the rear and top visual field could thus not be stimulated by the device.

To produce a stimulus movie, a virtual three dimensional environment had to be designed. Within this virtual environment a trajectory was defined that represented the motion of an observer. We then calculated a movie from the observer's perspective following the trajectory within the virtual environment.

Both, trajectory and the virtual environment were designed to meet the requirements for different conventional stimulus modes:

- translational self-motion (five movies)
- rotational self-motion (one movie)
- a looming object (five movies)
- a special stimulus for the estimation of the receptive field of a neuron

For self-motion tests, we constructed a virtual 'star field' environment model consisting of 640 bright globes (30 cm radius) in front of a dark background. Enclosing the area in which the movement took place, the spheres were pseudo-randomly distributed in a spherical area with a minimum distance of 7.5 m from the starting point to a maximum distance of 25 m. This 'hull' of spheres provided the background for the virtual movements that took place within the enclosed area.

Self-motion stimuli always comprised four phases of one second each: still image, motion in one direction, still image and motion into the opposite direction. The simulated velocity of the moving bird was always 3.5 m/s (translational stimuli) or  $400^\circ/\text{s}$  (rotational stimuli). These velocities fall well within the range of velocities measured in a previous behavioral study on zebra finch flight [7].

Self-translation stimuli were presented in 10 directions: forwards, backwards, to the upper left, to the lower right, leftwards, rightwards, to the upper right, to the lower left, downward and upward (upper/lower:  $+45^\circ/-45^\circ$  elevation, left/right:  $+45^\circ/-45^\circ$  azimuth; origin for elevation and azimuth is frontal,  $-/+180^\circ$  for both is the rear).

For self-rotation we only present the data from one stimulus that consisted of left and right turns about the vertical axis in the horizontal plane (yaw rotation). Two additional stimuli used in preliminary tests that differed in head pitch orientation (looking  $45^\circ$  up or  $45^\circ$  down) were skipped later because there were no significant differences between according neural responses.

A preference score for rotational versus translational self-motion was calculated as follows: We averaged the mean responses to all self-motion stimuli as were recorded during the last 500ms of each stimulus period for translation (Rt) and rotation (Rr) stimuli. The score was calculated by dividing the difference between these values by their sum:  $(Rr-Rt)/(Rr+Rt)$ . The score ranges from -1 (response to translational motion only) to 1 (response to rotational motion only).

For looming objects the 3D model comprised only one object (30 cm diameter) which was approached by the bird at constant velocity (3.5 m/s) until collision. The resulting image was an expanding disc that was centered at five different angular positions: frontal ( $0^\circ$  elevation and azimuth), above frontal ( $45^\circ$  elevation;  $0^\circ$  azimuth),

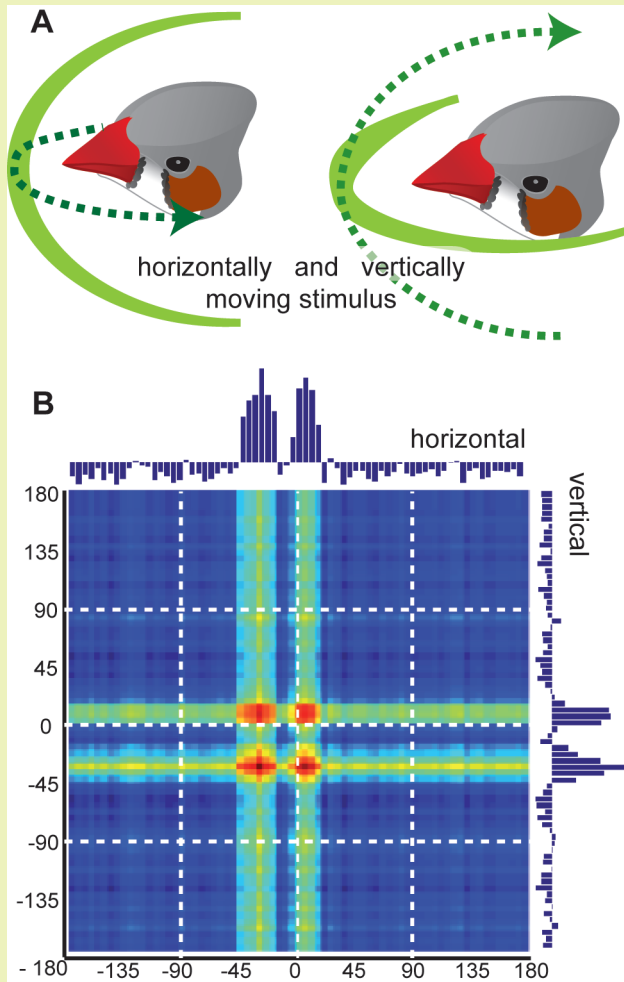


**Figure 3. Estimation of the receptive field: response to horizontal and vertical scans reveal rims of the receptive field.**

A schematic depicting the movement of the moving semi circle. Left: vertically oriented semi circle moves horizontally to scan azimuth. Right: horizontally oriented semi circle moves vertically to scan elevation. In B normalized (z-score) response histograms to horizontal and vertical scans are depicted regarding position of the semi-circle in the visual field for azimuth and elevation. Transient responses mark the borders of the receptive field. To build the map, horizontal response was included row-wise and vertical response was added column-wise. This produces lines of activation across the map according to transients in the horizontal and vertical response, respectively. The borders of the receptive field are indicated where these response peaks coincide, the receptive field is in between the four red areas. Dashed white lines indicate 90° sections.

below frontal (-45° elevation, 0° azimuth), frontal right (45° azimuth, 0° elevation) and frontal left (-45° azimuth, 0° elevation).

For a rough estimate of the receptive field of a given recorded neuron, a vertically or horizontally oriented semi-circle was rotated around the bird's field of view either in the vertical (horizontal semi-circle) or horizontal direction (vertical semi-circle; figure 3). The center of the semi-circle was at the center of the bird's head, the rotation axes were running through the transverse or the long axis of the head, respectively. The semi-circle rotated for a complete 360° in one direction and then 360° in the opposite direction for both, the horizontal and the vertical scan. Rotundal single neurons often respond to optic flow corresponding to self-rotation with a short but prominent motion onset response and only a small tonic or no response to ongoing motion. Thus, we expected transient responses each time the bar entered the recorded neurons's receptive fields. We combined the response to vertical and horizontal scans to a 36x72 map showing -90° to 90° elevation and -180 to 180° azimuth.

For each recording, all stimuli were presented in one out of three different sequences of 15 or 17 stimulus movies each of which was repeated 30 or 35 times. Between the presentations of two consecutive movies the last frame of the first movie was visible for the time the computer loaded the second movie, and an additional pause of 0-3 seconds was included between movies for technical reasons. Also, each stimulus movie began with a still image of the first stimulus movie frame presented for one second. Consecutive stimuli always differed in motion direction to avoid habituation effects. The whole stimulation sequence took 35 to 45 minutes.

Response latencies were calculated from the responses to stimuli that included sharp motion onsets. All responses to such transitions were summed up for each neuron, regardless of the stimulus direction (there was no inhibitory response). A threshold was defined by adding the standard deviation of the resting activity in the last 500 ms before stimulus onset to its average value four times. Then the time difference between stimulus motion onset and the moment at which the neuronal response raised above the threshold was measured.

## Naturalistic Visual Stimulation and Data Analysis

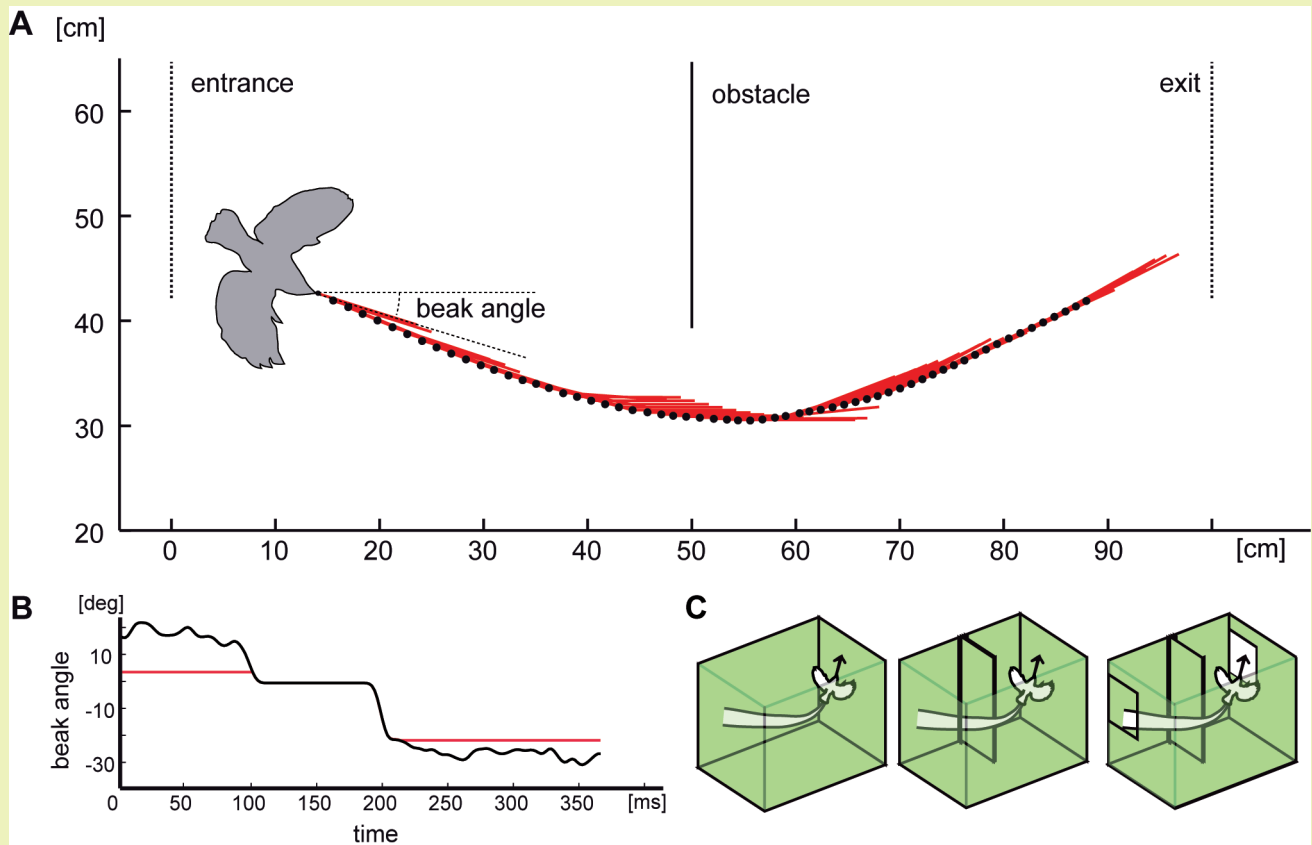


**Figure 4. Naturalistic stimulus: a real flight trajectory and head orientation was used for reconstruction of optic flow in three different virtual environments.**

In A the black dots show the position of the basis of the beak for every third frame of the movie (every 6th ms). Red lines indicate head orientation. Obstacle, entrance and exit are depicted as solid or dotted lines. The bird contour is approximately correct size. B shows the progression of the beak orientation angle (in space) over time for the used naturalistic stimulus. Black line shows beak orientation as measured including residual yaw rotations. Red line shows progression of the head orientation without the small fluctuations to test the influence of head movement on response properties. In C the different cage models are shown. As control condition for the object-no-object test we used an empty cage (left). In the first test condition, the obstacle was introduced (center). In the test for the influence of changing or not changing head orientation, the cage also included entrance and exit windows (right). For stimulus rendering the models were textured with a  $1/f$  distribution of contrast.

We presented naturalistic image sequences which resembled what a zebra finch had seen during a free-flight sequence as recorded in a previous study (figure 4, [7]). In the behavioral experiment the bird navigated around an obstacle within a flight arena.

The original test cage consisted of a central flight arena of 1 m width and two outer compartments. The birds entered the flight arena through a window from one outer compartment and left it through an exit window into the outer compartment on the opposite side. Another window in the front of the cage allowed high speed video recording from that side. A second camera was positioned at the ceiling. In order to reach the exit window the test animals had to circle around an incomplete wall.

For the first test (object-no-object test) with naturalistic stimuli we simplified the cage in the reconstructed stimulus sequence by removing the openings (exit, entrance, and opening for the camera) in the walls. In one version we also removed the obstacle, so that we can compare the response of neurons to a flight in an empty cage in one condition and the same flight in a cage that possesses an obstacle in the other condition (figure 4 C).

In the second test (head-rotation-no-head-rotation test) we wanted to study the influence of residual rotational head motion on the processing of optic flow. In our behavioral study we found residual head rotations during intersaccadic intervals [7]. On the one hand we had good evidence for an artifactual origin of these rotations in the data. On the other hand, if they were genuine, compensatory eye movements would be necessary to eliminate the effect of head rotations on the retinal image flow. We wanted to find out whether the neuronal activity differs when these residual rotations were present or were eliminated. Therefore, rotational head motion during intersaccadic intervals was removed in one condition and unchanged in the other. The virtual cage comprised exit and entrance windows and the obstacle (figure 4 B, C).

To find out which of the optic flow (local / global) or optic flow related environmental characteristics (distance to environment) is represented in the responses, it was necessary to determine the velocity parameters of the optic flow within the receptive field of the recorded neuron.

Therefore, we calculated and averaged local velocities and distances to the environment within the receptive field for each frame of the stimulus by using a toolbox developed for Matlab® at the Department of Neurobiology at Bielefeld University (Germany). The resulting time courses of vertical and horizontal velocities as well as distances were compared to the time course of the response.

## Results

We recorded from 76 units in nucleus rotundus of 18 birds. Sixty-four were recorded in the right hemisphere, twelve in the left one.

### Responses to Conventional Self-Motion Stimuli

All neurons showed an enhanced activity during stimulus motion, but the difference to resting activity levels was not always significant. A typical response to stimuli mimicking the optic flow resulting from self-motion is shown in figure 5 A. Often the onset of movement caused a strong phasic response followed by a tonic phase.

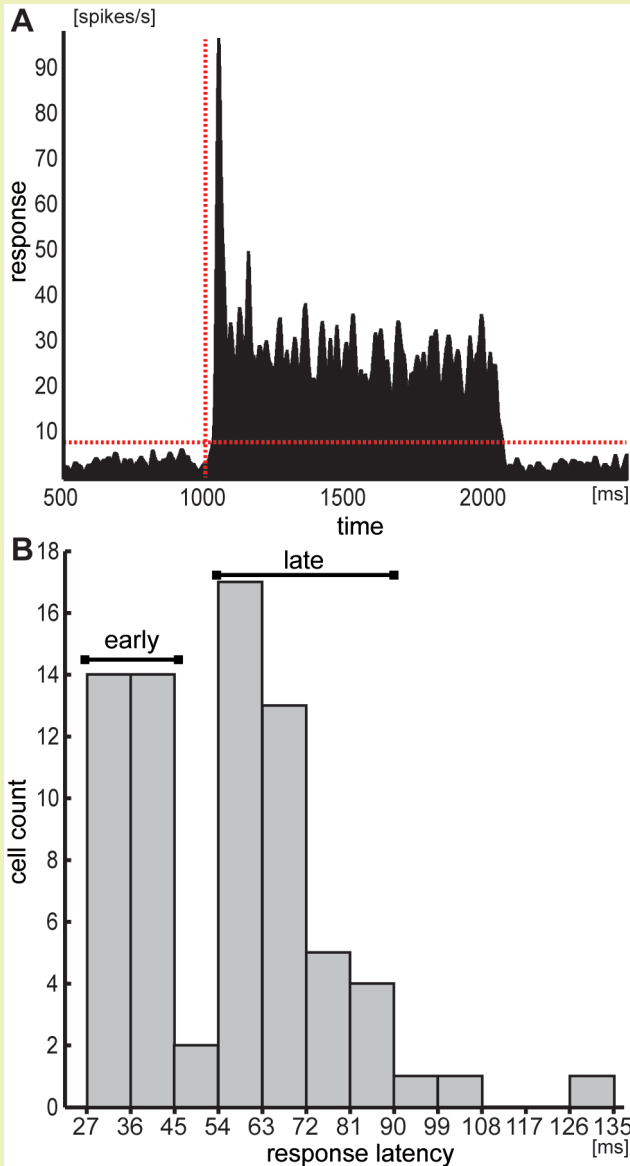


**Figure 5. Two different groups of response latencies were found.**

A: example of latency measurement. Response was averaged over 360 repeats of 12 self-motion stimuli (30 repeats each). Horizontal stippled red line indicates threshold. Vertical stippled red line indicates motion onset. Response latency was measured as time difference between motion onset and the moment at which the response rose over threshold. B: histogram of response latencies: cell count over response latency (bin size: 9 ms). X axis indicates bin edges. We found 28 early responding neurons in the range between 27 to 44 ms response latency. And 39 late responding neurons had latencies ranging from 54 to 85 ms.

The response latencies after movement onset ranged between 27 ms and 135 ms. Two latency groups of neurons could be distinguished (figure 5): Twenty-eight early responding neurons had short response latencies ranging from 27 to 44ms, 39 late responding neurons exhibited longer response latencies ranging from 54 to 85 ms. Response latencies exceeding 85 ms were found only rarely ( $n=3$ ). The latencies of only two neurons were located between the two groups. The activity of four neurons was too irregular for a reliable response latency determination.

To evaluate the strength of responses to different stimuli, we analyzed three aspects: the average transient response, the response peak and the average response rate over the last 500ms of the stimulus. The average tonic response turned out to be the least fluctuating and was used for the following analysis.

Comparison of the averaged response rates for rotational versus translational self-motion revealed some neurons that responded stronger to rotation, others to translation (figure 6), but most did not show any preference. To illustrate this we calculated a preference score leading to values between -1 (response only to translation) and 1 (response only to rotation). Neurons with a score above 0.33 ( $n=25$ ) were classified as self-rotation preferring neurons, neurons with a preference score below -0.33 ( $n=5$ ) as translational self-motion preferring. Neurons re-

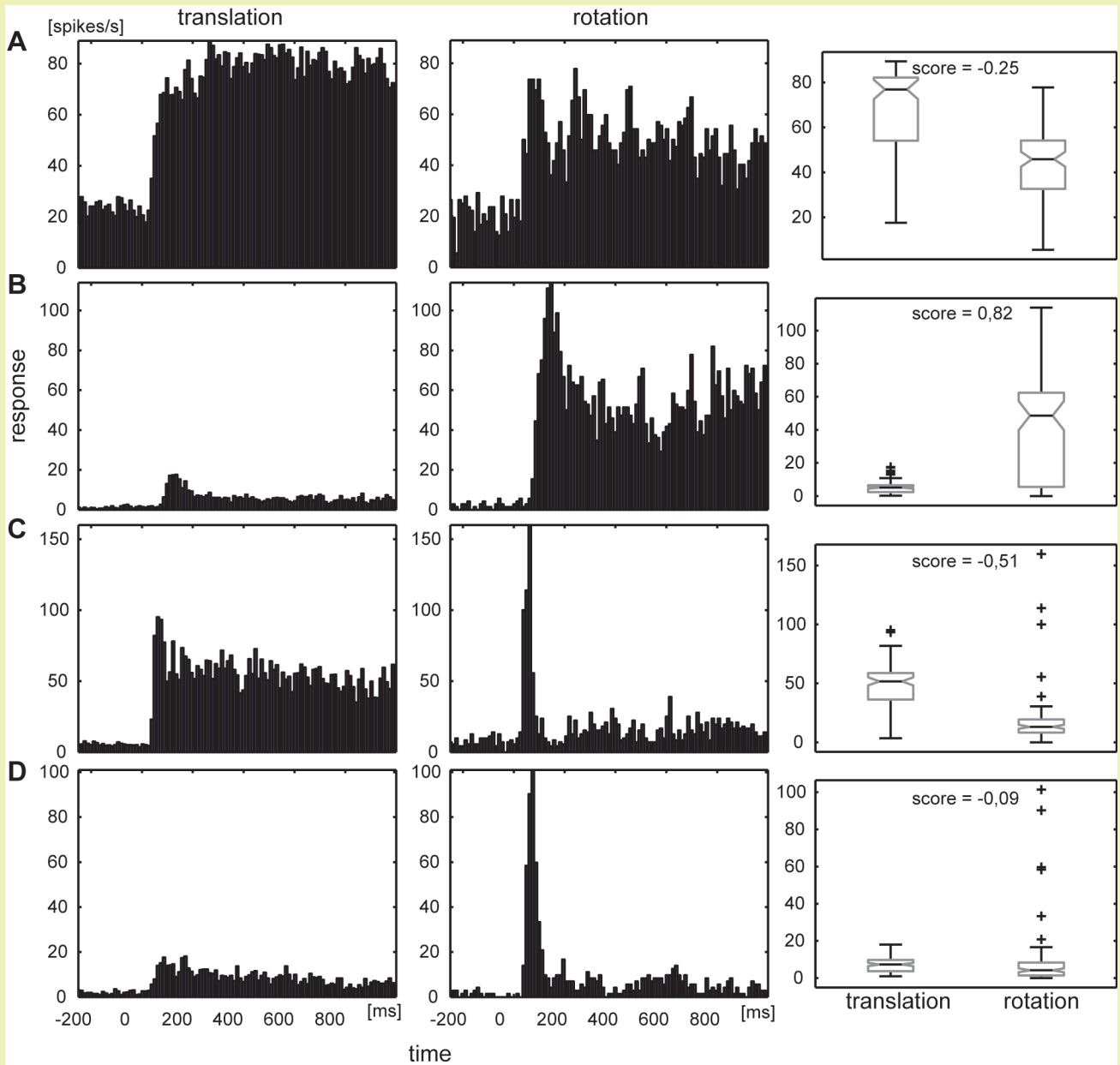


**Figure 6. Four examples of different response patterns to optic flow corresponding to translational and rotational self motion.**

Each row (A-D) corresponds to one neuron. Left column: response to translational self motion averaged across 10 stimuli representing different self motion direction. Middle column: response to rotational self motion averaged across left and right rotation. Right column: boxplot of average response across time for translational (left) and rotational (right) self motion. The preference score is depicted. A: Neuron with a slight preference for translational self motion. B: Neuron with a preference for rotational self motion. C indicates another translation preferring neuron, D a non-preferring neuron. C-D show that neurons not responding significantly to rotational self-motion in the tonic phase still produce a strong transient response. This is not the case for translational self-motion (B and D).

sponsive to rotational self-motion mostly were late responding neurons (15 out of 25) while those responsive for translational self-motion were exclusively early responding neurons (n=4; figure 7).

We found a habituation effect in the response to global motion stimuli. In pairs of self-motion directions tested consecutively, the second movement direction was on average responded to with only 70 - 84% of the response to the first direction (figure 8, blue data).

The question arose whether there was an additional effect from possible direction selectivities. We therefore tested 24 neurons with reversed stimulus order, e.g. a stimulus pair that started with forward movement followed by backward movement was altered to first show backward movement and then forward movement. For reversed stimuli, the second stimulus evoked a response of 84 -107% (figure 8, red data) related to the response rate during presentation of the first stimulus.

According to this result, stronger activation during the first presentation in a pair of opposing self-motion stimuli may result from a combination of both, habituation and directional preferences. If this effect were due to habituation alone, the neurons in the reversed stimulus sequence should have responded to movement into the second direction also with only 70-84% of the activation to the first stimulus. If the effect had only resulted from direction selectivity, inverted stimuli would induce inverted results compared to the original ones, with the activity rate for the second stimulus being 119 - 143% of that for the first (reciprocal result). Instead, our results are intermediate between these two extremes, supporting our idea of a combination of direction selectivity and habituation affecting the responses of the neurons.

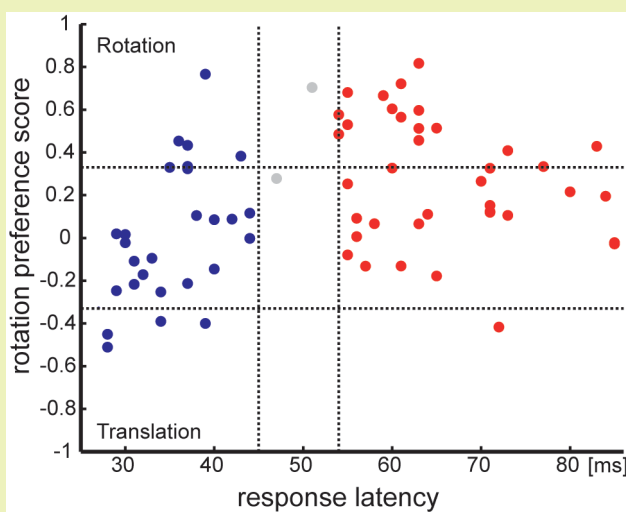


**Figure 7. Correlation of response latency to a preference score for a mode of self motion.**

Plot of the self motion preference score over response latency. Blue dots indicate early responding neurons, red dots indicate late responding neurons, and grey dots indicate unclassified neurons. Score values above 0.33 indicate rotation preference, values below -0.33 indicate translation preference (borders indicated by horizontal dotted lines).

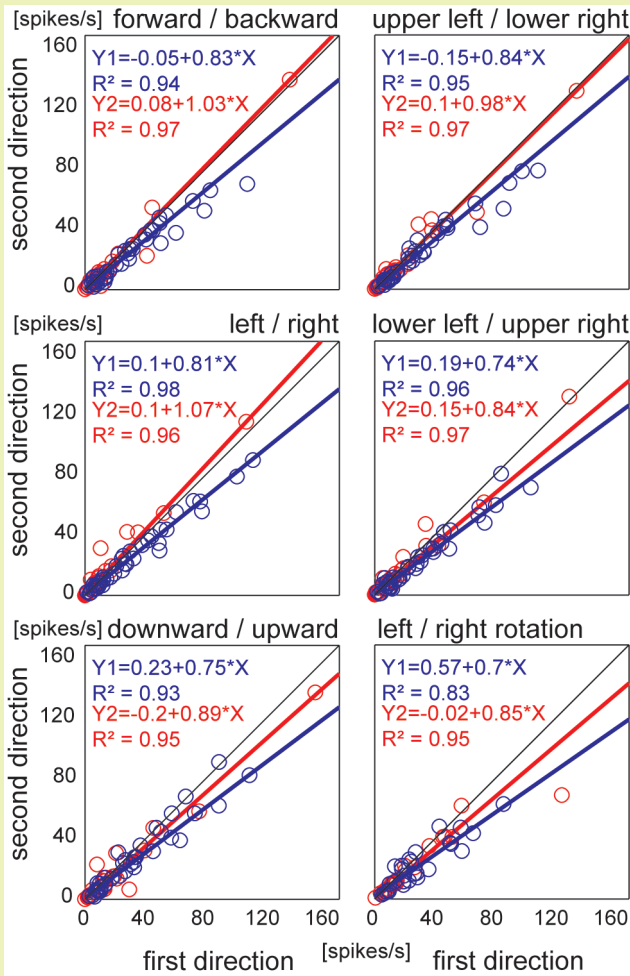


**Figure 8. Habituation or direction selectivity.**

Each graph shows the response ratio between 1st and 2nd stimulus direction tested pair wise in one stimulus. Blue indicates the original sequence as described above the graph. Red indicates inverted sequence. Circles indicate single neurons, lines indicate linear regression curves. Black diagonal represents equal response activity for both directions. Equations and  $R^2$  values are given. On average, the second stimulus evokes weaker responses – the effect is reduced when the stimulus sequence is reversed. Both, direction selectivity and habituation determine the response strength.

## Receptive Field Estimation

In order to understand the responses of a given neuron to complex stimuli, we had to estimate the size and position of the receptive field of the neuron and, thus, to determine whether its visual input originated from the ipsilateral or contralateral eye, or both. Since we tested many different stimuli and had to cope with limited recording times, we were not able to use a method for receptive field estimation that would provide us detailed information about it.

We developed a fast method that uses rotating semi-circle to roughly estimate the size and position of the receptive field. In tests preliminary to this study, rotational self-motion stimuli usually elicited a transient response onset. We presumed that a moving stimulus that has a local motion pattern similar to a rotating self-motion stimulus – i.e. a rotating semicircle – would also elicit such a transient response whenever it enters the receptive field of the recorded neuron. The semi-circle were moved across the entire extent of our panoramic stimulator once for each opposing direction vertically and horizontally (figures 3 and 9) to cover the whole visual field and to enter the receptive field from four directions (from above, below, left and right). The response was then correlated to stimulus position using the timing of both. The response latency of the neuron was taken into account.

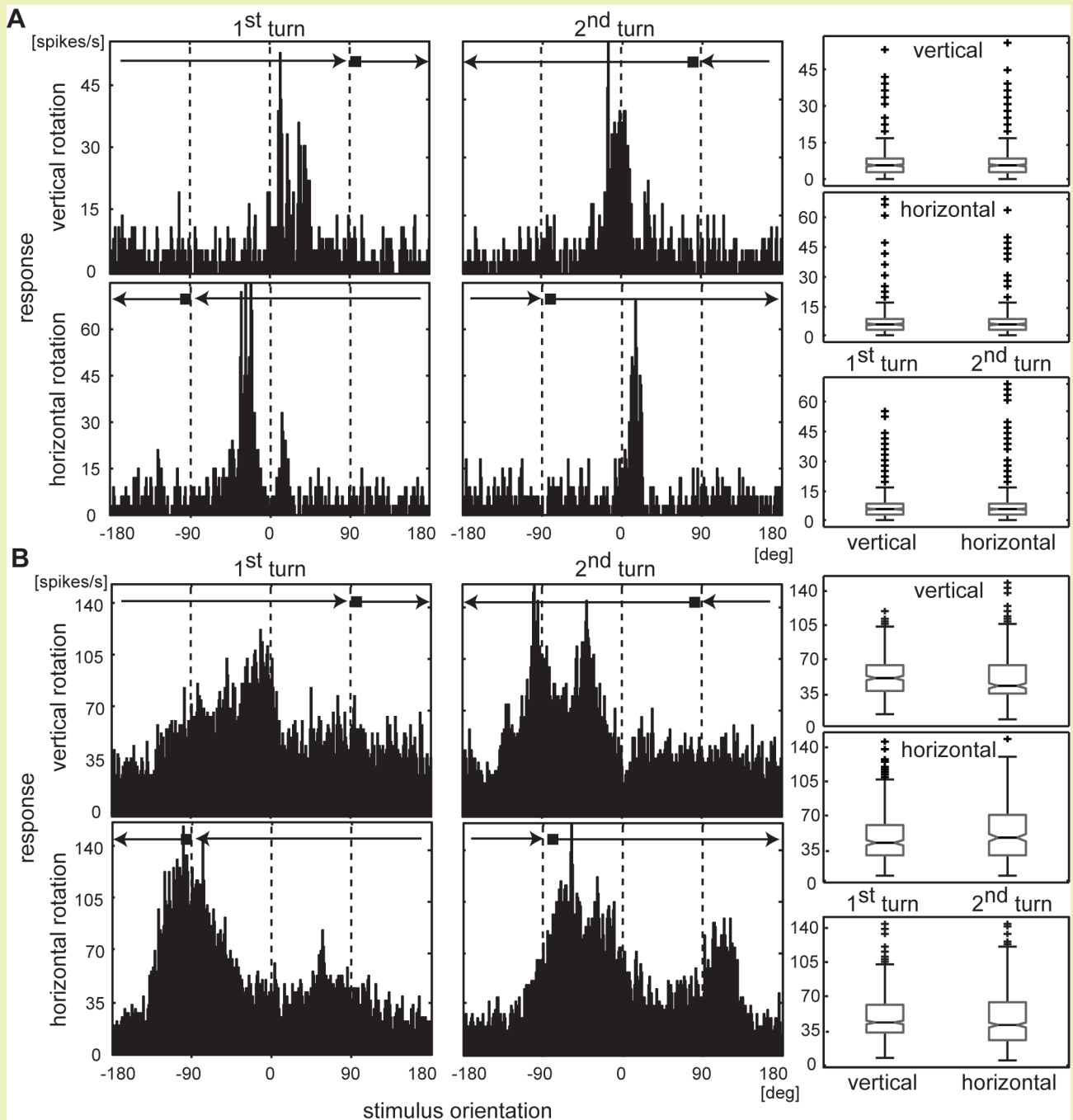


**Figure 9. Response to vertical and horizontal rotating semi circles.**

Histograms are averaged over 30 repeated presentations of the stimulus for both directions (1st and 2nd turn) of stimulus motion. X axis indicates the stimulus position for either azimuth (horizontal rotation) or elevation (vertical rotation) of the visual field. Start and end position of the stimulus as well as its direction are indicated by arrows and black square. Box plots show response values within 12 ms bins for both turns of a scan and for the two scans (horizontal and vertical). Black horizontal line indicates median, boxes indicate upper and lower quartile (edges at 25th and 75th percentile), whiskers indicate data variance, + indicate outliers, notches indicate uncertainty (5% percentile) A: Neuron with the receptive field in the frontal area of the receptive field. B: Neuron with the receptive field in the contralateral visual field, facing the axis of rotation in the vertical scan. Note different scaling of y-axes!

The method turned out to generate reliable results. Neurons with frontal receptive fields responded to the scans in the predicted transient manner (figure 9 A). However, when the receptive field of a recorded neuron was localized about  $90^\circ$  laterally, vertical scans evoked a deviating response pattern (figure 9 B). This result can be explained by the fact that the rotation axis of the moving semi-circle laid within the receptive field. The response of such neurons increased and decreased over the course of stimulus motion (figure 9 B). This was probably related to the changing coverage of the receptive field by the stimulus.

Another property of the responses to the rotating semi-circle could be explained by the size of the stimulus device. The responses to horizontal stimuli moving at the rear always showed low to zero spike rates. Often there was even a sharp edge visible (figure 9 B, horizontal). These areas were identical with the areas within the receptive field not covered by FliMax.

Finally, neurons with lateral receptive fields often revealed a small artefactual response peak with stimulation  $180^\circ$  away from the area evoking the peak response (in the ipsilateral visual field). Although visual input from the ipsilateral eye has been reported for nucleus rotundus [36,37], it is not very likely that a neuron has two receptive fields monitoring opposite directions. The artifact was induced by the moving reflection of the stimulus on the contralateral side when the circle moved on the ipsilateral side of the FliMax. This was corroborated by an experiment with a black semi-circle on a bright background as stimulus to avoid such a reflection. As expected, the neurons recorded in this experiment did not show ipsilateral activation.

In order to test for possible direction selectivities in the response to the semicircle stimuli, we calculated average response rates for both turns of the vertical and the horizontal scan ( $n=64$ ; horizontal: left and right moving semi-circle; vertical: up and down moving semi-circle). In 35 cases we did not find a significant difference for the two directions of one scan. The remaining neurons, however, showed preferred directions. Sixteen neurons preferred upward over downward motion of the semi-circle, only four neurons preferred downward motion. Seven neurons preferred leftward over rightward motion, while six preferred the opposite direction. Whether these results were due to habituation was not tested specifically.

The receptive field size and position was analyzed with the semicircle stimuli for 56 out of 64 rotundal neurons. Eight neurons were not analyzed because the response latency data were too noisy to produce a clear result or the overall response was not sufficiently high. Fifty-one neurons of the remaining sample could be assigned to one of three classes (figure 10), while 5 neurons showed individual activity patterns which we could not interpret. The neurons of the smallest group ( $n=10$ ; figure 10A) are characterized by relatively small receptive fields covering approximately  $40^\circ$  of the visual field with very clear responses to the stimuli used for receptive field estimation. The largest group ( $n = 25$ ; figure 10B) was defined by a medium-sized receptive field (approx.  $90$ - $110^\circ$  horizontal width) contralateral to the recorded hemisphere, approximately centered around  $90^\circ$  azimuth for neurons in the left hemisphere ( $n = 2$ ) or  $-90^\circ$  azimuth for neurons in the right hemisphere, respectively ( $n = 23$ ).

A third group of neurons ( $n = 16$ ) revealed receptive fields bigger than the area covered by the stimulation device. Strong transient response peaks marked in these cases the rims of the stimulus array instead of those of the receptive field (figure 10C).

The group with short response latencies consisted of four neurons with a small receptive field, three neurons with a medium sized receptive field and four neurons with a large receptive field (receptive fields of the other neurons in this group were not tested or not conclusive). The group of neurons with longer response latencies consisted of two neurons with a small receptive field, 19 neurons with a medium sized one and six neurons with a large receptive field. Neurons with a medium sized receptive field in the lateral visual field therefore tended to have longer latencies compared with neurons exhibiting a small frontally positioned receptive field.

Sixteen neurons with a preference for rotational self-motion stimuli exhibited medium sized lateral receptive fields, while six had small frontal receptive fields. In other words, 60 % of the neurons with frontal receptive field and 64 % of the neurons with lateral receptive field showed a preference for motion patterns as they emerge from

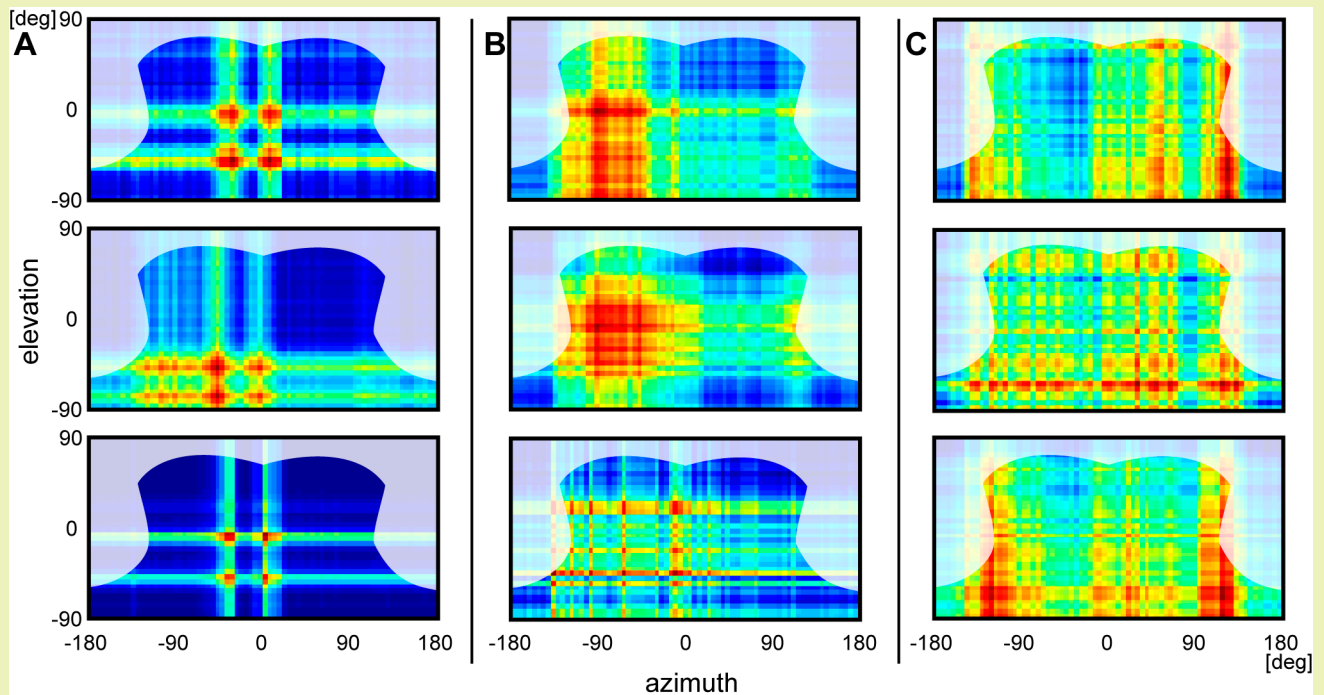


**Figure 10. Three categories of receptive fields were found in motion selective neurons in *n. rotundus*.**

Shaded areas were not covered by the stimulus apparatus. The cylinder projection causes an over-representation at  $+90^\circ$  and  $-90^\circ$  elevation which explains the seemingly broad coverage at the bottom. Due to the method used and response properties of the neurons, red areas indicate the edges of the receptive field. In B the red areas are broad due to the position of the receptive field which is monitoring the rotation axis of the vertical scan. For each category, three examples are given. A: small receptive field in the ventro-frontal visual field. B: medium sized receptive field in the lateral visual field. C: receptive fields covering the whole area of presentation.

rotational self-motion, but none of those with a large receptive field. In contrast, for neurons preferring translational self-motion stimuli ( $n=5$ ) we could only estimate the receptive field size of one cell which turned out to be large.

## Looming Stimuli

Five different stimuli presented a looming object that was positioned at different locations in the visual field.

We found a high variability in the response of neurons that were difficult to classify. All 76 neurons were tested. Twelve neurons did not respond to any “looming” stimulus, eleven responded in one of the five conditions tested, four neurons responded in three conditions, 10 neurons responded in four conditions and the others (35) responded in all five conditions.

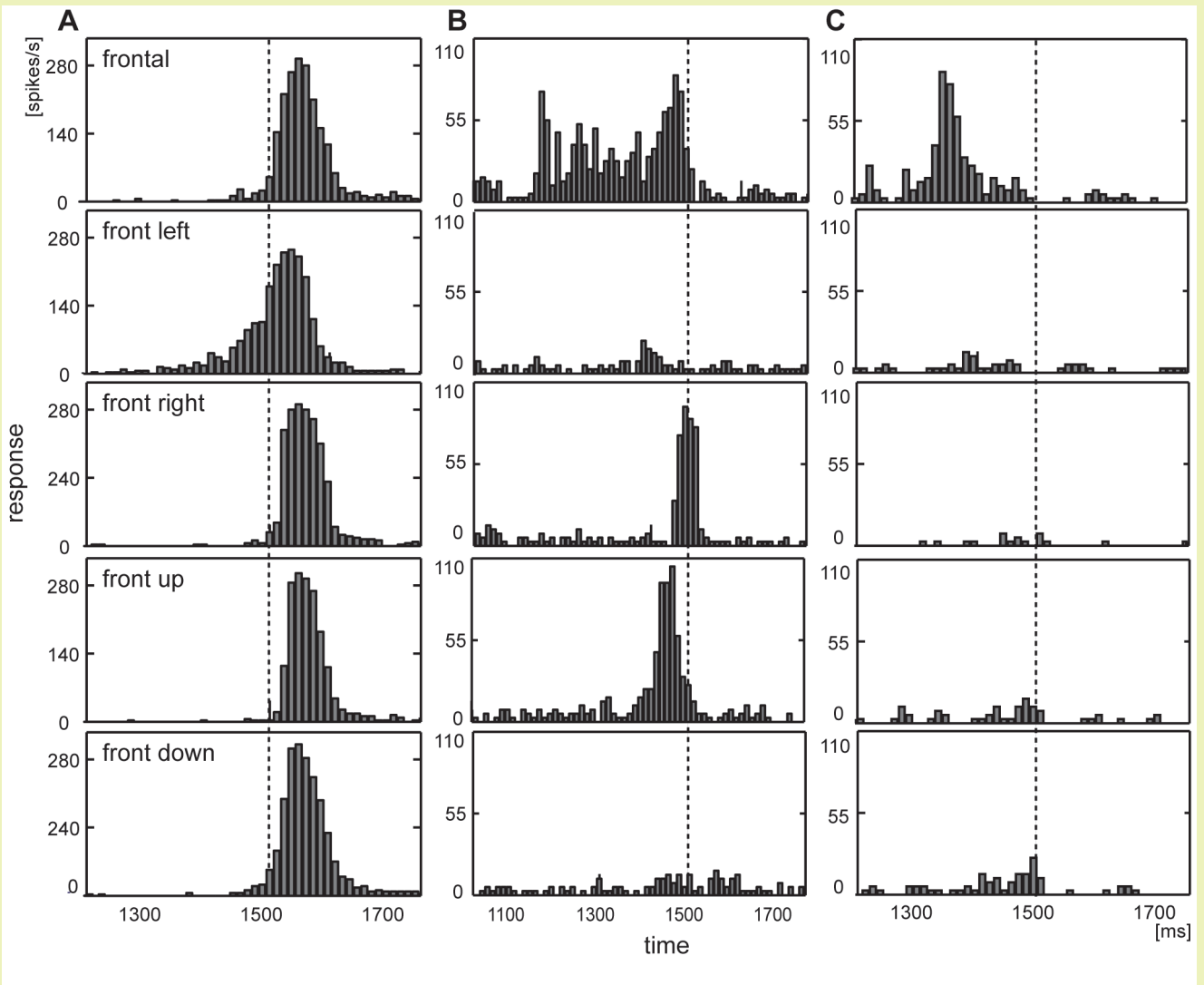


**Figure 11. Response to looming objects.**

Three examples of neurons are given that respond to bright looming disc in front of a dark background at different positions in the receptive field. Histograms depict the average response for 30 repeats of each stimulus. The position is indicated row-wise. Vertical dotted line indicates time of collision with the object. A: typical response. Most neurons show a response peak shortly after collision when the monitor is completely lit. Only the response to the approach from the frontal left shows a short earlier progression. B and C are examples for neurons differentiating between the directions of object approach showing early response, no response or a response near collision for different directions. Note different scaling of y-axes.

The most common type of response was observed in 28 neurons in all conditions (figure 11 A) and for most conditions in the other neurons. Here, the spiking rate rose over resting activity significantly only in a time window within the last 200 ms of stimulus presentation (duration: 1s). The spiking rate then increased rapidly and in some cases followed an approximately exponential course which correlates with the change in size of the object in the receptive field. The peak in spike rate was close to the virtual collision time, preceding or following it. For the remaining 36 neurons the responses to looming objects were very variable regarding preferred conditions or shape of the response.

In order to test whether the position of the receptive field had an influence on the response to the looming object, we calculated the time at which each neuron first reached an activity stronger than 33.3% of peak activity for neurons in the right hemisphere (n=64). There is a tendency towards earlier increments of activity for objects positioned at the frontal left (figure 11 A), which corresponds to the receptive fields being predominantly located on the left side of the visual field. Objects approaching from the frontal right, in contrast, elicited late responses.

### Naturalistic Replay

In the first step of the naturalistic replay experiment, we wanted to find neurons that would respond to objects in the visual scene (object–no-object test) and, as predicted by the work on the pigeon [23], signal the bird's approach towards them. In the next step, we wanted to test whether objects in the visual field were signaled differently when residual head movements we measured in the preceding behavioral study [7] were eliminated (head-rotation-no-head-rotation test).

### Defining the stimulus

When using a complex stimulus it is necessary to carefully analyze not only the response of the neuron but also the stimulus itself. Otherwise it would not be possible to interpret the response correctly. Here, we wanted to find out which optic flow parameter(s) the neuron responded to. It was therefore necessary to find a way to compare motion velocity values and distance values occurring within the receptive field of a neuron during stimulation in the different conditions.

We calculated the direction and size of image displacements between consecutive stimulus frames from the original data used to generate the movies. The result was illustrated with a cylindrical projection of vectors that point from the original position in one frame to the new position in the next frame for a set of coordinates in the visual field. Since the vectors refer to the time interval between the frames, they equal the velocity vectors of local image displacements.

In a movie of such cylindrical projections over the course of the virtual obstacle avoidance flight, the effects of objects on the optic flow can be demonstrated. The motion vectors produced by the obstacle are considerably longer compared with those generated by the walls in the background (figure 12 B; video 1).

The area of interest within the vector map was the area covered by the receptive field of the neuron. Using the knowledge we had of the receptive field, we calculated the average velocity and distance values within this area for each inter-frame-interval for all naturalistic stimuli. By this we acquired the time dependent changes of the optic flow parameters over the course of each stimulus and between different stimulus conditions as they were perceived by the neuron.

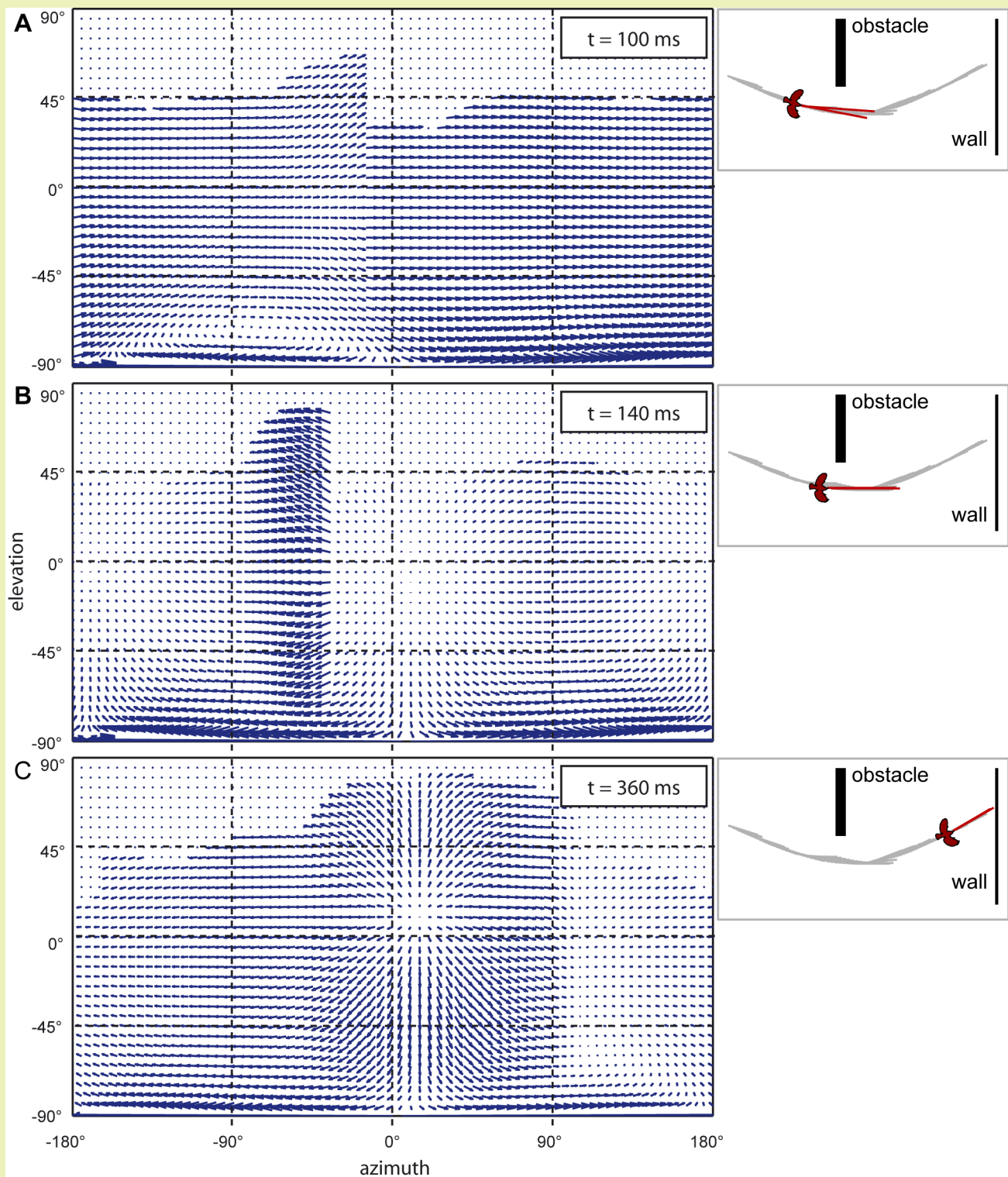


**Figure 12. Effects of rotational self motion, translational self motion and objects in the visual field.**

Blue arrows indicate velocities of image displacements. Arrows are 5 times original length for means of illustration. The timestamps indicate the points in time after stimulus begin. Y axis gives position in degrees of the elevation, X axis the same for azimuth. Insets on the right indicate bird position and gaze direction at according times. A: At 100ms the bird performs a head saccade during forward flight. Overlying vectors do not indicate objects. B: At 140 ms the bird is about to pass the obstacle. The image of the obstacle induces high velocity vectors in the left visual field. Heading direction is associated with small motion vectors and the focus of expansion near the centre of the visual field ( $0^{\circ}/0^{\circ}$ ). C: At 360 ms the bird approaches the wall at the end of the stimulus. The focus of expansion close to the centre of the visual field ( $0^{\circ}/0^{\circ}$ ) is visible.

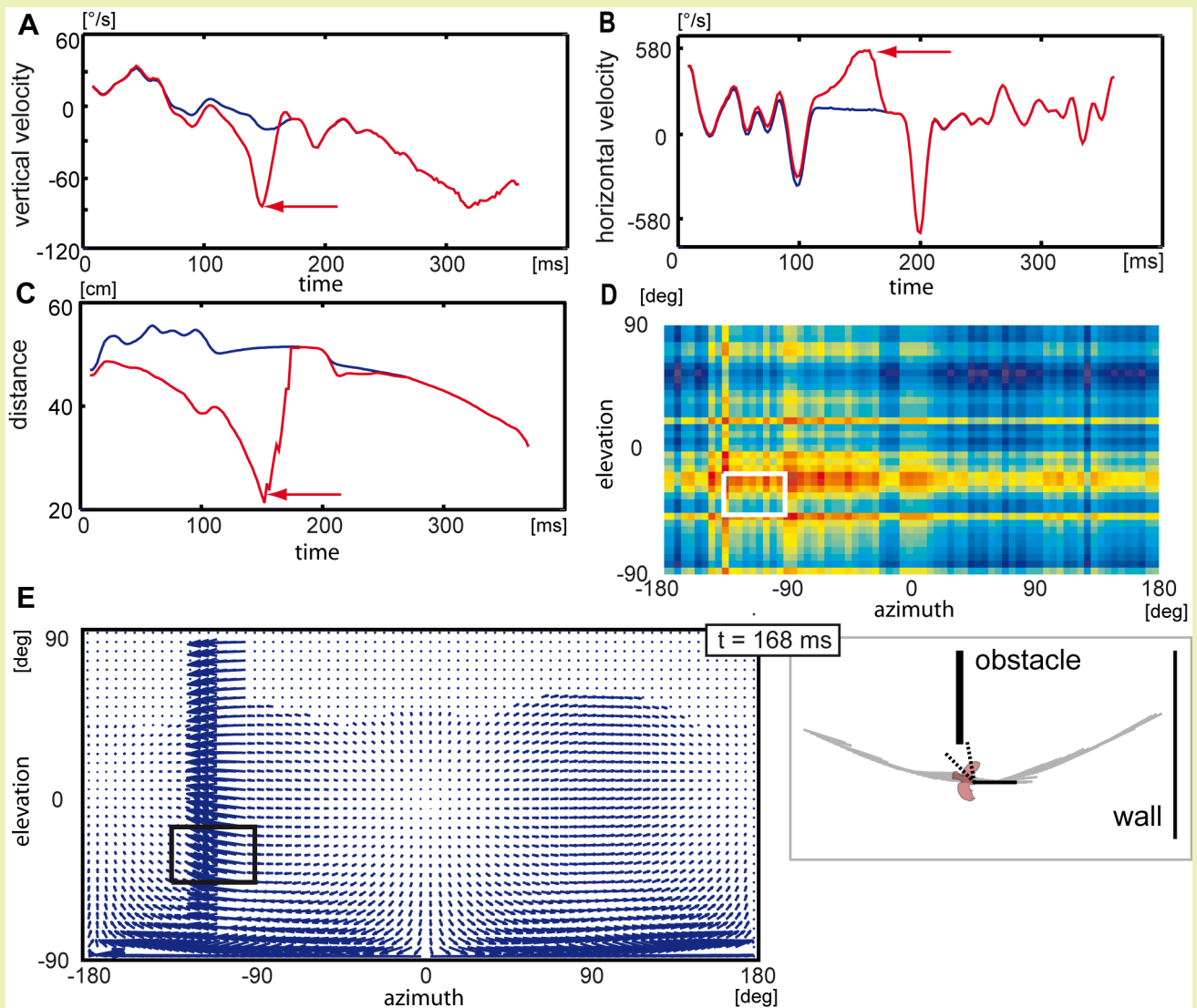


**Figure 13. Average values for different stimulus parameters within the receptive field of a neuron over the course of stimulus presentation.**

A-C: Values are averages of stimulus parameters given by the cylindrical projection within the area of the receptive field (Gaussian filter: sigma 5, window size 22 ms). Blue line corresponds to the no-object condition while the red line corresponds to the object condition. A: Vertical velocities show a distinct peak when the object is passed. B: Horizontal velocities show a peak when the obstacle is passed but also two additional peaks corresponding with saccadic head turns in the stimulus. C: Distance values reach a minimum when the obstacle is passed. D: The colour map indicates the result of the receptive field estimation. White rectangle indicates the area which was averaged. E: The map shows velocities of image displacement when peaks occur in the optic flow parameter values. The object is inside the receptive field (black rectangle). Inset on the right shows the bird's relative position to the obstacle and the angular width of the receptive field is indicated by broken black lines, accordingly.

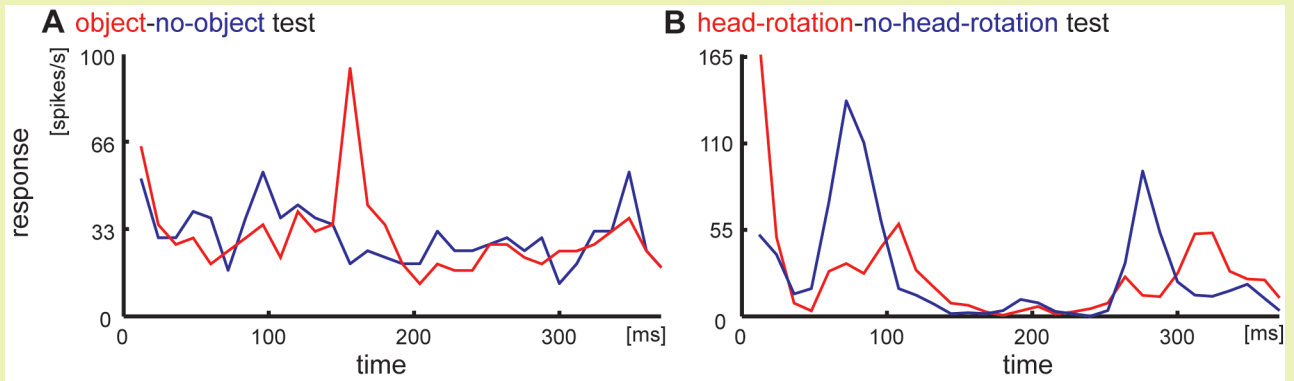


**Figure 14. Response to naturalistic stimuli.**

The response of two single neurons averaged over 30 repeats (bin size 12 ms). A: red line indicates response to the original flight trajectory in a cage including the obstacle (no windows); blue line indicates the response to the original flight trajectory in an empty cage (no obstacle, no windows). B red line indicates response to the original flight trajectory in a cage including obstacle and windows; blue line indicates response to an altered flight trajectory with stabilized head yaw orientation in the same cage.

In figure 13 we show the time-dependent distance and velocity data averaged over the receptive field of one of the neurons that showed reliable responses in the object-no-object test. The vertical (figure 13 A) motion component (image shift in elevation) reveals smaller velocities than the horizontal (figure 13 B) component (image shift in azimuth) since the trajectory of the original bird changed only little in altitude. Fast horizontal gaze shifts that occurred during saccadic changes in head orientation (figure 4 B) had a high impact on the horizontal velocities found in the stimulus but not on the vertical velocities. Instead, the vertical velocities correlated more closely with the distance to objects (figure 13 C) in the receptive field.

Both velocity components were affected by the presence of the obstacle. In the case depicted in figure 13 the obstacle generated a negative peak for vertical velocities (downward motion) and increasing horizontal velocities (front-to-back motion). The rapidly changing velocities coincide with a shrinking distance to the obstacle.

## General results

Many neurons of our sample could not be used for the following analysis. An accurate correlation between-stimulus and response demands both reliable response latency and an estimation of the receptive field from the according neurons. Due to these qualifications, 22 out of our 76 neurons were analyzed for the object-no-object test and 31 of the population of neurons were analyzed for the test with differing head rotation.

All of these neurons responded to the naturalistic stimulus with increased activity compared to resting activity. Among neurons we found a high variability of responses to the naturalistic stimuli. Within neurons differences between the responses to the control (no object / slow head rotations) and test conditions (object / only saccadic head rotation) were very small in many cases. Clearly visible response differences between control and test condition were found only in very few neurons which makes a statistical analysis impracticable (figure 14). Most neuronal responses were located between the depicted extremes and show very noisy response patterns which do not obviously show a time course correlated with the stimulus.

**Responses to objects in the naturalistic replay**

Two neurons responded to optic flow induced by static objects in the natural environment. The one with a lateral receptive field signaled the passing of the obstacle (figure 14A). The other one with a frontal receptive field signaled the approach towards the obstacle and towards the exit window (figure 15). The response peak of the neuron with lateral receptive field occurred immediately before the bird passed the obstacle. This coincided with peak velocities of optic flow within the receptive field of this neuron (figure 13). However, the strongest optic flow experienced during the naturalistic stimulus appeared when saccadic head turns occurred. None of the analyzed neurons showed any changes in response correlated to that.

The response properties of the neuron with a frontal receptive field could not be explained in a similar manner. Over the course of the stimulus, the focus of expansion appeared within the receptive field. In other words, motion vectors were found that pointed in all directions. This led to a nullified average velocity vector which did not provide information about objects. Instead we viewed the cylinder plots of those stimulus frames that were correlated with response peaks, manually, taking response latencies into account.

We found this neuron to signal the approach towards an object (video 1). When the object was present, we found two peaks 72 ms and 120 ms after stimulus onset, that did not occur within the empty cage (figure 15 A). The cylindrical projection (figure 15 C) of motion vectors in the receptive field revealed that at time 72 ms, the obstacle (wall) is in heading direction eliciting a strong response. At 120 ms, the focus of expansion was within the receptive field of the neuron but did not coincide with the object. In this case, the response was much smaller. Between these frames the object moved out of the receptive field but returned when a fast head turn was performed by the bird (video 1).

We extended the tests of this neuron by a third condition. Here the entrance and exit windows were introduced into the virtual flight arena in addition to the obstacle. The exit window evoked another high activity peak (figure 15 A, black curve). The cylindrical projection of the optic flow vectors at the same moment showed that the rim of the window generated high velocities and the focus of expansion was located well within the window.

At the very end, spike rates rose in the first two conditions due to an approach of the cage wall, in the third condition the neuron returned to resting activity as the bird was about to (virtually) exit by the window. At this moment, no optic flow occurred within the receptive field of the neuron.

**Influence of slow head rotations on the signaling of objects**

One neuron tested in the head-rotation-no-head-rotation test showed significant responses to objects and it had a frontal receptive field (figure 14 B). Like in the neuron described above, we found response peaks that could be correlated to the obstacle and exit window by viewing vector maps of the optic flow in the receptive field of the neuron.

In the condition where head yaw rotations were eliminated, these approaches were signaled with a considerably clearer signal. In the test condition when original head rotations were presented, the spike rates in response to the objects were relatively low. The corresponding response peaks found when the head rotations were eliminated, reached significantly higher spiking rates and were more pronounced. They also tend to occur earlier but this is mainly due to an altered head orientation rather than the reduced head yaw rotation.

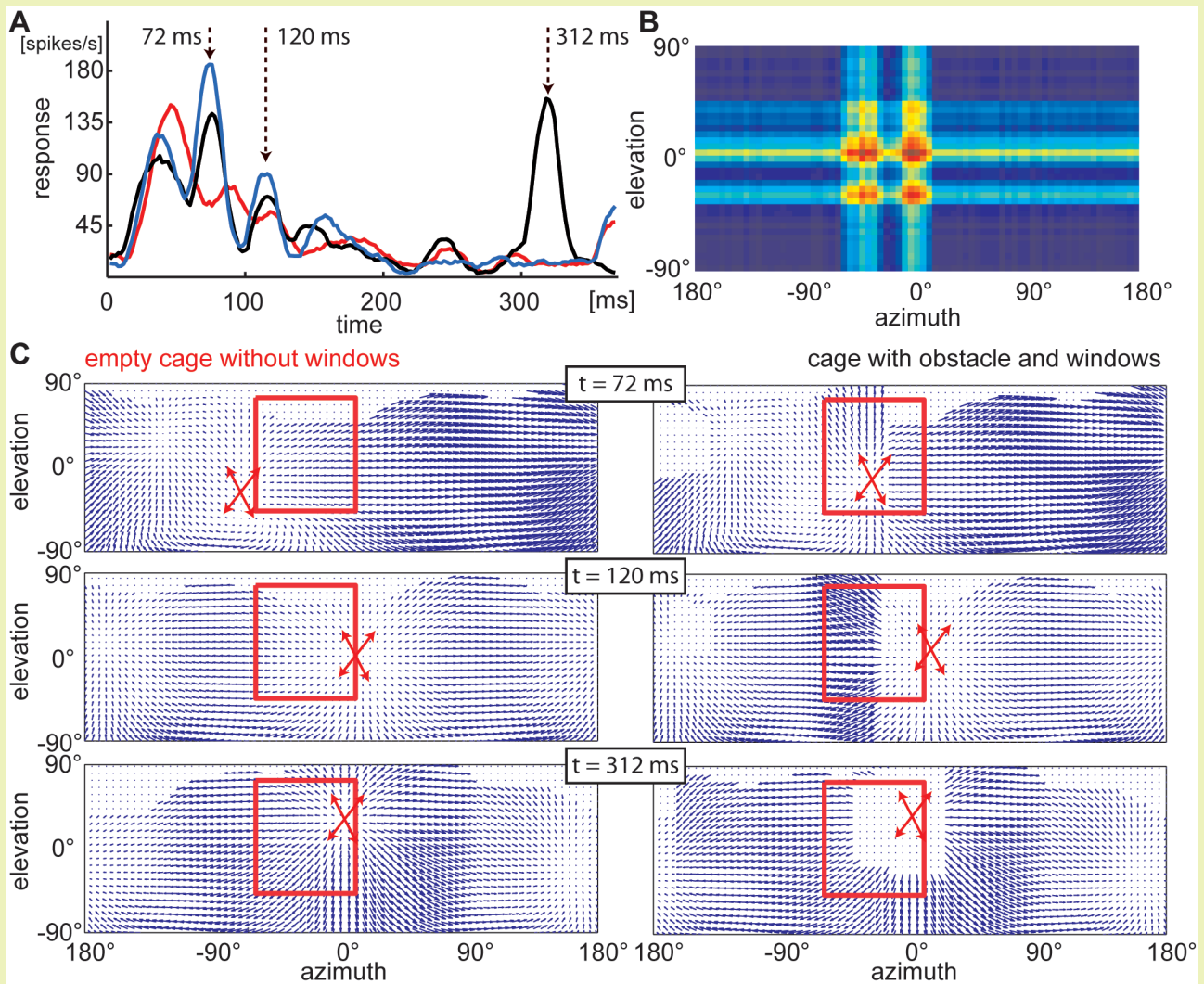


**Figure 15. Approach signalling neuron: response peaks occur when object position and focus of expansion are collocated.**

A: Averaged response to the three naturalistic test conditions over 30 repeats each (Gaussian filter: sigma 5, window size: 22 ms). Red line corresponds to no-object-condition. Blue line corresponds to first object-condition (cage + obstacle) and the black line corresponds to the second object-condition (cage + obstacle + windows). Arrows indicate peak responses of interest. B: The neuron exhibits a small frontal receptive field on the lower contralateral side. C: Velocities of image displacements at the three moments of interest. At 72 ms the focus of expansion (centre of red cross) is collocated with the obstacle eliciting a peak in response activity in both conditions including the obstacle. At 120 ms the local velocities generated by the obstacle are even stronger but the focus of expansion is not collocated with the object – the differences between the control and test conditions are small. At 312 ms there are no velocities detectable close to the focus of expansion but the edges of the window generate strong velocity vectors (from which the focus of expansion was estimated) – only the stimulus including a window elicits a very high peak in response activity.

### Further Properties of Neurons Responding to the Naturalistic Replay

The two neurons with frontal receptive fields that we identified as ‘approach signaling neurons’ belong to the very few neurons that had short response latencies (44 and 37 ms) and at the same time showed a preference for horizontal self-motion (figure 7). They did not show a preferred direction for the movement of the stimulus during receptive field estimation.

Within conventional stimuli, the looming object would be most similar to an approached object. One of the approach signaling cells did not respond differently to the different looming conditions. The other one showed a preference for the frontal position of the stimulus, according to the position of the receptive field. However, the response in this case was not similar to that found in the naturalistic stimulus.

The one neuron with the receptive field in the lateral field also responded early (35 ms). It showed a preference for upwards moving stimuli in the receptive field test but no response to looming stimuli.

## Discussion

Our experiments confirm earlier data on avian motion selective neurons, mostly obtained in the pigeon. They also add a new perspective, namely the responses of these neurons to more complex stimuli as they appear in a natural flight situation. Using “FliMax”, a panoramic stimulus device with an LED display, which has already been used for investigations in the fly [33,38-44], allows comparison of the behavioral and neurobiological mechanisms underlying orientation during flight in two phylogenetically very diverse animals, a bird and a fly.

We found that neurons in nucleus rotundus of the tectofugal visual system respond to global motion. Some of these neurons could further be categorized by preferential responses to optic flow corresponding to translational or rotational self-motion. We also found a strong decrease of spiking activity for consecutive self-motion stimuli. Finally, using the response latencies to the onset of global motion, the rotundal neurons could be categorized into two discrete groups.

In the naturalistic replay experiment we found neurons that responded to objects. The neuron with a lateral receptive field responded to the obstacle when the bird flew by. The neurons with a frontal receptive field responded to objects that were being approached. These response characteristics could not be predicted from the response to conventional stimuli. Especially, one neuron signaling approach did not respond selectively to looming stimuli. Actually, we did not find evidence for looming specific neurons at all since the responses to looming stimuli were too diverse. However, neurons signaling approach responded to horizontal self-rotation. Slow rotational head movements disrupted the signal coding for approaching objects while fast saccadic turns did not elicit changes in spike rates.

### I. Comparison of our findings to those from other studies on birds:

(1) We confirm that global stimulation affects the response of rotundal neurons, as it was demonstrated in studies from other labs [28-32].

We would hypothesize that the self-motion preferences we found were mediated by the accessory optic system. In principle, the cause of a response to self-motion stimuli could either be that the objects in our star-field-scene constantly entered the receptive field of the neuron during global stimulation or an input from self-motion processing areas. For neurons with a frontal receptive field, yaw rotation and left/right translation generate very similar retinal motion patterns. For neurons with a lateral receptive field this is the case for yaw rotation and back/forth translation. However, the preference for rotational self-motion in those neurons is still significant as compared to respective translational directions only (not shown), indicating another source of self-motion specificity, like the accessory optic system.

(2) Our data on response latency indicate two categories of neurons: early and late responding. This has also been shown by Schmidt and Bischof [36], who described a variation of response latencies due to the origin of input from the ipsi- (late response) or contralateral eye (early response).

In the pigeon, Folta et al. [37,45] also found short and long response latencies for input from contra- and ipsilateral eye, respectively. They explained this finding with two different anatomically known pathways by which information reaches the nucleus rotundus. Signals from the contralateral eye reach the nucleus rotundus either in an ascending stream via the contralateral tectum opticum or by a descending stream originating from the visual Wulst which is part of the thalamofugal visual pathway. Folta et al. [37,45] estimated the latency from a theoretical approach taking into account the length of the axons and the number of synapses that transmit the signal. The measured latencies fit the tectofugal bottom up connection for contralateral and bilateral stimulation whereas latencies found for ipsilateral stimulation fit the approximated latency from the top down input via the visual Wulst.

Our results indicate that this may not be the only explanation for difference in response latency. A significant number of neurons we recorded had receptive fields exclusively in the lateral monocular area but had long latencies. It seems that these neurons with long latencies do not necessarily get input from the ipsilateral eye.

However, latencies of late responding neurons found in the pigeon were longer than those of late responding neurons in the zebra finch. Folta et al. [37] classified late responding neurons as top-down neurons that exhibited latencies of at least 70 ms. Latencies of late responding neurons measured in our lab in the zebra finch usually ranged from 55 to 85 ms. Early responses found in all studies ([36,37,45]) including the present one, on the other hand, ranged about 30-40 ms.

We considered differences between stimuli to cause the differences in response latencies between the species. However, Schmidt and Bischof [36] and Folta et al. [37] both used flash evoked responses and got different latencies for the two species. In our present study we used global motion onset instead of flashes and found the same range of response latencies as Schmidt and Bischof [36].

The finding that the late responding neurons in the zebra finch respond earlier than those in the pigeon seems to have physiological reasons. The brain of the zebra finch is much smaller than that of the pigeon. It therefore has shorter axonal traveling times. Longer latencies in the late responding neurons of pigeons could also be a problem of anesthesia. The two species may react differently to urethane which was used in all studies, or the relative doses were different.

(3) Looming objects did not elicit responses in zebra finches that hint towards different types of time to collision processing neurons as described by Wang and Frost for pigeons [22-25]. Instead, most neurons seemed to respond to the size of the moving edge or the increasing size of the area covered by the object. In fact, we compared the responses of rotundal neurons to responses in nucleus lentiformis mesencephali or DLM (not shown)

and did not find any differences. However, in contrast to Wang and Frost [23] we did not apply a battery of tests to identify time to collision signaling neurons.

### II. Adding realism to a stimulus gives rise to unexpected response properties

(1) The reason why an increment of activity during pure global stimulation has not been reported for rotundal neurons so far may be due to stimulus characteristics. In our study the background presented a more realistic composition of global motion than was possible with other methods. Commonly used stimuli consist of moving gratings or dots on screens which covered only parts of the visual field or a planetarium projector [14,46,47] which covered the whole visual field but provided only one depth plane. In a study on a self-motion coding nucleus of the accessory optic system that processes horizontal optic flow, Xiao and Frost (at 9th International Congress of Neuroethology) found neurons that were maximally excited by a stimulus consisting of two depth planes, of which one moved in the preferred direction at a fast velocity, and the other one moved in the anti-preferred direction with slow velocity. From the details in response characteristics, Xiao and Frost suggest that these neurons derive relative depth from motion parallax. In general, this suggests that a more realistic composition of motion in depth enhances self-motion processing, and may explain why we were able to evoke responses to optic flow corresponding to self-motion.

(2) When taking another step towards more realistic stimuli in the naturalistic replay approach, we found two different types of response to the replay of motion sequences elicited during a flight around an obstacle in a flight arena [7]. One neuron with a lateral receptive field responded to the obstacle when the bird passed it. This response could be explained by the average size of motion vectors or average distance to obstacles in the receptive field of the neuron.

Two neurons with frontal receptive fields showed activity characteristics over the course of the stimulus similar to each other. Activity peaks correlated to the presence of the obstacle and exit window in the receptive field.

One of these neurons showed selective responses for situations at which the bird approached an object. The neuron showed highest response activity when in the receptive field the object coincided with the focus of expansion. This was the case, regardless of whether the bird virtually approached a textured wall which produced strong motion vectors or a window which only produced motion vectors at the rims but not in vicinity of the focus of expansion.

Signaling object related visual motion which is actually generated by self-motion in a static environment and does not refer to a moving object, can be interpreted as coding of ‘passive object motion’ to differentiate this type of motion from an ‘approaching-predator-scenario’.

### III. Flies and birds show similar aspects of response to a naturalistic replay.

(1) The decrease of response activity during stimulation with changing global stimuli is reminiscent of results in the blowfly [44] which were acquired using a naturalistic replay. There, motion sensitive neurons – mainly responding to motion stimuli by graded changes of their membrane potential – adapted to global motion. In the adapted state the base line of the membrane potential due to background motion was lower than in the non-adapted state. A novel object that evoked the same activation levels in both states was thus responded to with a clearer signal in the adapted state. In our study, the response to the naturalistic stimuli (figure 15) shows a high spike rate at the

beginning that decreases over the course of the stimulus. Both objects, obstacle and window, evoked similar spike rates, but due to the lower base line at the end of the stimulus the response to the window is a clearer signal than that to the obstacle (figure 15 A), since the difference to the corresponding baseline is bigger.

(2) Neurons that signal the three-dimensional structure of the environment from optic flow discontinuities in the blowfly and in the zebra finch, share common properties. The two neurons signaling approach found in the present study showed a preference for horizontal rotational self-motion (yaw rotation). The responses to objects were obscured by slow head turns while fast head turns did not have an effect on the response. This is similar to the situation in the blowfly. Kern et al. [39] showed that the motion dynamics generated by the saccadic gaze strategy of the blowfly lead to a representation of the spatial relation of a fly to its surroundings during inter-saccadic intervals. They also found that these responses showed a clearer signal when residual body yaw rotations were compensated during intersaccadic intervals by stabilizing head movements [40]. From studies that used conventional stimuli, the neurons they recorded (HSE; a neuron responsive to horizontal motion) were previously thought to signal self-rotation. The neurons also did not reliably signal saccadic gaze shifts as would have been expected for a self-rotation coding neuron.

To our knowledge, we were the first to use panoramic naturalistic stimuli for research on optic flow processing in vertebrates. Our stimuli included a virtual environment built to reflect the three dimensional structure of a real flight arena as well as a natural course of gaze position and orientation as it was behaviorally generated by a real bird in the real flight arena. In similar studies on blowflies it was shown that motion selective neurons may respond very differently to stimuli when they are embedded in a realistic context and include natural gaze shifts [39,43,44]. Here we found similar differences between the response to conventional and naturalistic neurons in birds which may lead to a more realistic idea about the function of an object coding brain area in a naturally behaving bird.

## Acknowledgements

We want to thank Claudius Strub for the development of the optic flow toolbox for Matlab® we used for some calculations.

## References

1. **Bischof HJ (1988) The Visual-Field And Visually Guided Behavior In The Zebra Finch (*Taeniopygia-Guttata*).** J Comp Physiol A 163: 329-337.
2. **Martin GR (2007) Visual fields and their functions in birds.** JOrnithol 148 (Suppl 2): S547-S562.
3. **McFadden S (1993) Constructing the Three-Dimensional Image.** In: Zeigler, HP und Bischof, H-J(eds): Vision, Brain and Behavior in Birds MIT Press, Cambridge, Mass, London (1993).
4. **Gibson JJ (1950) The perception of visual surfaces.** Am J Psychol 63: 367-384.
5. **Koenderink JJ (1986) Optic flow.** Vision Res 26: 161-179.
6. **Vaina L, Beardsley S, Rushton S (2004) Optic Flow and Beyond.** Synthese Library 324.
7. **Eckmeier D, Geurten BR, Kress D, Mertes M, Kern R, et al. (2008) Gaze strategy in the free flying zebra finch (*Taeniopygia guttata*).** PLoS ONE 3: e3956.
8. **Davies MN, Green PR (1990) Optic flow-field variables trigger landing in hawk but not in pigeons.** Naturwissenschaften 77: 142-144.
9. **Davies MNO, Green PR (1991) The Adaptability of Visuomotor Control in the Pigeon During Landing Flight.** Zoologische Jahrbucher-Abteilung fur allgemeine Zoologie und Physiologie der Tiere 95: 331-338.
10. **Lee DN, Davies MNO, Green PR, Vanderweel FRR (1993) Visual Control of Velocity of Approach by Pigeons When Landing.** Journal of Experimental Biology 180: 85-104.
11. **Lee DN, Reddish PE (1981) Plummeting Gannets - A Paradigm Of Ecological Optics.** Nature 293: 293-294.
12. **Mey J, Thanos S (2000) Development of the visual system of the chick. I. Cell differentiation and histogenesis.** Brain Res Brain Res Rev 32: 343-379.
13. **Wohrn JC, Puelles L, Nakagawa S, Takeichi M, Redies C (1998) Cadherin expression in the retina and retinofugal pathways of the chicken embryo.** J Comp Neurol 396: 20-38.
14. **Wylie DR, Frost BJ (1999) Responses of neurons in the nucleus of the basal optic root to translational and rotational flowfields.** J Neurophysiol 81: 267-276.
15. **Wylie DR (2000) Binocular neurons in the nucleus lentiformis mesencephali in pigeons: responses to translational and rotational optic flowfields.** Neurosci Lett 291: 9-12.
16. **Brauth SE (1977) Direct accessory optic projections to the vestibulo-cerebellum: a possible channel for oculomotor control systems.** Exp Brain Res 28: 73-84.
17. **Brecha N, Karten HJ (1979) Accessory optic projections upon oculomotor nuclei and vestibulocerebellum.** Science 203: 913-916.
18. **Gioanni H, Rey J, Villalobos J, Richard D, Dalbera A (1983) Optokinetic Nystagmus In The Pigeon (*Columba-Livia*).2. Role Of The Pretectal Nucleus Of The Accessory Optic-System (Aos).** Experimental Brain Research 50: 237-247.

19. **Gioanni H, Villalobos J, Rey J, Dalbera A (1983) Optokinetic Nystagmus In The Pigeon (*Columba-Livia*).3. Role Of The Nucleus Ectomamillaris (Nem) - Interactions In The Accessory Optic-System (Aos).** Experimental Brain Research 50: 248-258.
20. **Fite KV, Reiner A, Hunt SP (1979) Optokinetic nystagmus and the accessory optic system of pigeon and turtle.** Brain Behav Evol 16: 192-202.
21. **Warrick DR, Bundle MW, Dial KP (2002) Bird maneuvering flight: Blurred bodies, clear heads.** Integrative And Comparative Biology 42: 141-148.
22. **Wang YC, Jiang S, Frost BJ (1993) Visual processing in pigeon nucleus rotundus: luminance, color, motion, and looming subdivisions.** Vis Neurosci 10: 21-30.
23. **Wang YC, Frost BJ (1992) Time To Collision Is Signaled By Neurons In The Nucleus Rotundus Of Pigeons.** Nature 356: 236-238.
24. **Wu LQ, Niu YQ, Yang J, Wang SR (2005) Tectal neurons signal impending collision of looming objects in the pigeon.** European Journal Of Neuroscience 22: 2325-2331.
25. **Xiao Q, Li DP, Wang SR (2006) Looming-sensitive responses and receptive field organization of telencephalic neurons in the pigeon.** Brain Research Bulletin 68: 322-328.
26. **Engelage J, Bischof HJ (1996) Single cell responses in the ectostriatum of the zebra finch.** J Comp Physiol A 179: 785-795.
27. **Wylie DR, Linkenhoker B, Lau KL (1997) Projections of the nucleus of the basal optic root in pigeons (*Columba livia*) revealed with biotinylated dextran amine.** J Comp Neurol 384: 517-536.
28. **Frost BJ, Wylie DR, Wang YC (1990) The processing of object and self-motion in the tectofugal and accessory optic pathways of birds.** Vision Res 30: 1677-1688.
29. **Wang Y, Gu Y, Wang SR (2000) Modulatory effects of the nucleus of the basal optic root on rotundal neurons in pigeons.** Brain Behav Evol 56: 287-292.
30. **Diekamp B, Hellmann B, Troje NF, Wang SR, Gunturkun O (2001) Electrophysiological and anatomical evidence for a direct projection from the nucleus of the basal optic root to the nucleus rotundus in pigeons.** Neurosci Lett 305: 103-106.
31. **Sun H, Frost BJ (1998) Computation of different optical variables of looming objects in pigeon nucleus rotundus neurons.** Nat Neurosci 1: 296-303.
32. **Xiao Q, Frost BJ (2009) Looming responses of telencephalic neurons in the pigeon are modulated by optic flow.** Brain Res 1305: 40-46.
33. **Lindemann JP, Kern R, Michaelis C, Meyer P, van Hateren JH, et al. (2003) FliMax, a novel stimulus device for panoramic and highspeed presentation of behaviourally generated optic flow.** Vision Res 43: 779-791.
34. **Bischof HJ (1981) A stereotaxic headholder for small birds.** Brain Res Bull 7: 435-436.
35. **Nixdorf-Bergweiler B, Bischof H-J (2007) A stereotaxic atlas of the brain of the zebra finch, *Taeniopygia guttata*, with special emphasis on telencephalic visual and song system nuclei in transverse and sagittal sections.** Bethesda (MD): National Library of Medicine (US), National Center for Biotechnology Information.

36. Schmidt A, Bischof HJ (2001) Integration of information from both eyes by single neurons of nucleus rotundus, ectostriatum and lateral neostriatum in the zebra finch (*Taeniopygia guttata castanotis* Gould). *Brain Res* 923: 20-31.
37. Folta K, Diekamp B, Gunturkun O (2004) Asymmetrical modes of visual bottom-up and top-down integration in the thalamic nucleus rotundus of pigeons. *Journal Of Neuroscience* 24: 9475-9485.
38. Boeddeker N, Lindemann JP, Egelhaaf M, Zeil J (2005) Responses of blowfly motion-sensitive neurons to reconstructed optic flow along outdoor flight paths. *J Comp Physiol A Neuroethol Sens Neural Behav Physiol* 191: 1143-1155.
39. Kern R, van Hateren JH, Michaelis C, Lindemann JP, Egelhaaf M (2005) Function of a fly motion-sensitive neuron matches eye movements during free flight. *PLoS Biol* 3: e171.
40. Kern R, van Hateren JH, Egelhaaf M (2006) Representation of behaviourally relevant information by blowfly motion-sensitive visual interneurons requires precise compensatory head movements. *J Exp Biol* 209: 1251-1260.
41. van Hateren JH, Kern R, Schwerdtfeger G, Egelhaaf M (2005) Function and coding in the blowfly H1 neuron during naturalistic optic flow. *J Neurosci* 25: 4343-4352.
42. Karmeier K, van Hateren JH, Kern R, Egelhaaf M (2006) Encoding of naturalistic optic flow by a population of blowfly motion-sensitive neurons. *J Neurophysiol* 96: 1602-1614.
43. Liang P, Kern R, Egelhaaf M (2008) Motion adaptation enhances object-induced neural activity in three-dimensional virtual environment. *J Neurosci* 28: 11328-11332.
44. Liang P, Kern R, Kurtz R, Egelhaaf M (submitted) Enhancement of object responses by visual motion adaptation and its dependence on the temporal characteristics of optic flow. *Journal of Neurophysiology*.
45. Folta K, Troje NF, Gunturkun O (2007) Timing of ascending and descending visual signals predicts the response mode of single cells in the thalamic nucleus rotundus of the pigeon (*Columba livia*). *Brain Research* 1132: 100-109.
46. Wylie DR, Kripalani T, Frost BJ (1993) Responses of pigeon vestibulocerebellar neurons to optokinetic stimulation. I. Functional organization of neurons discriminating between translational and rotational visual flow. *J Neurophysiol* 70: 2632-2646.
47. Winship IR, Wylie DR (2001) Responses of neurons in the medial column of the inferior olive in pigeons to translational and rotational optic flowfields. *Exp Brain Res* 141: 63-78.

